ATTRACTOR DYNAMICS IN THE HIPPOCAMPAL REPRESENTATION OF THE LOCAL ENVIRONMENT

Thomas Joseph Wills

Thesis submitted for consideration for the degree of Doctor of Philosophy

Department of Anatomy and Developmental Biology
University College London
August 2005

ProQuest LLC
789 East Eisenhower Parkway
P.O. Box 1346
Ann Arbor, MI 48106-1346

Abstract

Pyramidal cells of the CA1 field of the hippocampus fire at relatively high rates only when the animal is in a restricted region of the environment (Place cells). A collection of these cells may form the neural substrate of a map-like representation of the animal's environment.

Previous work has shown that place cells have different firing patterns, or 'remap', in different environments.

In this thesis, it was found that exposing rats to environments differing in the shape (square vs circle), colour (brown vs white) and texture of their walls resulted in rapid remapping between the environments. The environments were then substituted, so that both were constructed from the same deformable box, and only differed in their shape (square vs circle). The place cells remained remapped in this condition.

In order to investigate the nature of the remapped place cell representations, rats were then exposed to a series of octagonal environments which varied incrementally from square-like to circle-like. Despite environmental shape changing continuously, all recorded place cells switched abruptly between square and circle representations: no intermediate firing patterns were observed. Furthermore, all simultaneously recorded cells switched between representations at the same point in the octagon series.

In 2 animals, remapped place cells were tested in a series of hybrid shapes which were octagonal at one end and square at the other. Place cells always responded to these shapes as either an octagon or a square but different cells responded differently to each hybrid.

These results can be interpreted as evidence for the existence of attractor networks in the hippocampal representation of space. Under some circumstances, representations of familiar environments form stable attractors, and environmental inputs sufficiently similar to these cause the place cell representation to converge onto them. The results also suggest that place cells can form a coherent, map-like representation of the environment.

Contents

Chapter 1

Anatomy of the Rat Hippocampal Formation

This chapter will review the main aspects of the anatomy of the rat hippocampal formation. The first section will introduce the gross morphology and general connectivity of the hippocampal formation, as well as giving a definition of nomenclature. The second section will review hippocampal formation anatomy in more detail, describing cytoarchitectonics, intrinsic and extrinsic connections. The third section will describe some aspects of the parahippocampal region, important for understanding input to the hippocampal formation. Finally, there will be a brief summary, which will try to extract the important anatomical principles for considering hippocampal function.

Introduction to the Hippocampal Formation

Nomenclature

The nomenclature used in this thesis will follow the scheme proposed by Scharfman *et al* (2000). In this scheme, the hippocampal formation and the parahippocampal region are defined on the basis of both connectivity and laminar organisation.

The hippocampal formation is defined as the dentate gyrus, the CA (*Cornu Ammonis*) fields (CA1, CA2, CA3) and the subiculum. All these regions (which will be referred to as 'fields' of the hippocampal formation) share a laminar organisation, in that they all are three-layered cortex (also referred to as allocortex or archiocortex). The hippocampal formation can also be defined on the basis of the connectivity between fields. Hippocampal formation connectivity differs from that of neocortex by lacking much of the strong, reciprocal innervation between different areas. It is much simpler, and more serial: the connections between different hippocampal formation fields are overwhelmingly in one direction only.

Following previous definitions, the term 'hippocampus' will be used to refer to the CA fields of the hippocampal formation only.

The parahippocampal region is defined as the pre- and parasubiculum, the entorhinal cortex, the perirhinal cortex and the postrhinal cortex. (The primate homologue of the latter is thought to be the parahippocampal cortex (Burwell *et al*, 1995; Witter *et al*, 2000)). All these areas consist of six-layered cortex. Pre- and parasubiculum, and the entorhinal cortex, have a prominent cell-free layer IV, the lamina dissecans. The parahippocampal region can be thought of as a forming the transition between allocortex and neocortex (Scharfman *et al*, 2000). The connectivity of the parahippocampal region shows a more neocortical pattern of connectivity than that of the hippocampal formation. There are at least two sets of reciprocal connections, one between peri- and postrhinal cortices and entorhinal cortex, the other between pre- and parasubiculum and entorhinal cortex.

Gross morphology

In the rat, the hippocampal formation is a rather large structure, occupying about half the cortical volume of the brain. Figure 1.1 is a sketch depicting where the hippocampus sits in the rodent brain. Its long axis extends from the septal nuclei of the basal forebrain rostrally and bends caudo-ventrally into a cashew-nut shape, reaching the temporal lobe. The long axis of the hippocampus is referred to as septo-temporal (or dorso-ventral) axis. Orthogonal to this, running medial to lateral, is the transverse axis. Along the transverse axis, regions closest to the dentate gyrus are referred to as proximal, those closest to the peri- and postrhinal cortices are referred to as distal. A radial axis can also be defined through each field (the curves of this axis following the curves of the field). Regions close to the ventricle are referred to as deep, while regions close to the pia or hippocampal fissure are referred to as superficial.

The horizontal section in Figure 1.2, through the hippocampal formation and the parahippocampal region, shows its basic components and highlights the cyto-architectonic features described above. The darkly stained, interlocking, V-shaped structures are the granule cell layer of the dentate gyrus, and the pyramidal cell layers of CA1-3. This section illustrates the tri-laminar organisation of the structures which

Figure 1.1

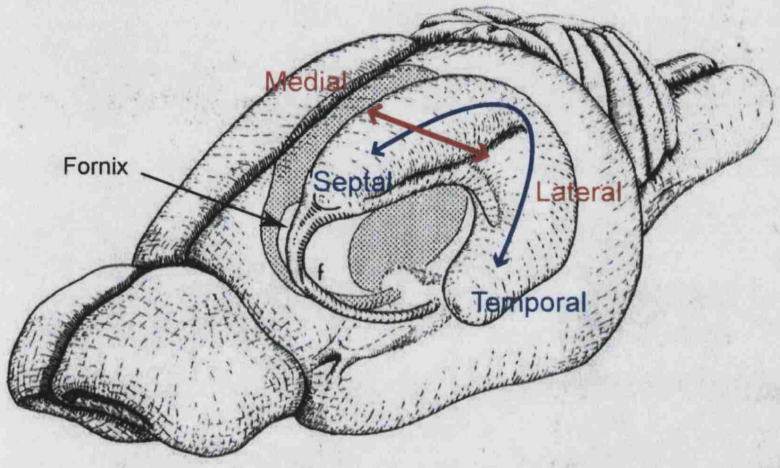

Figure 1.1. Drawing showing the position of the hippocampal formation within the rat brain. The septo-temporal axis (blue) runs between the poles of the hippocampal formation marked septal and temporal. The transverse axis (red) runs medial to lateral. (Adapted from Amaral and Witter, 1995).

Figure 1.2

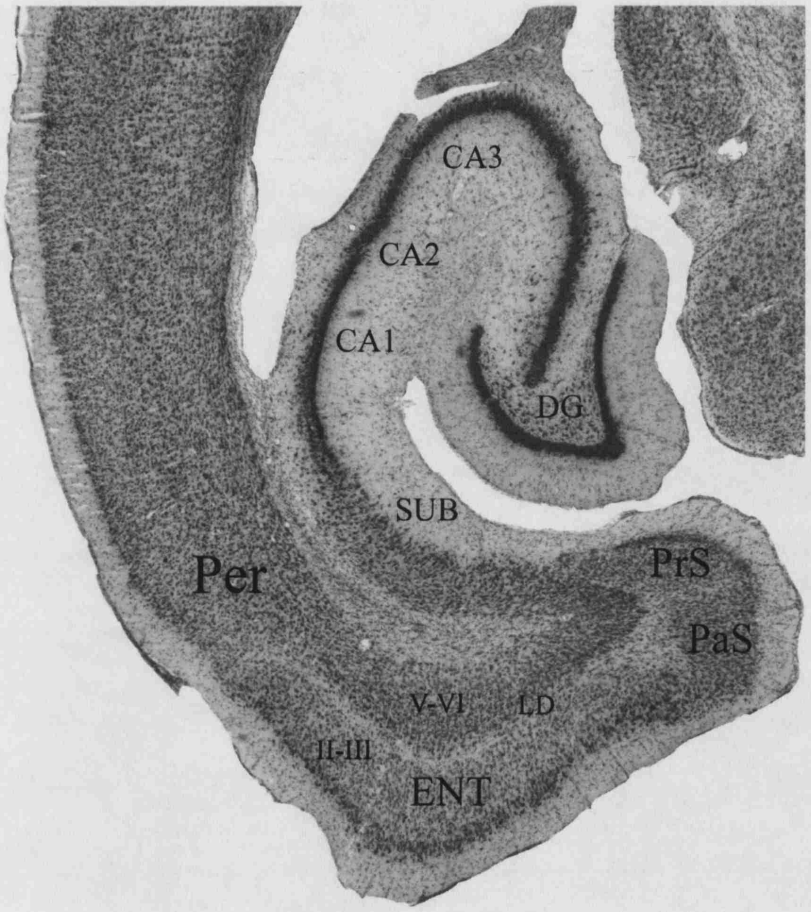

Figure 1.2. Horizontal section through hippocampal formation and parahippocampal region of the rat brain. The trilaminar structures that compose the hippocampal formation are the Dentate Gyrus (DG), CA1-3 pyramidal cell layers, and the subiculum (SUB). The parahippocampal region is composed of the Presubiculum (PrS), Parasubiculum (PaS), Entorhinal cortex (ENT) and Perirhinal cortex (Per). The transition to the parahippocampal region is marked by an abrupt increase in the number of layers. The newly appearing layers form the superficial parts of these structures (II-III), while the deep layers (V-VI) are a continuation of the Subiculum. The transition between the Entorhinal and Perirhinal layers is marked by the disappearance of the cell-free zone, lamina dissecans (LD). (Adapted Witter et al, 2000).

make up the hippocampal formation (dentate gyrus, CA1, CA2, CA3 and subiculum), and shows the emergence of new layers at the border between subiculum and presubiculum. It also shows how the deep layers of pre- and parasubiculum appear to be a continuation of the pyramidal cell layer of the subiculum.

The major fibre bundle associated with the hippocampus is the fimbria-fornix. The deep surfaces of the hippocampal formation are covered in a thin sheet of efferent and afferent fibres, the alveus. These fibres collect in a bundle along the lateral edge of the hippocampal formation, named the fimbria. At the septal extreme of the hippocampal formation, these fibres descend into the basal forebrain, at which point the bundles are referred to as the fornix (see Figure 1.1). The fornix then splits into several components, innervating different regions including medial and lateral septal nuclei, anterior and posterior hypothalamic areas and anterior thalamic nuclei (see Gloor (1997){} for further details). It should be emphasised that fornix fibres are both afferent and efferent to the hippocampal formation, and therefore represent sub-cortical input to, and output from, the hippocampal formation.

Hippocampal Formation Connectivity: Introduction

The diagram in Figure 1.3 illustrates the major connections of the parahippocampal-hippocampal regions. The entorhinal cortex has a crucial position in the hippocampal-parahippocampal network, in that it forms the gateway through which most neo-cortical input reaches the hippocampal formation. Cortical afferents reach the hippocampal formation through the entorhinal cortex, both directly or channelled through peri- and postrhinal cortices. The hippocampal formation also receives substantial sub-cortical input. Some sub-cortical afferents directly innervate the hippocampal formation (medial septum, basal nucleus of the amygdala, midline thalamic nuclei, hypothalamic nuclei, and brainstem nuclei), while others (dorsal thalamic nuclei) are channelled through pre- and parasubicular cortices.

The entorhinal cortex gives rise to the "perforant pathway" to the hippocampal formation, which can be subdivided into two major streams:

1) originating from layer II of entorhinal cortex and innervating DG and CA3;
2) originating from layer III of entorhinal cortex and innervating CA1 and subiculum.

Figure 1.3

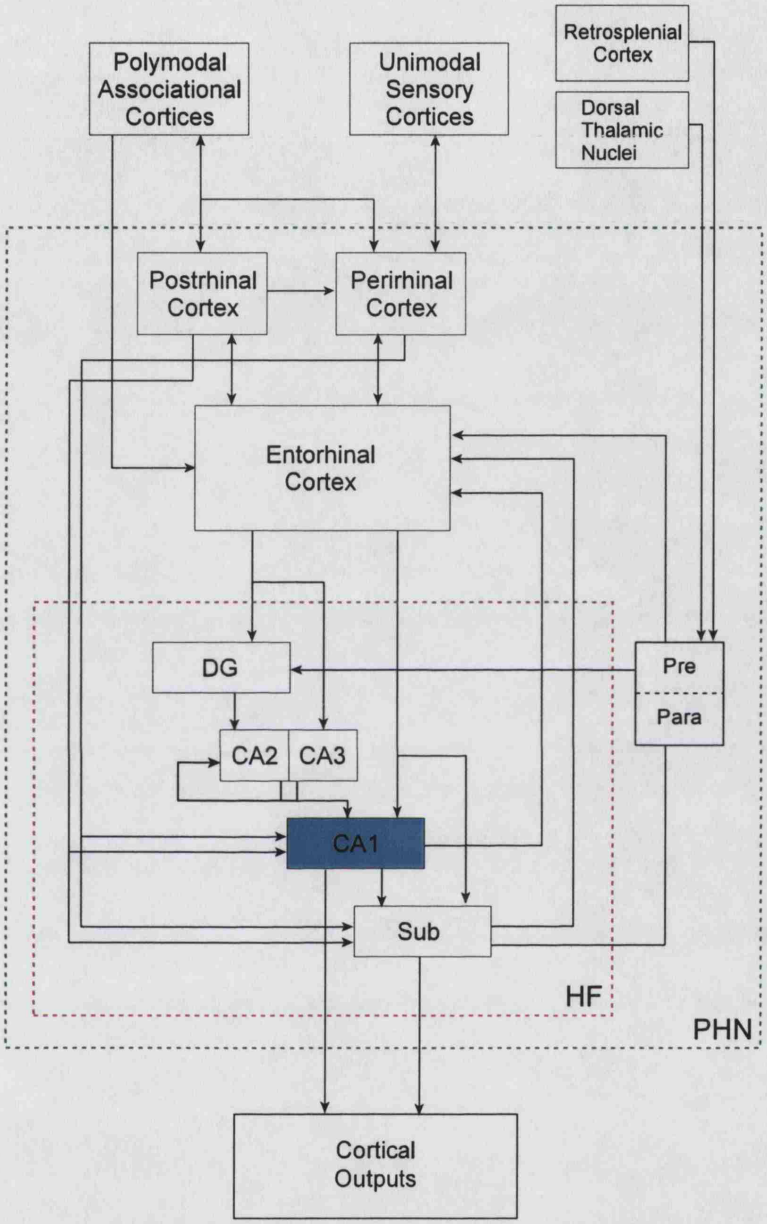

Figure 1.4. Diagram showing the internal connections of the hippocampal-parahippocampal regions, plus cortical input and output to these regions. The dashed boxes demarcate the hippocampal formation (HF, red box) and the parahippocampal network (PHN, green box). For details of cortical outputs of subiculum and CA1, see main text. All place cells in this thesis were recorded from CA1, blue.

The main intrinsic connections of the hippocampal formation are:

1) mossy fibre projection from dentate gyrus to CA3;
2) CA3/CA2 to CA3/CA2 recurrent collaterals;
3) Schaffer collaterals, from CA3/CA2 to CA1;
4) Projections from CA1 to subiculum.

The output from the hippocampal formation originates in three fields; the subiculum, CA1 and CA3. The subiculum projects to a number of cortical and sub-cortical regions, and, in the parahippocampal region, to the deep layers of entorhinal cortex, perirhinal cortex, pre- and parasubiculum. CA1 field also projects to deep layers of the parahippocampal region, and to a number of neo-cortical and sub-cortical regions, although not as strongly as the subiculum. The only major output from CA3 targets the lateral septum.

The Fields of the Hippocampal Formation

This section will review the anatomy of each of the fields of the hippocampal formation. In this discussion, the terms 'intrinsic' and 'extrinsic' will be taken to mean 'intrinsic to the hippocampal formation' and 'extrinsic to the hippocampal formation'.

Dentate Gyrus

Lamination and Cell Types

The dentate gyrus comprises three layers: the molecular, granule and polymorph layer. Closest to the hippocampal fissure is the molecular layer, with few cells. Deeper to this lies the granular layer, a densely-packed cellular layer. The deepest layer is polymorphic layer, which contains a variety of cell types.

The principle cell type of the granular layer is the granule cell. The packing density of granule cells is relatively high: it is estimated that, in the rat, there are around $0.6x10^6$ to $2.2x10^6$ granule cells (Amaral *et al*, 1990). One very interesting feature of granule cells is that they continue to proliferate well into adult life (Bayer, 1982; Bayer *et al*, 1982).

Just deep to the granular layer is a morphologically heterogeneous population of cells (including 'basket' cells) most of which are GABA-ergic, and appear to be inhibitory interneurones (Ribak & Seress, 1983; Seress & Ribak, 1983, Freund & Buzsaki, 1996 for a review). The most prominent cell type of polymorphic layer is the mossy cell. These cells are glutamatergic, receive inputs from granule cell axons, and give rise to fibres projecting back to the granule cell layer (Ribak *et al*, 1985; Frotscher *et al*, 1991; for projections, see below).

Intrinsic Inputs/Outputs

The main intrinsic input to the dentate is the associational/commissural input from the dentate gyrus itself, in the form of the feedback projection from mossy cells to granule cells, originating both contra- and ipsilaterally (Blackstad, 1956; Laurberg & Sorenson, 1981; Swanson *et al*, 1978; 1981).

In addition to this, some collaterals from CA3 and CA2 axons terminate in the polymorphic layer (Ishizuka *et al*, 1990; Li *et al*, 1994). These connections form the only exception to the rule of uni-directional excitatory projections between fields of the hippocampal formation.

There is one intrinsic output, the mossy fibre projection to CA3, which will be discussed in the CA3 section, below.

Extrinsic Inputs

Almost all cortical input to the dentate gyrus originates in the entorhinal cortex. The nature of these inputs will be discussed in the section on the entorhinal cortex, below. One exception is that the dentate gyrus also receives a dense projection from the parasubiculum (Kohler, 1985).

The dentate gyrus receives sub-cortical afferents from several different regions. In common with all other fields of the hippocampal formation, there is a

substantial projection from the septal region. This originates from the medial septal nucleus and the vertical limb of the diagonal band of Broca, and the fibres of this projection (travelling mainly via the fornix) terminate throughout the hippocampal formation (Daitz & Powell, 1954; Mosko *et al*, 1973; Swanson, 1978{}; Amaral & Kurz, 1985). Of the septal cells that contribute to this input, approximately half are cholinergic (Lewis & Shute, 1967; Amaral & Kurz, 1985; Wainer *et al*, 1985) and of the others, many are GABA-ergic (Kohler *et al*, 1984). GABA-ergic septal cells terminate preferentially on the GABA-ergic interneurones of the dentate (Freund & Antal, 1988).

Brainstem afferents to the dentate gyrus consist of; a) noradrenergic projections, from the nucleus locus coeruleus, mainly to the polymorphic layer (Swanson & Hartman, 1975; Haring & Davis, 1983), b) serotonergic projections, from the raphe nuclei to the polymorphic layer (Conrad *et al*, 1974), and c) weak and diffuse dopaminergic projections from the ventral tegmental area to the polymorphic layer (Swanson, 1982).

The dentate gyrus also receives hypothalamic afferents, the major projection being from the supramammillary nuclei. This projection terminates in a narrow zone just superficial to the granule layer (Segal & Landis, 1974; Haglund *et al*, 1984).

Extrinsic Outputs

The dentate gyrus makes no projections extrinsic to the hippocampal formation.

CA3

Lamination and Cell Types

The principle cell layer of CA3 (and of all CA fields) is called the pyramidal cell layer. Deep to the pyramidal cell layer is a narrow cell-free layer, *stratum oriens*, and deep to this is the fibre-containing alveus. Just superficial to the pyramidal cell layer, in CA3, is *stratum lucidum*, occupied by mossy fibre axons projecting from the dentate granule layer. Superficial to this is *stratum radiatum*, in which CA3-CA3

projections are located. Finally, the most superficial layer is *stratum lacunosum-moleculare*.

The principle cell type of all CA fields is the pyramidal cell. CA pyramidal cells have a basal dendritic tree that extends into *stratum oriens*, and an apical dendritic tree that extends to *stratum lacunosum-moleculare*.

There are several types of non-pyramidal cell throughout all CA fields of the hippocampus, the vast majority of these being immuno-reactive for markers of GABA (Ribak *et al*, 1978), and therefore presumed to be inhibitory interneurones. These cells have been classified on the basis of target specificity, morphology, stratification and expression of molecular markers (for a review, see Freund & Buzsaki, 1996). Principle types include axo-axonic cells (whose axons innervate the initial segment of pyramidal cell axons), basket cells (whose axons form 'basket' plexuses around pyramidal cell bodies), bistratified cells (whose axonal plexuses run through *stratum oriens* and *stratum radiatum*) and O-LM cells (so-called because their cell body lies in *stratum oriens*, while their axonal terminals lie in *stratum lacunosum-moleculare*). In a recent review, Somogyi & Klausberger (2005) further classified CA1 interneurones in at least 16 different types. Each of these classes of interneurones may play a specific role in hippocampal physiology (see chapter 2).

Intrinsic Inputs/Outputs

The intrinsic input to CA3 is the mossy fibre projection. This projection consists of un-myelinated axon fibres, arising in the granule layer and making synaptic contacts with CA3 pyramidal cells at the level of *stratum lucidum*. A single mossy fibre can make up to 37 contacts with a single CA3 pyramidal cell (Chicurel & Harris, 1992), at characteristic 'thorny excrescence' synaptic processes. This, combined with location of the synapses (proximal to the cell body) may give mossy fibres a powerful influence over CA3 pyramidal cell activity. It is estimated that each granule cell will, therefore, influence 14-28 pyramidal cells, while each CA3 pyramidal cell receives contact from around 50 granule cells (Claiborne *et al*, 1986). The mossy fibre projection to CA3 therefore represents a relatively sparse projection (summarised in Amaral *et al*, 1990).

One major intrinsic output of CA3 is the associational/commissural projection, to CA3 itself. A striking feature of the CA3 hippocampal field is its extensive

associational projections. A crucial feature of this associational network is that the recurrent collaterals of CA3 pyramidal cells are highly divergently distributed along the hippocampal septo-temporal axis (Ishizuka *et al*, 1990; Li *et al*, 1994). In the rat (but not in primates), there is also a similarly widespread commissural projection to the contra-lateral CA3 (Blackstad, 1956; Amaral *et al*, 1984). Swanson *et al* (1980) showed that one CA3 cell can give rise to both associational and commissural projections. This organisation means that the CA3 system can be viewed functionally as a single network, within which each CA3 pyramidal cell can transmit information to every other pyramidal cell within a small number of synaptic steps.

The other major intrinsic output is the projection from CA3 to CA1, referred to as the Schaffer collaterals. Schaffer collateral axons terminate, both ipsi- and contra-laterally, on the basal (*stratum oriens*) and apical (*stratum radiatum*) dendrites of CA1 pyramidal cells. There is a complex topographical organisation to the projection (see Ishizuka *et al* (1990) for details). An important point, though, is that projections spread broadly from the cell of origin, in both the transverse and septo-temporal axes.

Extrinsic Inputs

As with the dentate gyrus, the only cortical input to CA3 is from the entorhinal cortex, and will be discussed below.

The major sub-cortical afferent to CA3 is from the medial septum. Similarly to the septal afferents of the dentate gyrus, this projection arises in the medial septal nucleus and the vertical limb of the diagonal band of Broca. It terminates mainly in *stratum oriens*, but also in *stratum radiatum* (Gaykema *et al*, 1990). As in the dentate, GABA-ergic septal cells terminate preferentially on GABA-ergic interneurones, in all CA fields, including CA3 (Freund & Antal, 1988).

Brainstem inputs to CA3 consist of; a) noradrenergic afferents from the nucleus locus coeruleus, terminating in *stratum lucidum* and *stratum lacunosum-moleculare*, and b) a weak, diffusely terminating serotonergic projection from the raphe nuclei (Swanson *et al*, 1987){}.

There is also a projection from the amygdala to CA3, from the parvicellular division of the basal nucleus (Pikkarainen *et al*, 1999).

Extrinsic Outputs

The only extrinsic output of CA3 is to the lateral septal nucleus (Swanson & Cowan, 1977). This projection originates from both pyramidal and non-pyramidal (GABA-ergic) CA3 cells (Toth & Freund, 1992) and runs, via the fornix, to terminate in both the ipsi- and contra-lateral lateral septal nuclei.

CA2

Lamination and Cell Types

CA2 is a thin strip of the hippocampus, lying between CA3 and CA1. Traditionally, CA2 has been defined as the hippocampal region which, like CA3, contains large pyramidal cells, but, unlike CA3, receives no mossy fibre input from the dentate gyrus. CA2 pyramidal cells therefore lack the 'thorny excrescences' characteristic of mossy fibre termination sites. The laminar organisation of CA2 is the same as that of CA3, apart from the lack of a *stratum lucidum* layer (Lorente de No, 1934; Tamamaki *et al*, 1988; Ishizuka *et al*, 1995).

In addition, a number of recent studies have observed differential immuno-histochemical staining of CA3 and CA2. For example, CA2 shows a denser staining for the calcium-binding protein parvalbumin (Sloviter *et al*, 1991; Leranth & Ribak, 1991[primates]). Fibroblast growth factor 2 (Williams *et al*, 1996), adenosine A1 receptor (Ochiishi *et al*, 1999), and epidermal growth factor receptor (Tucker *et al*, 1993) are, within hippocampal pyramidal cells, uniquely expressed in CA2. Lein *et al* (2005) described the differential expression of a range of mRNAs, which, collectively, gave genetic definitions of the fields of the hippocampal formation. This study also demonstrated a clear distinction between CA2 and other hippocampal areas.

Intrinsic Inputs/Outputs

As mentioned above, CA2 does not receive mossy fibre inputs from the dentate gyrus. Otherwise, the intrinsic connections of CA2 are similar to those of CA3. CA2 cells send projections to ipsi- and contra-lateral CA1 and CA3, and there is an associational/commissural projection to ipsi- and contra-lateral CA2 (Tamamaki *et al*, 1988; Ishizuka *et al*, 1990). CA3 and CA2 projections can be differentiated, however. CA2 fibres are thinner, more sparsely distributed, and show less topographic organisation than those originating in CA3 (Ishizuka *et al*, 1990).

Extrinsic Inputs/Outputs

In general, CA2 shares the extrinsic inputs and outputs of CA3. One notable exception is that, unlike CA3, CA2 receives hypothalamic afferents, in particular from the supramammillary area (Haglund *et al*, 1984) (similarly to the dentate gyrus) and from the tuberomammillary nucleus (Kohler *et al*, 1985).

CA1

Lamination and Cell Types

CA1 largely shares the cell types (pyramidal and non-pyramidal) of CA3 and CA2 fields. (Originally being differentiated on the basis of the smaller size of CA1 pyramidal cell bodies (Ramon y Cajal, 1911; Lorente de No, 1934)). Like CA2, CA1 receives no dentate gyrus afferents, and therefore has no *stratum lucidum.*

Intrinsic Inputs/Outputs

The intrinsic input to CA1 is the Schaffer collaterals of CA3/CA2, described above. There is no input from the dentate gyrus.

CA1 pyramidal cells give rise to one prominent intrinsic projection, which is to the subiculum. This projection is highly topographically organised, in a columnar fashion. CA1 cells located proximally (closest to CA3, along the transverse axis)

project to the distal-most third of the subiculum (closest to the presubiculum), throughout the radial extent of the subiculum, while cells located distally in CA1 project into the proximal portion of the subiculum. Projections terminate at approximately the same septo-temporal level as CA1 cells of origin, over roughly one third of the septo-temporal extent of the subiculum (Tamamaki *et al*, 1987; Amaral *et al*, 1991).

There is a weak associational and commissural CA1-CA1 connection. There are a small number of projections to contra- and ipsilateral CA1, but far fewer than in CA3/CA2 (Tamamaki *et al*, 1987; Van Groen & Wyss, 1990c; Amaral *et al*, 1991).

Extrinsic Inputs

As well as cortical input via the perforant pathway, CA1 (in common with the subiculum) receives direct input from the peri- and postrhinal cortices. In CA1, the projection from the perirhinal cortex is much denser than that from the postrhinal cortex (Suzuki & Amaral, 1990[primates]; Witter *et al*, 2000).

Sub-cortical inputs to CA1 include the medial septal afferents already described for other fields, although this projection is somewhat lighter to CA1 than to other areas (Nyakas *et al*, 1987).

CA1 receives a projection from the amygdala, originating in a greater number of amygdaloid nuclei than that to CA3. These fibres originate in the lateral, basal, and accessory basal nuclei, and terminate in different CA1 layers, depending on the site of origin (Pikkarainen *et al*, 1999). Unlike CA3, CA1 receives a projection from the thalamus, specifically the small, midline nucleus reuniens (Dolleman-Van der Weel & Witter, 1996).

Extrinsic Outputs

CA1 and the subiculum are the only fields of the hippocampal formation that give rise to cortical efferents. Much of the output of CA1 is similar to that of the subiculum (see below). In particular, prominent targets of CA1 cortical efferents (excluding those to the parahippocampal region) are retrosplenial cortex and the medial prefrontal cortex (Van Groen & Wyss, 1990c). CA1 also projects to parahippocampal cortex: to the deep layers of the entorhinal cortex, predominantly

layer V, and to the perirhinal cortex (Swanson & Cowan, 1977; Van Groen & Wyss, 1990c). CA1 (along with the subiculum), therefore, gives rise to 'loop-back' projections, terminating in parahippocampal areas that form the main sites of cortical input to the hippocampal formation.

CA1 also gives rise to several prominent sub-cortical projections, in addition to the lateral septum efferents already described for CA3. These terminate in the anterior olfactory nucleus, the olfactory bulb, the nucleus accumbens, the basal nucleus of the amygdala and the anterior and dorso-medial hypothalamus (Van Groen & Wyss, 1990c).

Subiculum

Lamination and Cell Types

The CA1/subiculum boundary is marked by an abrupt widening of the pyramidal cell layer. *Stratum oriens* of CA1 disappears, and *stratum radiatum/stratum lacunosum-moleculare* are replaced by the subiculum molecular layer. Each of these subicular layers appear cyto-architectonically homogeneous. The pyramidal cell layer contains many smaller neurones, presumably the interneurones of the subiculum (Swanson *et al*, 1987{}; Amaral & Witter, 1995{}).

Intrinsic Inputs/Outputs

The intrinsic input to the subiculum is represented only by afferents from CA1, described above. There are no subicular efferents intrinsic to the hippocampal formation.

Extrinsic Inputs

The only cortical afferents to the subiculum arise in the parahippocampal cortices. In addition to perforant path input from the entorhinal cortex, the subiculum also receives direct input from perirhinal and postrhinal cortices. Unlike CA1, the

strength of projections from these two areas are roughly equal (Naber *et al*, 1999; Witter *et al*, 2000; Naber *et al*, 2001).

In general, the subiculum shares the same sub-cortical afferents as those already described for other hippocampal formation fields, and this section will briefly describe them. For a full review, see Swanson *et al* (1987){}, Lopes da Silva *et al* (1990). Projections from the septum (medial septal nucleus, diagonal band of Broca) terminate in the pyramidal and molecular layers (Nyakas *et al*, 1987). Thalamic afferents originate mainly in the nucleus reuniens (Wouterlood *et al*, 1990). There are dense projections from the supramammillary region of the hypothalamus (Haglund *et al*, 1984). Amygdaloid afferents arise in the basal nucleus, the posterior cortical nucleus and the amygdalohippocampal area (Krettek & Price, 1977; Canteras *et al*, 1992). However, monoaminergic projections from the brainstem to the subiculum are sparse.

Extrinsic Outputs

As emphasised in the introduction to hippocampal connectivity, the subiculum is one of the major output regions of the hippocampal formation, with both cortical and sub-cortical targets. Prominent projections of the subiculum include:

(Parahippocampal region):
a) pre- and parasubiculum
b) entorhinal cortex
c) perirhinal cortex

(Cortical):
d) portions of medial prefrontal cortex, particularly to the medial and ventral orbitofrontal cortices, and to the prelimbic and infralimbic cortices
e) retrosplenial cortex

(Sub-cortical)
f) lateral septum
g) medial anterior olfactory nucleus
h) nucleus accumbens, particularly its caudomedial part

i) ventromedial hypothalamic nucleus
j) medial mammillary nuclei (the lateral mammillary nucleus, important in generating the directional signal in anterior thalamus and presubiculum is only sparsely innervated by the subiculum)
k) medial thalamic nuclei, including nucleus reuniens and inter-anteromedial nucleus

(Amaral & Witter, 1995; Groenewegen *et al*, 1987; Naber & Witter, 1998; Witter *et al*, 1989; Witter & Groenewegen, 1990; Wyss & Van Groen, 1992).

The Parahippocampal Region

The following section will cover the anatomy of the parahippocampal region, but in less overall detail than that for the hippocampal formation. Rather, the emphasis will be on those aspects of parahippocampal anatomy important for understanding the hippocampal formation, with particular emphasis on the nature of the inputs to the hippocampal formation.

The following section will refer to the lateral entorhinal area (LEA) and the medial entorhinal area (MEA). These are cyto-architectonically defined regions of the entorhinal cortex. Briefly, LEA has a more clearly demarcated layer II, as compared to MEA, and LEA layer II cells are smaller, more densely packed and clustered into islands (see Amaral & Witter, 1995 for further details). They are also differentiated in terms of their inputs and outputs, and are therefore relevant to the discussion below.

Cortical Afferents to the Entorhinal Cortex

The entorhinal cortex occupies a pivotal position in the parahippocampal-hippocampal circuit. It channels cortical inputs from the perirhinal and postrhinal cortices, and gives rise to most of the cortical input into the hippocampal formation via the perforant pathway. The origin of entorhinal cortex afferents is therefore crucial for understanding the nature of input to the hippocampal formation.

Afferents to peri- and postrhinal cortex

Much of the entorhinal input to hippocampus comes via the postrhinal and perirhinal cortices. The peri- and postrhinal cortices receive most of their inputs from uni-modal and poly-modal neocortical association areas. Of the uni-modal input, particularly prominent efferents are olfactory (originating in piriform cortex) and visual. Visuo-spatial input, originating in the retrosplenial, cingulate, and posterior parietal cortices, also forms a robust projection (Burwell & Amaral, 1998a). There is some differentiation between peri- and postrhinal cortices: postrhinal cortex receives stronger visual and visuo-spatial inputs, whereas perirhinal cortex receives a stronger projection from olfactory areas.

Afferents to entorhinal cortex

The entorhinal cortex also receives direct neocortical inputs. Similarly to peri- and postrhinal afferents, most projections are from uni-modal or poly-modal association areas. A particularly dense projection is from the piriform cortex (Burwell & Amaral, 1998a). There is a differentiation between inputs to MEA and LEA, with the MEA receiving a higher proportion of cortical afferents from visual or visuo-spatial areas (Burwell & Amaral, 1998a).

Projections from the peri- and postrhinal cortices also differentiate between MEA and LEA, with the postrhinal cortex sending more efferents to the MEA, and the perirhinal cortex preferentially projecting to the LEA (Burwell & Amaral, 1998b; Naber *et al*, 1997). The pattern of differentiation between MEA and LEA is therefore similar both for direct neocortical inputs to entorhinal cortex, and inputs via the peri- and postrhinal cortices.

Afferents from pre- and parasubiculum

An important sub-cortical input enters the hippocampal-parahippocampal network via the pre- and parasubiculum. These are afferents from dorsal thalamic nuclei, specifically the antero-dorsal, antero-ventral and latero-dorsal, which terminate in layers I, III and V of pre- and parasubiculum (Van Groen & Wyss, 1990a; 1990b; 1995). The functional significance of this projection is that cells which

code for the allocentric head direction of the animal have been found in dorsal thalamic nuclei (Taube, 1995). This input reaches the hippocampal formation mainly via the entorhinal cortex. Both pre- and parasubiculum send efferents to entorhinal cortex, presubicular efferents terminating in MEA layer III, and parasubicular efferents terminating in layer II of MEA and LEA (Caballero-Bleda & Witter, 1993; Kohler, 1985; Van Groen & Wyss, 1990a; Swanson & Cowan, 1977). There is also, however, a direct projection from parasubiculum to the dentate gyrus (Kohler, 1985).

It should also be noted that presubiculum receives projections form visuo-spatial neocortical areas, including retrosplenial cortex (Swanson & Cowan, 1977; Van Groen & Wyss, 1990a; 1990b) and visual area 18b (Vogt & Miller, 1983).

The Perforant Pathway: Entorhinal Efferents to the Hippocampal Formation

The perforant pathway is the major source of cortical afferents to the hippocampal formation. All fields of the hippocampal formation have a direct input from the perforant pathway. The organisation of the pathway is somewhat complex, however, it being possible to classify the projections according to three orthogonal divisions. These divisions, and the nature of the projections, will be briefly reviewed here.

Layer II projections vs. layer III projections

Fibres originating in layer II of the entorhinal cortex project to the dentate gyrus, CA3 and CA2. The projections to the dentate gyrus terminate in the most superficial two-thirds of the dentate molecular layer, mainly on granule cell dendrites, but also on some GABA-ergic cells (Nafstad, 1967; Zipp *et al*, 1989). Entorhinal layer II efferents to CA3/CA2 terminate in *stratum lacunosum-moleculare* (Nafstad, 1967; Steward & Scoville, 1976; Witter, 1993).

Projections originating in entorhinal layer III, by contrast, project to CA1 and the subiculum. As in CA3/CA2, projections to CA1 terminate in *stratum lacunosum-moleculare* (Steward & Scoville, 1976). Projections to the subiculum terminate in the molecular layer (Witter, 1993).

MEA projections vs. LEA projections

The perforant pathway can also be sub-divided on the basis of whether it originates in the MEA or the LEA. As discussed above, these cyto-architectonically defined regions of the entorhinal cortex receive input from different cortical areas, and may therefore carry different information.

Termination sites of layer II MEA and layer II LEA projections are segregated along the radial axis of their target areas. LEA originating fibres terminate in the outer-most third of the dentate molecular layer, while MEA originating fibres terminate in the middle third. Projections terminating in *stratum lacunosum-moleculare* of CA3 show a similar organisation (Steward, 1976; Witter, 1993). In the dentate and CA3/CA2, therefore, the same cells are likely to be influenced by both MEA and LEA inputs (McNaughton & Barnes, 1977). By contrast, MEA and LEA components of the layer III perforant path show a non-overlapping terminal distribution in CA1 and the subiculum, discriminating along the transverse axis. Projections from the MEA terminate in the proximal part of CA1 (that closest to CA3) and the distal part of the subiculum (that closest to the presubiculum), whereas fibres originating in the LEA terminate in the distal part of CA1 and the proximal part of the subiculum (Witter *et al*, 2000a).

If inputs from the MEA and LEA represent different types of information, therefore, it is apparent that these inputs are merged in the dentate and CA3/CA2, but remain distinct in CA1 and the subiculum (Witter *et al*, 2000b).

Projections to septal vs. temporal hippocampal formation

The entorhinal cortex can be further subdivided into three strips, on the basis of where perforant path fibres terminate along the septo-temporal axis of the hippocampal formation (Fyhn *et al*, 2004; Dolorfo & Amaral, 1998a; Witter *et al*, 1989; Ruth *et al*, 1988; Ruth *et al*, 1982). Each of these strips contains portions of both MEA and LEA (see Figure 1.4 for illustration).

Burwell (2000) reanalysed the data of Burwell & Amaral (1998a), looking at the origin of cortical afferents to these three bands of entorhinal cortex. It was found that, especially in the MEA, septally projecting bands received more visuo-spatial input, while temporally projecting bands received more olfactory inputs. This could,

Figure 1.4

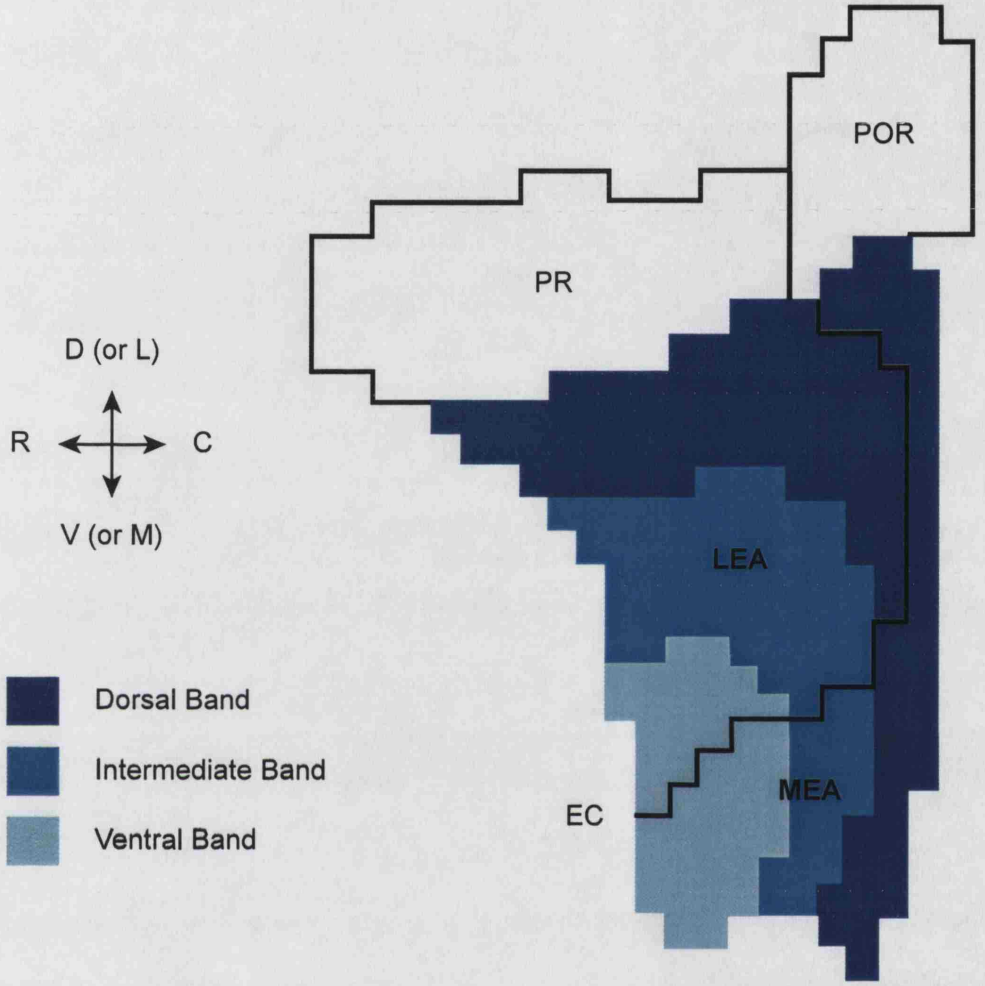

Figure 1.4. Diagram showing an unfolded map of the perirhinal (PR), postrhinal (POR) and entorhinal (EC, coloured) cortices. Black line within EC demarcates lateral entorhinal area (LEA) and medial entorhinal area (MEA). Shades of blue show the approximate location of the dorsal, intermediate and ventral dentate-projecting bands in the entorhinal cortex. Note that each band includes portions of both LEA and MEA. Adapted from Burwell & Amaral (1998a).

therefore, represent another functional differentiation in the perforant pathway, one which leads to the septal hippocampal formation receiving more visuo-spatial input than the temporal hippocampal formation.

Summary

Some important principles can be drawn from the anatomy of the hippocampal formation regarding its possible function.

First, a striking feature of the hippocampal formation is its pattern of serial connectivity between fields. The organisation of the perforant pathway also means that neocortical input reaches the hippocampal formation (with the exception of the dentate gyrus) by mono-synaptic and multi-synaptic routes simultaneously. This anatomical organisation therefore allows for both serial and parallel information processing. Furthermore, the anatomy allows for re-entrant information processing, both in the hippocampal outputs directed at the parahippocampal region, and in the CA3 recurrent collaterals.

Secondly, the neo-cortical inputs to the hippocampal formation originate in many different areas, mostly in association cortices, poly-modal and uni-modal. The hippocampus is therefore well placed to receive highly-processed, multi-modal sensory information. Interestingly, these inputs are channelled through a gateway, in the form of the rhinal cortices, from which the flow of information enters intra-hippocampal pathways described above.

Unlike cortical inputs, sub-cortical afferents directly innervate fields of the hippocampal formation. The information processing taking place in the hippocampus, therefore, can be directly influenced or controlled by sub-cortical structures, such as the septum, amygdala and thalamus, as well as by neuromodulatory inputs originating in the brainstem.

Finally, the output of the hippocampus is directed at many different areas, cortical and sub-cortical. The pattern of input and output described, spanning a large number of different brain structures, suggests that the hippocampal formation is most likely involved in general, abstract functions, for example memory or spatial cognition.

Chapter 2

Physiology of the Hippocampus

This chapter will briefly summarise physiological aspects of the hippocampus, concentrating on the different global EEG states found in the hippocampus. Various EEG states have been described in the hippocampus, with oscillations ranging in frequency from slow (7-12 Hz, theta), to fast (40-100 Hz, gamma), and ultra-fast (200 Hz, "ripples"). There is a basic distinction between two different functional states of the system, each correlating with a particular set of behaviours. Theta and gamma oscillations occur in the rat during voluntary activity, exploratory activity, alert attention and rapid eye movement sleep. In contrast, during immobility, consummatory behaviours, and slow-wave sleep, the hippocampus enters a state termed Large Irregular Activity (LIA: Vanderwolf, 1969).

Theta

Theta is characterised as a 5-12 Hz quasi-sinusoidal oscillation in various animals, including rats, cats, dogs, and rabbits. Recently, theta oscillations have also been observed in humans (Tesche, 1997; Kahana *et al*, 1999). In the rat, it can be recorded from several brain regions, including the hippocampal formation, the superficial layers of presubiculum and entorhinal cortex, septum, hypothalamic and brainstem nuclei.

On the basis of work primarily, but not exclusively, on the rat, Vanderwolf (1969; 1971) reported the following behavioural correlates of theta:

> walking, running straight ahead or backing up, turning, rearing, jumping, climbing, struggling when held, swimming, head movements, postural changes, manipulation (such as pressing a lever in a Skinner box), and digging in sawdust.

Vanderwolf originally interpreted these correlates as suggestive of voluntary motor activity and contrasted it with the automatic activity correlating with LIA-related behaviours. O'Keefe and Nadel (1978) reinterpreted the behaviours associated with theta as those which involve displacement of the rat. Theta is also associated with REM sleep in the rat. Theta can be associated with alert attention (for example in cats), but it has been a matter of debate whether theta can be associated with arousal in rats.

Mechanisms of theta generation

Theta generation appears to depend on three factors: 1) external control circuits in the medial septum/diagonal band of Broca complex (MS/DBB) and other areas; 2) network properties in the hippocampal formation; and 3) cells' intrinsic oscillatory properties.

Evidence for the importance of the MS/DBB comes from experiments in which the MS/DBB is inactivated, and hippocampal theta rhythm is completely lost (Mizumori *et al*, 1990; Lawson & Bland, 1993). It is likely that both cholinergic (muscarinic) and GABA-ergic projections from the MS/DBB are important. The MS/DBB is not the only important external region in controlling theta. Many other brain areas are implicated, among the most important of which are the posterior hypothalamus/supramammillary complex and the pons (Bland & Colom, 1993).

The idea that there might be intrinsic hippocampal generators of theta results from current density analysis of electrical activity in the hippocampus. A study by Buzsaki *et al* (1986), looking at current sink positions along the radial axis in CA1, proposed that hippocampal theta rhythm is the result of two inputs: one from the medial septum, and one from a theta generator in the entorhinal cortex. A later study by Brankack *et al* (1993) proposed that, in addition to the excitatory inputs from the entorhinal cortex, the excitatory connections between cells in the 'tri-synaptic loop' (the dentate gyrus to CA3 to CA1 pathway) also provide rhythmic inputs.

Evidence that hippocampal neurones act as oscillators comes from *in vitro* slice work. There is evidence that application of carbachol (a cholinergic agonist) to hippocampal slices induces membrane potential oscillations at theta frequencies in pyramidal cells in region CA1 (Bland *et al*, 1988) and CA3 (MacVicar & Tse, 1989).

However, how this relates to the situation in the intact animal is controversial. For instance, Bland *et al* (1975) found that carbachol infusion does not produce theta oscillation in CA3. Colom *et al* (1991) found that, in septal lesioned rats, both carbachol and bicuculline (a GABA antagonist) were necessary to produce theta frequency oscillations in CA1.

Hippocampal Cell Firing and Theta

The firing of cells throughout the hippocampal formation is modulated by the theta rhythm. Ranck (1973) subdivided extracellularly recorded hippocampal single units into two broad classes: 1) theta cells, which fire at high rates (10 Hz to > 30 Hz), have short action potentials (<0.35 ms), and fire single spikes in bursts, synchronous with theta; 2) complex spike cells, which fire at low rates (generally around 2 Hz and not greater than 30 Hz), have long duration action potentials (0.4-1.2 ms), and show complex spikes, i.e. bursts of two to ten spikes of decreasing amplitude and an inter-spike interval between 2 to 6 ms. The relationship between cell firing and theta, for both of these cell types, will be briefly discussed.

Theta Cells

Theta cells increase their firing rates in the presence of the hippocampal theta rhythm, and preferentially fire at the negative peak of the extra-cellularly recorded CA1 theta wave (Fox *et al*, 1986; Csicsvari, 1999). However, different theta cell units fire at varying times of the theta cycle (Skaggs *et al*, 1996). For example, unidentified putative interneurones, recorded from *stratum oriens* and the pyramidal cell layer of CA1, fire 60 and 20 degrees, respectively, before pyramidal cells during the theta cycle (Csicsvari *et al* 1999).

Recently, the relationship to theta of a subset of CA1 interneurones has been characterised in some detail (for a review, see Somogyi & Klausberger, 2005). Coupling intra- and extracellular recording with intracellular dye injection, Klausberger *et al* (2003; 2004) identified four classes of GABA-ergic interneurones within CA1, each displaying a characteristic pattern of firing with respect to theta. The highest firing probability of parvalbumin positive basket cells and axo-axonic

cells coincides with the peak of the theta wave recorded extracellularly from the CA1 pyramidal cell layer (Klausberger *et al*, 2003). This time corresponds to the highest degree of hyperpolarisation of pyramidal cells during each theta cycle. Basket cells and axo-axonic cells are therefore assumed to provide inhibitory inputs to the soma and the initial axonal segment, respectively, of pyramidal cells, and contribute to the hyperpolarisation of pyramidal cells at the peak of the theta wave.

OL-M cells and bistratified cells fire maximally in conjunction with the trough of the extracellularly recorded (pyramidal cell layer) theta. This coincides with the highest probability of pyramidal cell firing. The axons of OL-M cells and bistratified cells target the dendrites of pyramidal cells (the axonal terminals of OL-M cells preferentially target pyramidal apical dendrites, at the level of *stratum lacunosum-moleculare*, while bistratified cells contact both the apical and the basal dendrites, in *stratum radiatum* and *oriens* respectively). As both OL-M and bistratified cells are known to be GABA-ergic interneurones, it is surprising that these cells are most likely to fire at the same point in the theta cycle as CA1 pyramidal cells.

Complex-Spike Cells

Hippocampal complex spike cells (presumptive pyramidal cells) show an interesting relationship between their firing and the concurrent locally recorded theta oscillation, firing at progressively earlier phases of the theta wave, as the animal crosses the place field of the cell (O'Keefe & Recce, 1993, see Chapter 3 for details of place cells and place fields). This phenomenon, named phase shift, has since been observed in dentate gyrus and CA3 cells, with the precession occurring over more restricted phase ranges than that observed for CA1 cells (Skaggs *et al*, 1996).

O'Keefe and Recce (1993) proposed that the phase precession observed in CA1 was generated by two oscillators of slightly different periods converging onto the hippocampus. They also suggested a functional role for phase precession, postulating that hippocampal pyramidal neurones (place cells) might encode information in two independent ways: a rate code (rate of firing), and a time code (phase of theta oscillation at which firing occurs).

Two recent studies have proposed that phase shift does not represent independent time and rate codes. Harris *et al* (2002) claimed that the theta phase of pyramidal cell firing is best predicted by the instantaneous firing rate of the cell, and

therefore proposed that phase shift results from the dynamics of the spike train. Mehta *et al* (2002) reported that, during initial runs through the place field, place firing became more asymmetric (see Mehta *et al*, 2000, for details), and phase shift strengthened. They therefore proposed a causal link between these two phenomena. However, when Huxter *et al* (2003) looked at phase shift on sub-sections of the place field, and on individual runs through the place field, they found that the strongest correlation of phase shift was still the animal's position. They therefore maintained that place cells could represent position with independent rate and time codes.

Gamma

Buzsaki and colleagues have described gamma oscillations in the hippocampus of the awake, behaving rat (Bragin *et al*, 1995). Gamma oscillations occur during theta-associated behaviours (exploration, sniffing, REM sleep), and are nested to the concurrent theta waves, their frequencies span from 40-100 Hz and there is a high correlation between theta and gamma frequency shift. This suggests that similar mechanisms modulate the frequency of both gamma and theta rhythms. Gamma waves were seen most clearly in the dentate gyrus, where they were highly coherent. Average coherence decreased rapidly in CA3 and CA1 regions. Unlike theta, gamma oscillations persist after removal of all sub-cortical inputs to the hippocampal formation (Buzsaki *et al*, 1987), demonstrating that they are generated within the hippocampal circuits. Recorded theta cells (presumptive interneurones) in the dentate gyrus discharge at gamma frequency. These authors suggest that gamma oscillation emerges from an interaction between intrinsic oscillatory properties of interneurones and the network properties of the dentate gyrus. The function of gamma oscillations might be to synchronise the activity among of neurones within very short time windows (10-25 ms), complementing the role that theta waves have over longer time scales.

It has been demonstrated that gamma oscillations in the dentate gyrus can be elicited by the animal sniffing at an object, or by delivery of odours to the anaesthetised animal, but not by generalized sniffing in the air (Vanderwolf, 2001). Interestingly, beta oscillations (15-30Hz) in the dentate gyrus appear to be elicited specifically by predator-related odours (Heale *et al*, 1994). These results have

contributed to Vanderwolf (2001) proposing that the hippocampus is primarily an olfactory-motor mechanism.

Large Irregular Activity (LIA)

Sharp Waves

Vanderwolf (1969) used the term LIA to describe the large, irregular, slow waves in which the dominant frequency is slower than theta. In *stratum radiatum* of CA1 and the deep layers of the entorhinal cortex, LIA also produces sharp spikes of 40-100 ms duration and 1-3 mV amplitude (Chrobak & Buzsaki, 1994; O'Keefe & Nadel, 1978). Buzsaki and others refer to these EEG spikes as sharp waves. It is thought that CA1 sharp waves result from the excitation of the apical dendritic field of CA1 neurones by their CA3 Schaffer collateral input, due to a burst of activity in CA3. The sharp waves occur most frequently during slow-wave sleep and quiet sitting, less frequently during eating and drinking, and least of all during grooming; they are often inhibited by arousing stimuli, even when no movement occurs (O'Keefe & Nadel, 1978).

Ripples

The synchronous depolarisation of CA1 neurones and inhibitory interneurones results in a high frequency oscillation, the ripple, within and just superficial to the pyramidal cell layer of CA1. Ripples take the form of small sinusoidal wave bursts where each wave has a period in the range 4-8 ms, with about 4-10 waves in each burst.

The firing of both interneurones and pyramidal cells firing displays a clear relationship to the ripple oscillation. Pyramidal cells tend to fire a single action potential per ripple, phase locked to the troughs of the ripple oscillation (Chrobak & Buzsaki, 1996; Csicsvari *et al*, 1999).

Different populations of CA1 interneurones show different relationships to ripple events. Basket cells and bistratified cells both increase their discharge

frequency during the ripple event, whereas O-LM cells are specifically suppressed for the duration of the ripple. Axo-axonic cells increase their firing in the run-up the ripple episode, but are then silent after the highest amplitude ripple (Klausberger *et al*, 2003; 2004; Somogyi & Klausberger, 2005).

The mechanism by which this highly coherent discharge of pyramidal neurones is brought about along the whole extension of the dorsal CA1 region is still unknown. One hypothesis put forward recently assumes that the synchronisation of pyramidal cells is achieved through axo-axonic gap junctions. Ripple oscillations persist in the absence of chemical transmission, while inhibitors of gap junctions were shown to block ripple activity in hippocampal slices (Draguhn *et al*, 1998). Recently, (Bragin *et al*, 1999) ripple states have been described in the human.

Buzsaki (1989) has suggested a model of memory trace formation in the hippocampus in which the sharp waves, during rest or slow-wave sleep, play a major role in potentiating memory traces of information acquired during exploration (the theta state).

Chapter 3

Hippocampal Place Cells

Pyramidal cells in the CA1 and CA3 fields of the hippocampus will fire at relatively high rates only when the animal is in a specific portion of the environment (O'Keefe, 1976). This chapter will review some properties of these spatially specific cells (Place cells), and will also act as an introduction to the experimental findings of this thesis. It will therefore give emphasis to aspects of the place cell phenomenon relevant to the finding of this thesis: place cell remapping, and whether place cells constitute a coherent representation of space.

This thesis concentrates on spatial coding in the hippocampus. It should be noted, however, that other accounts of hippocampal function propose that spatial cognition is only one part of a more general role for the hippocampus in memory encoding and storage (see, for example, Cohen & Eichenbaum, 1993; Squire, 1987).

Basic Properties of Place Cells and Place Fields

The Place Field

The portion of the environment in which the place cell fires at a high rate is termed the place field of that cell. The shape of place fields can be approximated by a two-dimensional gaussian, though the exact shape of the field seems also to be influenced by the shape of the environment the animals are in. For instance, crescent shaped fields are often found in circular environments but are rare in square environments (Muller *et al*, 1987; O'Keefe & Burgess, 1996). It is also possible for a place cell to have two place fields in one environment (e.g. O'Keefe & Burgess, 1996). The firing rate of place cells depends on the parameters used in their quantification, but various methods of describing peak firing can show place fields with up to 30 Hz peaks. In contrast, the firing rate outside the field can approach 0 Hz.

Generally, in 'open' environments, place fields are not directional, i.e. the cell's firing is not affected by the animal's direction of travel (O'Keefe, 1976; Muller *et al*, 1987; Muller *et al*, 1994). In environments or tasks where rat traversals are spatially restricted, by environmental constraints (e.g. maze arms) or by reward-shaping, fields are often directional (McNaughton *et al*, 1983; O'Keefe & Recce, 1993; Markus *et al*, 1995). Directionality appears to emerge primarily in response to the animal moving along a spatially restricted path (Markus *et al*, 1995).

The multi-modal sensory basis of place fields

One hypothesis of the hippocampal cognitive map theory (O'Keefe, 1978) was that place field activity could be based on various different sensory modalities. Input necessary for spatial mapping, such as distance and orientation, could be obtained from several external (e.g. visual, somatosensory, olfactory, auditory) and internal systems (e.g. self-motion, proprioceptive, vestibular).

Early work by O'Keefe and others (O'Keefe & Dostrovsky, 1971; O'Keefe, 1976; O'Keefe & Conway, 1978) suggested that place cells could sustain firing by utilising many different types of sensory cues. Visual information alone is not necessary to produce place field firing, as place cells can continue to display place fields in the dark, in the same position as with the lights turned on (O'Keefe & Dostrovsky, 1971; O'Keefe, 1976). Further studies have also indicated that place field stability is greater if the lights are turned off whilst the animal is within the testing environment (Markus *et al*, 1994; Quirk *et al*, 1990). Non-visual information is capable of maintaining place fields when visual sensory input is removed, therefore, but visual input may be important for first establishing a place cell's spatial response. A study by Save *et al* (2000) showed that olfactory cues within the testing arena are crucial for maintaining place field firing in the dark. When the lights were turned off while the animal was in the testing arena, most cells showed stability of their place fields. If the floor was cleaned at the same time as the lights were turned off, most place fields were not stable.

Another approach to investigating the sensory basis of place cells firing is to completely and permanently remove a sensory modality from an animal. Hill and others (1979; reviewed in O'Keefe, 1979) attempted to eliminate entire sensory

modalities from rats, before undergoing place cell testing. Animals were blinded, or deafened, or had their vibrissae removed, or had their olfactory receptors destroyed. Place cells were found in all these animals, with no obvious differences from those found in normal rats. Place cells were also found in animals deprived of both vision and hearing (Hill & Best, 1981). Using quantitative approaches developed by Muller *et al* (1987) and Skaggs *et al* (1993){}, Save *et al* (1998) compared place cell firing in rats which were surgically blinded one week after birth with that of normal rats. No statistically significant differences were found except that the fields of blind rats were slightly more directional, and that blind rats' place cells had lower firing rates.

Place Field Emergence and Stability

Hill (1978) reported that initial fields (the first time an animal passes through the field) are indistinguishable from fields recorded later on, when the animal is familiar with the environment. This is in contrast with a study by Wilson & McNaughton (1993). To create novel and familiar environments, the authors used a rectangular box, with a partition dividing it into equal halves. Rats were trained in one half of the box for 10 days. On the first exposure to the other half, place fields took 6 to 10 minutes to be established, and these initial fields were not as stable as the ones recorded in the familiar half. Frank *et al* (2004) used previously unvisited arms of an 8-arm radial maze as a novel environment. This study found that place cells require 5-6 minutes to set up stable fields.

There is a general consensus that, once place fields are established, they are stable for as long as they can be recorded (providing sensory stimuli are kept constant). Thompson & Best (1990) recorded place cells with field positions that were stable for up to 153 days.

Head Direction Cells

In order to understand some properties of place cell firing, it is necessary to briefly describe another class of spatially selective cell, the head direction cells. The basic property of a head direction (HD) cell is that it fires maximally when the

animal's head is pointing in a given allocentric direction (Taube *et al*, 1990a; 1990b). Peak firing in the preferred direction (90-130° in width) is approximately 10-50 Hz, firing outside this approaches 0 Hz. In different environments, the preferred direction may change but the basic tuning properties remain. Several studies have shown that prominent cues, distal to the rat's current environment (e.g. large white card on the wall of the environment), can control the preferred direction of HD cells (e.g. Taube *et al*, 1990b; Taube, 1995). HD cells fire in every environment in which they are tested.

Since their discovery in the presubiculum (Ranck, 1984), HD cells have subsequently been found, among other areas, in the anterior-dorsal nuclei (ADN) of the thalamus (Taube, 1995), latero-dorsal nuclei (LDN) of the thalamus (Mizumori & Williams, 1993) and lateral mamillary nuclei (Stackman & Taube, 1998).

Angular Rotation of Place Fields and the Head Direction System

It has been clearly shown that place fields' angular location may be controlled by distal landmarks, for instance, a large white card either on the wall of the recording environment, or outside the environment. When the distal cues are rotated by a given amount, place fields can be observed to rotate both in unison and by a similar amount. Furthermore, simultaneously recorded place cells rotate in unison. (Jeffery *et al*, 1997; Jeffery and O'Keefe, 1999; Muller & Kubie, 1987; O'Keefe and Conway, 1978; O'Keefe and Speakman, 1987).

Cues placed distally to the environment are more likely to exert this form of control over the place fields. For instance, a set of distinct objects placed in a circular arena will only control field location when placed next to the wall of the environment (Cressant *et al* 1997; Cressant *et al*, 1999). However, local, intra-recording environment cues may control place fields under some conditions. Evidence for this in CA1 cells is disputed, but seems clearer for CA3 (see below).

When place cells and HD cells have been simultaneously recorded in this type of cue-control experiment, their signals have been shown to be strongly coupled (Knierim *et al*, 1995; 1998). Current indications are that the head direction system controls the hippocampal place system, rather than visa versa. In animals with complete dorsal hippocampal lesions it is still possible to record HD cells from the

presubiculum and ADN (Golob & Taube, 1997; 1999). The properties of these HD cells are very similar to those recorded from control animals. The converse is not true. Calton *et al* (2003) showed that lesions of the dorsal presubiculum and ADN degraded the spatial selectivity of hippocampal place cells, and also made their signal more directional. Dorsal presubicular lesions, in particular, disrupted cue control over angular position of place fields. Mizumori *et al* (1994) reversibly inactivated the LDN, showing a disruption of both hippocampal place fields and behavioural accuracy on a spatial memory task (radial arm maze).

In conclusion, therefore, cue-control over angular position of place cells may reflect cue-control of head direction cells, which in turn control the directional bearing of the place cell representation.

Place Cells in Different Regions of the Hippocampal Formation

This review has so far focused on the pyramidal cells of the hippocampal CA1 and CA3 sub-fields. However, spatial firing correlates are found throughout the hippocampal formation. As one theme of this thesis is how anatomical connections may create functional networks, it is worthwhile to review briefly the nature of the spatial signal in different parts of the hippocampus.

Entorhinal Cortex

The entorhinal cortex represents one of the major input structures to the hippocampal formation. Quirk *et al* (1992) recorded cells in the superficial layers of the medial entorhinal cortex (MEC). They found that entorhinal cell firing was spatially restricted, though entorhinal place fields were larger and less reliable than CA1 fields. Frank *et al* (2000) also found cells with similar properties in the superficial MEC. Deep layer MEC units were found to have place fields with size and spatial selectivity intermediate between superficial MEC and CA1 cells.

However, a recent study has shown a strongly spatially selective signal in the entorhinal cortex (Fyhn *et al*, 2004a). Cells were recorded in the dorsolateral band of the entorhinal cortex, which projects to more dorsal areas of the hippocampal formation (see Chapter 1). Cells in this area showed sharp and coherent place fields,

with nearly all cells displaying many small fields that were stable across recording sessions. Hafting *et al* (2005) demonstrated that these cells ('grid cells') are active whenever the animal's position coincides with the corners of a regular grid of equilateral triangles, spanning the surface of the environment. Grid cells are an interesting finding, as they show that highly spatially selective cell firing is not unique to the hippocampal formation, and their pattern of firing is suggestive of a path-integration based map of the environment.

Dentate gyrus

Due to the technical difficulties in identifying dentate gyrus granule cells, few studies have looked at the physiological correlates of these cells (Jung *et al*, 1993; Gothard *et al*, 2001). They tend to discharge at relatively low firing rates (mean rates below 0.5 Hz). They show stable place fields on the 8-arm maze and the fields appear to be as directional as CA1 fields under similar conditions. Granule cell place fields are somewhat smaller than those of CA1 cells and a higher proportion of granule cells show multiple sub-fields.

The Hippocampus Formation: Dorsal vs. Ventral

The anatomy of the hippocampal formation suggests that the septal pole of the hippocampus receives more visuo-spatial sensory input than the temporal pole (see Chapter 1). Jung *et al* (1994) recorded from dorsal and ventral CA1 cells, and found significant differences in several measures of spatial coding. Dorsal CA1 cells had more spatial information content per spike, higher spatial information rates, greater sparsity, and smaller place fields than ventral CA1 cells. It must be pointed out, however, that Poucet *et al* (1994) reported no differences in the size and shape of fields from dorsal and ventral sites.

Differences between CA1 and CA3

Olton, (1978) and Muller *et al*, (1987) found that place fields of CA3 cells were indistinguishable from those in CA1. However, some authors have shown that CA3 fields have higher spatial specificity (Barnes *et al*, 1990; Markus *et al*, 1995) and higher information content and greater spatial stability (Mizumori *et al*, 1999) than

CA1 fields. Further comparative studies of CA1-CA3 have concerned the way in which place cells change their firing in response to changes in the environment, a phenomenon known as 'remapping'. These studies will be dealt with in a later section.

Subiculum

The subiculum is the main output structure of the hippocampal formation. Subicular neurones have significantly larger place fields than those in CA1 (Sharp, 1994). Spatial coherence is higher, field size smaller, and overall rate lower in the distal, as opposed to proximal, subiculum. Unlike entorhinal and hippocampal cells, subicular cells show a weak directional signal, even when recorded in an open environment.

Investigating the Role of the Parallel Perforant Pathway Inputs

CA1 receives input along two parallel pathways. The 'tri-synaptic' pathway (Entorhinal > Dentate Gyrus > CA3 > CA1) was traditionally considered the main route for information processing in the hippocampus. However, there are also direct connections from Entorhinal Cortex to CA3 and to CA1 (see Chapter 1). What are the functional contributions of these different pathways to place cell firing?

McNaughton *et al* (1989) used colchicine to destroy selectively at least 75% of dentate gyrus granule cells. They found, however, little effect on the spatial selectivity of CA1 place cells (recorded on an 8-arm radial maze). The authors conclude that direct projections from the entorhinal cortex to CA3 and CA1 are capable of maintaining place field firing. Interestingly, however, there was a dissociation between place cell firing and behaviour: learning on a spatial forced-choice behavioural task was severely impaired.

Brun *et al* (2002) disconnected the tri-synaptic pathway using two different methods (selective lesion of CA3 pyramidal cells and knife cuts through the Schaffer collaterals). In both cases, the authors were able to record CA1 cells with normal place fields. Place fields in the disconnection animals were the same size as in the normal animals, and as stable over one hour and 24-hour periods. The only

differences were that the fields in the disconnection animals were less sharp, and had lower peak rates. A behavioural deficit was also found in the disconnection animals, though only in some tasks. Performance was impaired on the open field water maze task, but not on the annular maze version of the task.

Input via the tri-synaptic pathway, therefore, is not the sole route through the hippocampus for spatial information. Direct input from the entorhinal cortex is sufficient to drive spatially selective firing in CA1. Further study is required to understand what (if any) are the differences between an entorhinal-only place representation and a normal one, and what behavioural deficits are induced by these manipulations.

Place Cells and Remapping

Early studies of place cells demonstrated that place cells fire differently in different recording environments. It is also possible for place cells to display different fields even when the animal is in the same absolute position in space (relative to the laboratory), if the stimuli available to the animal, or the behaviour of the animal, are different. The phenomenon of place cells changing their firing fields in response to changing stimuli or behaviour has become known as 'remapping'.

'Complete' Remapping: Switching Between Place Representations

O'Keefe & Conway (1978) looked at fields of place cells in two different recording environments: a small raised platform open to the laboratory, and a 3-arm maze curtained-off from any uncontrolled visual cues. The position of a place field in one environment did not predict the position in the other. Furthermore, a place cell with a field in one environment might not have a firing field at all in the other. Kubie & Ranck (1983){} showed that place cells could change their firing fields unpredictably (including turning off altogether) even when the different environments (8-arm radial maze, operant chamber, home cage) were in the same absolute position in the laboratory and common distal visual cues were available in all of them.

From these studies, however, it is was not possible to say whether the changes in place cell firing were due to changes in the stimuli available, the behaviour of the animals, or both. In order to address this problem, Muller and colleagues (Muller *et al*, 1987; Muller & Kubie, 1987) designed an apparatus in which rat behaviour was held constant while stimuli were changed. Rats were trained to forage for food pellets scattered randomly over the floor of a recording environment approximately 1 m^2. Curtains were used to isolate the rat from all visual cues except the walls of the recording environments. The environments were either circular or rectangular, coloured grey, 50 cm high and included a white card across one quarter of their inner wall, to act as a constant directional reference. All environments were in the same position in the laboratory. Under these conditions, place cells fields in the circular environment did not predict fields in the rectangular environment (Muller & Kubie, 1987). Of a sample of 22 CA1 place cells, 12 had fields in only one environment and 9 had fields in both that could not be related by any 'simple' (rotational or radial) transformation. Changing the geometry of the enclosure walls therefore seemed to produce an 'all-or-none' switch in the responses of place cells, with almost all cells changing their place response in an unpredictable way. This basic finding became known as 'remapping' (Bostock *et al*, 1991; Muller, 1996), and was further replicated by other studies (Quirk *et al*, 1992; Sharp *et al*, 1997).

To investigate which cells fire in any environment, Thompson & Best (1989) recorded from CA1, first with the animals under barbiturate anaesthesia, to activate maximally pyramidal cells (pentobarbital, at low doses, inhibits theta cell activity, and may therefore reduce postsynaptic inhibition of pyramidal cells), then in three different recording environments (though behaviour was not controlled across environments). The distribution of place field occurrence across the different environments implied that an independent population, or active subset, of cells was active in each environment. A more recent study used RNA imaging to address the same question (Guzowski *et al*, 1999). This technique assesses neurone activity by looking for the presence of activity-dependent Immediate Early Gene mRNA (in this study, *Arc* and *zif268*) in hippocampal pyramidal cells. As *Arc* mRNA shows time-dependent changes in its intra-cellular distribution after cell activity (moving from nucleus to cell body to dendritic processes), cells which were active at different times can be distinguished. It is therefore possible to examine which pyramidal cells are active in two different environments. Using these methods, the authors came to

similar conclusions as Thompson & Best (1989): that independent subsets of CA1 pyramidal cells were active in each different environment.

Bostock *et al* (1991) investigated the time-course of remapping after changing the environment. The basic set-up was as for Muller & Kubie (1987), but the stimulus manipulation was to replace the white cue card with a black one. This experiment was repeated for several days. Cells were classified as either rotated (probably due to the disturbance caused to the head direction system by manipulating the cue card: see above) or remapped. Different responses were seen in different rats. In the majority of animals, cells were not remapped (rotated only) on the first day of the manipulation, but were remapped on subsequent days. Other rats had remapped cells on Day 1, whilst others still showed no remapped cells even after 5 days of stimulus manipulation. Once remapped cells were observed in any given animal, only remapped cells were observed from that point onwards. The process of place cell remapping therefore entails a learning process, with the time course of that learning being different in different animals. The authors also claimed that their results supported an 'all-or-none' model of remapping, as no remapped and non-remapped cell were ever simultaneously recorded. While this is true, the fact that no more than two cells were recorded together does not allow strong conclusions to be drawn.

These studies therefore produced the concept of 'complete' remapping. If a sufficiently large manipulation were made to stimuli, place cells would change their fields in an entirely unpredictable way, including ceasing to fire. Though this change may take some time to occur, when it happened it would be all-or-none, and would correspond to a different active subset of cells representing that environment.

'Partial' Remapping

The 'complete' model of remapping was challenged by several studies. Skaggs & McNaughton (1998) recorded CA1 place cells in two visually identical environments connected by a corridor, through which the rat walked between them. When place fields in the two boxes were compared, cells were fairly evenly split into those which had similar fields, and those whose fields were completely different. There was, therefore, 'partial' remapping between environments. Swapping the physical boxes controlled for cues on the walls of the boxes. During training, rats

were always placed first into the same box. When rats were then introduced first into the opposite box, place cell responses were based on the box rats expected to be in, not the one in which they were. In this case, remapping could have been produced by two simultaneously active representations of space: one for within the box, and one large-scale, encompassing both boxes. In order to determine its position on this large-scale map, the animal used path integration, and the expectation of which box it would be placed in first.

In contrast to previous studies, Lever *et al* (2002) found no remapping between square and circular environments on initial exposure (c.f. Muller & Kubie, 1987; Quirk *et al*, 1992; Sharp *et al*, 1997). After several days of repeated training, place cells did begin to develop different fields in different environments. Importantly, though, this was a gradual, incremental process, that occurred at different times for different cells. There did not appear to be any relationship between the responses of individual cells: remapping appeared to occur on a cell-by-cell basis.

Another study investigated systematically changing stimuli across modalities: the colour (black/white) and odour (vanilla/lemon) of the recording environment (Anderson & Jeffery, 2003; Jeffery & Anderson, 2003). Place cells were found to have heterogeneous responses, with some remapping in response only to colour changes, some only to odour changes, and some to both. Heterogeneous responses, and therefore partial remapping, were seen within each animal. However, a different study from the same group (Jeffery *et al*, 2003) reported almost complete (all-or-none) remapping in response to changing box colour from black to white. The animals in the study had been very extensively exposed to the recording environment beforehand (during behavioural training), which, as in the Lever *et al* (2002) study, may account for the different response.

In conclusion, several studies, using different techniques, have demonstrated partial remapping between environments. In partial remapping, significant proportions of simultaneously recorded place cells are both remapped and non-remapped. In the case of Skaggs & McNaughton (1998), this could be explained by more than one representation being simultaneously active in CA1. In Lever *et al* (2002), it seems more likely all individual cells are acting independently. A further question is why some manipulations produce complete remapping, and some produce partial remapping? Which response is seen appears to depend on the exact nature of the manipulation, and on the individual animal being studied. Further investigation is

required in order to elucidate what exactly are the crucial factors controlling remapping.

Remapping in Different Regions of the Hippocampal Formation

Entorhinal Cortex

Since it is the major input pathway to the hippocampal formation, the presence or absence of remapping in the entorhinal cortex is of crucial importance. If there were no remapping in entorhinal place cells it would strongly suggest that discrimination between two environments is a process that occurs in the hippocampal formation itself. Quirk *et al* (1992) recorded both CA1 and MEC cells during the same manipulation, the substitution of a circular for a square recording environment. CA1 place cells remapped under these conditions. However, MEC place cells did not remap: any change in firing fields could be accounted for by a simple radial transformation between shapes.

Fyhn *et al* (2004b) simultaneously recorded entorhinal dorsolateral band cells (see above) and place cells from the hippocampal formation, while the environment shape was changed between square and circle. CA1 cells did remap under these conditions, while entorhinal cells did not, as measured by quantifying temporal co-firing of cells. However, examination of firing rate maps appears to show that the spatial tuning of the entorhinal cells does change. There may be some discrimination between environments, therefore, even upstream of the hippocampal formation.

Dentate Gyrus

Fyhn *et al* (2004b), was also the first to examine remapping in the dentate granule cells. Under the same manipulations (i.e. changing environment shape from square to circle) it was found that dentate place cells would also remap. The neural representation therefore, is already discriminating between the environments, even before the information reaches CA3 or CA1.

Comparisons of CA3-CA1

In general, studies looking at remapping in CA3 pyramidal cells have found that they show the same responses as CA1 cells. Two recent studies, however, have found differences between the two regions.

Leutgeb *et al* (2004a) simultaneously recorded CA1 and CA3 place cells whilst animals were in two similar-looking square environments, each in a different laboratory room. Remapping was assessed by; 1) comparing cells' mean firing rate in the two environments, 2) examining which cells co-fire in short time windows in each environment (population vectors). These measures were used to determine the 'overlap' of the cell populations active in each environment. In both CA1 and CA3, overlap was lower than in repeated trials of the same environment, indicating some degree of remapping in both. However, the overlap between CA1 cell populations was much higher than the overlap between CA3 populations (after correcting for the overall sparser activity in CA3). The CA1 representations therefore shared more cells firing in both environments, whereas the CA3 representations were based on more independent active sub-sets of cells. The conclusion drawn from this study, therefore, was that CA1 cells showed partial remapping, as seen, for example, in Lever *et al* (2002) or Anderson & Jeffery (2003). Under the same conditions, CA3 cells remap by switching to a completely different, independent, active sub-set of cells.

A similar result was reported by Vazdarjanova *et al* (2004), in this case using time-dependent RNA imaging techniques to detect cell co-activity in two environments visited 20 minutes apart. The environments used were different in shape and colour, and in different rooms. In common with Leutgeb *et al* (2004a), the authors claim the amount of co-activity is lower in CA3 than in CA1. There is, therefore, a larger amount of overlap between CA1 representations, or, in other terms, less remapping. The obvious caveat to this result, however, is that assaying cell firing through gene activity cannot show the spatial nature of cell firing. If CA1 cells remapped by shifting field position, the techniques used in this study would not detect this.

It should also be noted that both of the above studies induced remapping by moving the recording environment to a different room: an environmental manipulation not used in other studies discussed so far. The more complete remapping observed in CA3 may therefore be due to CA3 place cells being more

sensitive to changes in large-scale environment, or to distal cues, rather than having a greater general propensity to remap.

Subiculum

Several studies (Sharp and Green, 1994; Sharp, 1997; Sharp, 1999) have explored the nature of subicular representations of differently shaped environments. They indicate that subicular cells tend to generalise, rather than remap, across different environments. In particular, subicular cells showed similar firing patterns in cylindrical and rectangular environments (Sharp and Green, 1994), and in cylindrical and square enclosures that were both geometrically and visually distinct. Hippocampal CA1 cells showed distinct firing patterns when tested under similar conditions (Sharp, 1997), suggesting a dissociation between remapping between CA1 and the subiculum. However, given that Lever *et al* (2002) showed CA1 remapping can take a long time to occur, the above finding is potentially confounded by the fact that CA1 and subiculum recordings were not simultaneous. However, recent unpublished data from simultaneous CA1/subiculum recording seems to confirm the original conclusion, i.e. that subicular cells will not remap under conditions in which CA1 cells will (Lever *et al*, in prep).

Remapping and Synaptic Plasticity

As remapping involves a change to a different neural representation, an important question is whether this process requires synaptic plasticity. All studies described here have focused on Long-Term Potentiation (LTP) as a model of synaptic plasticity (Bliss & Lomo, 1973; Bliss & Collingridge, 1993). Many studies have suggested that LTP may underlie synaptic changes in learning and memory (Bliss and Richter-Levin, 1993; Moser *et al*, 1998; Elgersma and Silva, 1999; Martin *et al*, 2000), though this remains to be firmly proven.

Kentros *et al* (1998) attempted to block synaptic plasticity by pharmacological blockade of N-Methyl-D-Aspartate receptor (NMDA-R), a glutamate receptor necessary for both LTP (Collingridge *et al*, 1983) and for spatial memory (Morris *et al*, 1986). Animals were familiarised with the baseline recording environment (set up

as in Muller *et al*, 1987) before being exposed to the novel environment (cue card and enclosure wall colour changed), on two consecutive days. On the first day of exposure to the novel environment, the animal was injected (intra-peritoneally) with an NMDA-R blocker, CPP (3-(2-carboxypiperazin-4-yl)propyl-1-phosphonic acid). CPP injection did not affect the place fields of cells in the familiar environment, thereby controlling for any general effects of drug infusion. Furthermore, it did not prevent remapping occurring on first exposure to the novel environment. The remapped representation was stable when re-tested 1 hour later. However, when tested the next day, the place cell representation of the novel environment was remapped again: different from that of the first day of exposure. The familiar environment representation was unchanged. NMDA-R function is not necessary for remapping to occur, therefore. It does appear to be needed in order to give long-term stability to the new, remapped, place representation.

Protein synthesis is necessary to maintain LTP for over 6 hours (Frey *et al*, 1993). Agnihotri *et al* (2004) used a very similar protocol to Kentros *et al* (1998) to demonstrate that protein synthesis is not necessary for remapping to occur, or be stable over short time periods. It is necessary, however, for long-term stability of the remapped representations. There are technical problems with this study, though, relating to the behavioural effects of the protein synthesis inhibitor (Anisomycin) and to place fields in all experimental conditions having low inter-trial map-to-map correlations.

Dragoi *et al* (2003) attempted a very different approach: inducing LTP whilst simultaneously recording place cells, in order to look for effects of LTP on place fields. Example cells presented in the figures appear to show that LTP induction induces place cell remapping, whereas a control stimulation procedure does not. However, a closer look at the entire data set casts doubt on whether remapping is occurring. Whatever change does occur, this result does not show that LTP is a normal, physiological part of place cell function. It is equally likely that the LTP protocol used resulted in a perturbation to the hippocampus sufficient to disrupt place cell firing.

Place Cells as a Coherent Representation of the Environment

An important aspect of the cognitive map theory (O'Keefe & Nadel, 1978) is that the hippocampus holds a holistic representation of space. As the hippocampal representation is presumed to be of absolute space (in the context of which the positions of objects and actions are encoded), there should be a fixed 'map' in every environment: it should not be susceptible to piecemeal change. O'Keefe & Nadel (1978) proposed that place cells form the neural substrate of this map. If that were the case, place cells should show evidence of this behaviour, for example, a tendency for all active cells to stably retain their field positions relative to each other, despite perturbations to the environment. In this thesis, the term 'coherent' will be used to describe place cells displaying these properties.

Angular Cue Dissociation.

As discussed above, the angular position of place fields in a rotationally symmetrical environment can be controlled by prominent distal cues. One way to investigate the coherent nature of the place representation, therefore, is to put these cues into conflict with others, for example by rotating them in a different direction to the local (i.e. intra-maze) cues. A coherent representation would be expected to rotate as a whole, following only one set of cues and ignoring others. If, on the other hand, different cells rotated with different cues, it would suggest that cells responding independently to individual stimuli.

The first studies to address this issue found a complex set of results (Tanila *et al*, 1997; Shapiro *et al*, 1997). Rats were trained to run on a four-arm plus maze, where the spatial reference was defined by both intra-maze (distinct materials on each arm of the maze) and extra-maze (four prominent objects surrounding the maze) cues. On some trials, these two cue sets were rotated 90° in opposite directions. Between 2 and 10 place cells were simultaneously recorded on each trial. Tanila *et al* (1997) reported that in only 37% of rotations did cells rotate as a coherent representation. Of the other cases, sometimes cells remapped, and sometimes different cells rotated with different cues. The latter phenomenon argues against a coherent representation,

suggesting, rather, that different cells are 'tuned' to different sets of cues. A weakness of these studies, though, are the low numbers of simultaneously recorded cells. Brown & Skaggs (2002) repeated the experiment, recording 4-70 cells simultaneously. They found that, initially, cells rotated coherently, all following the intra-maze cues. After repeated manipulations, the likelihood of cells remapping increased. When the effects of remapping were controlled for, the incidence of cells simultaneously following both cue sets was no more than expected by chance. Knierim & McNaughton (2001) came to a similar conclusion, although using a very different experimental protocol (3-dimensional rotation of the recording apparatus). In this case, no more cells were bound to the local cues than would be expected by chance.

Knierim (2002) substituted a circular track for the plus-maze as the recording environment. This study claimed to demonstrate clear split control of place fields. This certainly appears true of some of the animals in the study: some fields rotate with local cues, some with distal, and some develop double fields, as if rotating with both cue sets. The field rotation data, grouped over all animals, shows a corresponding bi-modal distribution. However, in most cases, the field rotation data for individual animals does not show this. Only 2/8 animals show an obvious bi-modal distribution, in the others, fields seem to rotate overwhelmingly with either one cue set or the other. (The study does not provide formal analysis of this data). This study therefore showed that split control over place fields is possible, but not necessarily that it is the normal response to cue dissociation.

All of the above studies were conducted on CA1 place cells. Lee *et al* (2004) repeated the experimental protocol of Knierim (2002), but simultaneously recorded CA1 and CA3 place cells. The principle claim of this study is that the CA3 place cell fields rotate together - they are a more 'coherent' representation than CA1 cells. This appears true to the extent that, of the CA3 cell fields not remapped or showing ambiguous responses, the vast majority rotate with the local cues. There is no clear conclusion regarding coherent representations in CA1. In 3/5 animals, CA1 cells appear split between local and distal cue control. In all animals, however, approximately 75% of CA1 cells remap or show ambiguous responses. The finding of increased coherence in CA3 place fields is interesting, given the common idea that CA3, with its extensive recurrent collaterals, may be able to act as an auto-associative network (see chapter 1, chapter 4). An alternative explanation, however, may simply be that CA3 receives different inputs to CA1, and that these are more controlled by

the local cues. Furthermore, given that place field rotation is, most probably, driven by cue control over head direction cells (see above), greater coherence in CA3 than in CA1 may reflect the different influences of HD cells on these regions. For instance, CA1 may be receive more input from HD cells, which are in turn controlled by distal cues.

All studies described so far have used angular dissociation of local and distal cues as their primary experimental technique. Local and distal cues exert control over place fields in different ways, however, and their effects may interact in non-obvious ways, making prediction or modelling difficult. Fenton *et al* (2000a; 2000b) also investigated angular cue dissociation, but with two similar distal cues (a white card and a black card on a circular environment wall). The amount of angular dissociation was also smaller: 25° together or apart, compared to 90° or 135° in other studies. Under these conditions, place fields neither followed different cues independently, nor remapped. Rather, place representation was topologically distorted, such that fields near each cue moved rotationally with the cue, while those away from the cues moved radially towards or away from the centre. This experiment does show a type of coherent representation, therefore, though a flexible and deformable one, rather than a rigid one.

In conclusion, if there is a coherent place representation in CA1, it is clear that it can be 'broken up' by a severe manipulation such as placing local and distal cues 180° in conflict. All studies using this protocol found that some cells rotate with the cues and others remap. However, this does not disprove the existence of a coherent representation under more normal conditions. Evidence for 'split control', i.e. different fields rotating with different cues, which would be stronger evidence against a coherent representation, is more contentious. Subjecting animals to a lesser cue manipulation, as in Fenton *et al* (2000), shows a place representation that is coherent, though deformable rather than rigid. Finally, one study has indicated greater coherence in CA3, though this may only reflect a bias to follow a particular set of cues.

Pattern Completion and CA3

One way in which place cells can act as a coherent representation is that place firing can withstand the removal of a sub-set of cues from the environment. If an animal is already familiar with an environment, then exposure to that environment, even with only some of usual cues present, will elicit normal place fields from all place cells that usually fire. This phenomenon is sometimes termed 'pattern completion'.

It is generally accepted that removal of sub-sets of cues does not disturb place fields. This was first demonstrated by O'Keefe & Conway (1978). Place cells were recorded on a 3-arm maze inside a curtained environment. Apart from the maze itself, the only cues inside the curtained environment were four prominent, distinct objects placed near the curtains. Rotation of these objects showed that they were controlling the position of all place fields on the maze. Eight cells were then tested with removal of one or two of the cue objects. All cells maintained the same fields despite removal of at least one object, and for most cells two objects. Hetherington and Shapiro (1997) claimed to have found a contrasting result, that place cell firing is selectively degraded, depending on the proximity of the place field to the removed cue. However, the effects on place firing reported were relatively minor, 20-30% decrease in peak firing rate. As an overall conclusion, the basic integrity of the place cell representation (i.e. which cells fire, and the spatial relationship of their fields) is not affected by removal of sub-sets of cues.

CA3 pyramidal cells are often proposed as an anatomical substrate of place cell pattern completion. Their extensive network of recurrent collaterals could act as an auto-associative network, allowing any cell missing its own particular input for that environment to be fired by others active in CA3. Additionally, plasticity in the recurrent collateral synapses may be crucial: the network created needs to be selective (some synapses stronger than others) if the entire CA3 is not to activate itself. (Marr, 1971; McNaughton & Morris, 1987; Treves & Rolls, 1992. Also see chapter 1, chapter 5).

Recent evidence for the role of CA3 in pattern completion has come from selective deletion of NMDA receptors from CA3 pyramidal cells (Nakazawa *et al*, 2002). CA1 place cells were recorded from mice as they foraged in a circular

recording environment with four prominent distal cues. The place fields from the NMDA-R knockout mice had the same firing rate and field size as those of control mice. When three of the four cues were removed, however, the spatial firing of cells in the NMDA-R mice was degraded, showing a significant decrease in firing rate and field size, compared to the control animals. This was paralleled by a behavioural deficit on a water maze: NMDA-R mice showed the same reduction in performance when removing three cues as when removing all four cues. By contrast, control mice showed little deficit when three cues were removed but a large drop in performance when all cues were removed.

The NMDA receptor (NDMA-R) is necessary for synaptic plasticity in the CA3 recurrent collateral synapses (Harris & Cotman, 1986). The removal of the NMDA receptors, therefore, may prevent the selective strengthening of synaptic connections needed to create an auto-associative network specific for an environment. Place cell spatial specificity, and behavioural performance, therefore become susceptible to removal of a sub-set of cues.

Coherent Representations and Remapping

The finding of complete remapping discussed above (e.g. Muller & Kubie, 1987; Thompson & Best, 1989), fits well with the concept of a coherent hippocampal representation. The place cell responses are resistant to small changes in the environment but, when the amount of change crosses a threshold, a different, wholly independent set of place cells are activated. On the other hand, gradual, piecemeal remapping such as seen in Lever *et al* (2002) seems to directly disprove that there is a coherent representation, at least under those particular experimental conditions. Partial remapping can be interpreted in different ways. It could be evidence against a coherent representation: some cells are responding to environmental features which change, and so remap, other to features which are constant, and so do not. It is possible to see partial remapping as overlapping coherent representations, one remapped, the other not, as in Skaggs & McNaughton (1998). Yet another interpretation is that partially remapped place cells belong to coherent representations which share some elements.

To assess whether partial remapping does involve changing between different coherent representations, a useful set of experiments would be exposing the animal to a range of environments with different degrees of contrast between them. If, in response, place cells showed incrementally different amounts of remapping, this would argue against a coherent representation. Two studies which investigated this were Leutgeb *et al* (2004a) and Vazdarjanova *et al* (2004).

Leutgeb *et al* (2004a) used a series of boxes that were different in colour, size and shape (though always in different rooms). The authors claim to observe incremental changes in CA1 remapping, depending on the degree of difference between environments. Their best example is that, using the mean rate overlap measure, there is a gradual increase in the amount of remapping as the environment changes colour, then size, then shape. However, when using the population vector method (which should also take into account field position shifts) to assess remapping, this effect is much less pronounced.

Vazdarjanova *et al* (2004) used four levels of difference between the two environments: (1) and (2) manipulations of intra-environment cues, (3) same environment but different room, (4) different shape and colour environment in a different room. In both CA1 and CA3, the number of co-active cells was lowest in condition (4) and intermediate for all of (1), (2) and (3). Place cells in both CA regions, therefore, show the lowest co-activity (presumed greatest remapping) when both the immediate, proximal environment and the large-scale, distal environment change simultaneously. Although conditions (1), (2) and (3) produce partial remapping in CA1, the amount of remapping appears roughly equal in all. The evidence for incremental amounts of remapping is weak, therefore. Only condition (4) produces more remapping, a result which is not surprising, given that all cues available to the animal change.

One methodological problem with both of the above studies is the somewhat random nature of the incremental differences. It is not known to what extent changing colour, size, shape, etc, are perceived as different by the rat. Furthermore, different neural systems may underlie place representation of different classes of cues, e.g. intra-environment and distal cues. A more systematic approach to producing incrementally different sensory stimuli would be useful.

One attempt at such an experiment has been published in abstract form (Leutgeb *et al*, 2004b). Rats were trained in square and circular environments until

remapped, similarly to Lever *et al*, (2002). A deformable wall was then used to create 5 environments, with shapes incrementally intermediate between square and circle. After an initial baseline (e.g. square) intermediates were presented to the animal by order of shape, i.e. most square-like first, then next most square-like, and so on until most circle-like and finally circle. (The opposite order was run on the following day). Remapping was assessed using rate overlap and population vector methods (see above). Both CA1 and CA3 place cells showed incrementally increasing remapping, as the environment shape became more different from the baseline. The authors claim CA3 place cells showed pattern completion, as, in the intermediate shapes, CA3 cells always showed more overlap with the baseline place representation, compared to CA1 cells. However, the gradual and incremental change in remapping argued against either CA1 or CA3 place cells acting as a coherent representation of place.

Chapter 4

Models of Hippocampal Function

This chapter will describe some models and theories of hippocampal function, particularly those that emphasise the spatial memory and cognition role of the hippocampus. The first section will review some influential models of hippocampal spatial function. The second part will review models that relate the hippocampus to attractor neural networks, as this theoretical concept has clear relevance to the idea of coherent representations in the hippocampus. All theories will be discussed with a particular interest in their relevance to remapping, and to coherent representations of space. Finally, this chapter will be limited to discussing the rat hippocampus only.

Models of Spatial Hippocampal Function

The Hippocampus as a Cognitive Map

Immediately after the isolation of place cells by O'Keefe & Dostrovsky (1971), O'Keefe and Nadel began elaborating the theory that the hippocampus acted as a cognitive mapping system (O'Keefe, 1976; O'Keefe and Nadel, 1978). The most important feature of the spatial cognition proposed by O'Keefe and Nadel is the conceptualisation of space as an absolute entity (following Kant), primary to the objects or behaviours within it. This was in contrast to other theories, in which space was relativistic, defined by the spatial relationships of objects and events encountered by the animal. For O'Keefe and Nadel, it is the hippocampal system that generates the organism's intuitive framework of absolute, unitary space. This framework is thought of as innate, and the underlying geometry of the system is Euclidean. The theory was motivated by features of hippocampal anatomy, correlates of the hippocampal EEG, behavioural studies of hippocampal lesioned animals and, primarily, by spatial correlates of single unit firing in the hippocampus. These cells were proposed to form the neural substrate of the cognitive map.

According to the theory, the hippocampus generates and stores cognitive maps of all environments the organism encounters during its life. The map of each environment is composed of a set of place representations (entailed by the place fields of hippocampal pyramidal cells) connected together by rules that represent the distance and directions among them. O'Keefe and Nadel described this map as underlying the *locale* system of navigation. The *locale* system automatically produces a map of an environment as soon as it is explored, and stores it indefinitely. The creation of the map is all-or-non, meaning that once a map for an environment exists, it is not modified. (References to changes in the environment could be added, but these do not effect the spatial structure of the map). The *locale* can 'act at a distance' allowing animals to move with reference to places they cannot perceive, for instance, taking short-cuts. By contrast, the non-hippocampal *taxon* navigation system is comprised of guidance and orientation strategies, and learns, incrementally, only those particular routes relevant to a given behavioural task.

There have been many attempts to describe how place cells (and other spatially specific cells) could implement a navigation system, some of which are described later in this chapter. For this thesis though, the most interesting aspect of the cognitive map theory is its conception of a coherent, integrated representation of space in the hippocampus. It is not a piecemeal set of responses to different cues. The cognitive map used by the *locale* system should, therefore, be resistant to the alteration of cues in the environment. When changes to the place representation do occur, they should be in an all or none fashion. This view is supported by place cell data on pattern completion (e.g. O'Keefe & Conway, 1978) and 'complete' remapping (e.g. Muller & Kubie, 1987, Bostock *et al*, 1991). However, it does not account for data showing incremental changes to place cell responses (Lever *et al*, 2002) or different place cells responding to different features of the environment (O'Keefe & Burgess, 1996). Even if place cells are capable of acting as a coherent representation, therefore, they may not do so in all circumstances.

The Hippocampus as a Cognitive Graph

The cognitive graph theory shares a fundamental assumption with O'Keefe & Nadel (1978): that the hippocampus functions as a cognitive mapping system. The

premise of the cognitive graph theory is that, in these maps, distances between places are represented entirely by synaptic strengths between neurones (Muller *et al*, 1991; Muller *et al*, 1996; Muller & Stead, 1996).

The model relies on two basic features, the dense recurrent connections of CA3 place cells, and an LTP-like process. The authors propose that during exploration of an environment, cells with adjacent place fields will show the coincident firing needed for LTP, and the efficacy of the synapse CA3 recurrent synapse between them will increase. This will organise the CA3 network into a "cognitive graph", in which cells with adjacent fields are strongly connected together, those with fields further apart have weak connections. As the connection strength codes for the distance between place fields, if a start and a goal location are defined, the network can easily compute the path of least resistance between them. The graph is also able to sustain detour navigation and short-cuts, provided the animal is given an opportunity to explore the newly opened path.

The model's strengths include the simple demonstration that the network implicitly contains a cognitive map within its structure and the fact that the "cognitive graph" is set up in a completely incidental manner, through spontaneous exploration of the environment. A general criticism of the model, however, is that it doesn't include a prediction or description of how the output generated by the graph could be read out, and implemented behaviourally. Which structures support this read-out and how do they accomplish it? Moreover, it is not clear how a goal could be selected (where is the goal represented in neural terms?).

The cognitive graph model does not address the issue of remapping in detail. It is proposed that the different active sub-sets of cells have different sets of connection strengths, forming independent 'graphs' for each remapped representation. It does not attempt to account for partial or gradual remapping, or more generally, how sensory changes induce remapping. Finally, it is interesting to compare the cognitive graph theory with attractor based models of place cell firing (e.g. Samsonovitch & McNaughton, 1997). Both use a very similar mechanism of encoding two-dimensional space in the connection strengths between recurrently connected CA3 neurones, but reach different conclusions on the dynamic behaviour of such a network.

Navigation models of O'Keefe, Burgess and colleagues

Burgess, O'Keefe and colleagues have developed a detailed model of what drives place cell firing, and how animals could use the place cells to navigate to a goal (Burgess *et al*, 1997; 1998; 2000; Burgess & O'Keefe, 1996a; 1996b; Hartley *et al*, 2000; O'Keefe, 1990; 1991; O'Keefe & Burgess, 1996).

The experimental findings of O'Keefe & Burgess (1996) are modelled by assuming that place fields result from summing together a set of gaussian tuning curves extending from a certain set of walls. The model of Hartley *et al* (2000) therefore proposed that the input signal to place cells was comprised of Boundary Vector Cells (BVCs). These cells fire when a wall (or other barrier) is at a certain distance from the animal, in a certain allocentric direction. Place fields are produced by performing a thresholded sum of these inputs. This model can predict place field behaviour in differently shaped boxes, and their response to inserting barriers into the environment. The model also incorporates goal cells, assumed to reside in the subiculum. When the rat encounters a goal, a one-shot Hebbian learning process takes place between goal cells and the currently active population of place cells. As a result, goal cells would have a spatially graded response, with the highest activity at the goal location. The animal would be able to reconstruct a path to the goal, by choosing a path that increasingly activates the relevant set of goal cells.

The major weakness of the model, from the perspective of this thesis, is the lack of a remapping mechanism. The BVC model can reproduce unpredictable changes in firing when walls are moved by large amounts (Hartley *et al*, 2000), but not when walls are in the same or similar positions (square and circle, for example). The model would not predict a switch to an unrelated active sub-set of cells ('complete' remapping) under these circumstances.

The Hippocampus as an Attractor Neural Network

Attractor Neural Network Models of Memory

The roots of the Attractor Neural Network (ANN) model of memory lie in Hebb's concept of the cell-assembly (Hebb, 1949). Hebb conceived that information could be represented in the brain by distributed networks of neurones, the connections between them selectively strengthened by coincident activity. Due to recurrent (feedback) connections within them, these networks would be able to maintain the representation even in the absence of the sensory input. Furthermore, even a sensory input comprised of only part of the original stimulus would be able to activate all cells in the assembly. These principles, representation independent of online input and associative recall, are fundamental to neural network models of memory. The ANN model, in its simplest form, is a neural network which displays these properties, and whose behaviour can be described using the well established mathematics of physical attractor dynamics.

The basis of the ANN is a recurrently connected neural network, with a pre-assigned set of synaptic efficacies. Given an initial set of inputs, the changing state of the network can be mapped as a path through N-dimensional state-space, where N is the number of neurones in the network. Depending on the connectional properties assigned to the network, 'fixed points' may appear in state-space, i.e. network states which, after they have occurred once, will persist indefinitely. Fixed points are also fairly insensitive to initial conditions - many different initial condition states will converge onto them. They are therefore also termed 'fixed point attractors', or simply 'attractors' (described in Amit, 1992).

If attractors are taken to be remembered representations, the ANN can therefore model the persistence of a representation in the absence of sensory input. It can also model associative recall, due to the fact that any starting condition 'close enough' to an attractor state will cause the network to converge onto the attractor (Hopfield, 1982). The distribution of encoded representations, and the way in which inputs to the system recall them, can be visualised as a 'landscape' function (Lyapunov function), where attractors are valleys in the landscape (Hopfield, 1982, Amit 1992). For a given input, the initial state can be plotted on the landscape, from

where the network state will always move 'downhill', until a local minimum attractor is reached. In its simplest form, there is no plasticity in the ANN: encoding representations by altering synapses requires adding further detail to the model (Amit, 1992).

The Hippocampus as an ANN: General Memory

Marr (1971) first proposed that the recurrent collaterals of the hippocampal CA fields played an important role in memory. Marr's model of hippocampal function was not formally an ANN, but the fundamental principle was network auto-association. In the model, the hippocampus forms a temporary memory store for representations active in the neocortex. During memory recall, a partial representation in the neocortex would activate the corresponding partial representation in the hippocampus. The full representation would then be generated within the hippocampus, by recurrent activation 'filling in' the missing parts. One weakness in Marr's model was its lack of anatomical specificity: it did not account for the hippocampal 'tri-synaptic circuit'. Furthermore, later tests of the model have shown its particular implementation to be flawed (Willshaw & Buckingham, 1990). Nevertheless, it remains an important study, as the first to point a memory role for the hippocampus based on the recurrent connection anatomy of CA3.

The model of Marr was updated by McNaughton & Morris (1987). This study used the correlation matrix as its formal model, but, as with Marr (1971), its fundamental principle was that recurrent collaterals within the hippocampus allow for completion of a partial representation. The model also adds anatomical detail. The mossy fibre input to CA3 is presumed to impose patterns on CA3, as each axon makes powerful synapses on relatively few pyramidal cells. Dentate gyrus granule cells, being substantially greater in number than CA3 or entorhinal cells, act to reduce the overlap between similar inputs, thereby increasing recall accuracy in CA3. According to this model, therefore, the hippocampus between entorhinal cortex and CA3 is involved in pattern separation (increasing the difference between neural representations of similar stimuli) and pattern completion (filling in the neural representation for missing sections of familiar stimuli). These properties would allow

the hippocampus to flip between two very different representations, even when presented with very similar input stimuli.

The pattern separation/completion model of the hippocampus was further developed by Treves and colleagues (for summary, see Treves & Rolls, 1994). This study modelled CA3 as a fixed point ANN, with the modification that neurones possessed continuously variable firing rates (Treves, 1990; Treves & Rolls, 1992). As in the McNaughton & Morris (1987) model, the role of the dentate gyrus is to decrease the correlation of representations of similar inputs, with the mossy fibre inputs driving the learning of new representations (Rolls, 1990; Treves & Rolls, 1992). The direct entorhinal-CA3 projections, by contrast, are used to recall full representations from partial inputs (Treves & Rolls, 1992). CA1 represents the output of the network in this model: the role of the direct entorhinal-CA1 projections being to provide any detail lost from the input representation during the pattern completion process. (See also O'Reilly & McClelland (1994) for further detail of the different roles of entorhinal to dentate, dentate to CA3 and entorhinal to CA3 connections in the pattern separation/completion model). The overall role of the hippocampus in this model is to provide a rapid 'snapshot' encoding of events (not specifically spatial). Encoded representations are distinct, even for similar inputs, and can be recalled in full, even from a partial stimulus input.

All the models described above focus on excitatory connections as the primary means of information processing. Inhibitory circuits are also important, however, one example being the formation of CA1 place fields from CA3 input. CA3 pyramidal cells have similar place-specific firing properties to those of CA1 (see Chapter 3). Approximately 20% of all CA3 pyramidal cells are active in any environment (Vazdarjanova *et al*, 2004; Leutgeb *et al*, 2004), and their place fields are distributed throughout the environment. A single CA3 pyramidal cell sends widespread projections to the CA1 field, and may make synaptic contact with between 8% and 66% of CA1 pyramidal cells (Li *et al*, 1994; see also Chapter 1). CA1 pyramidal cells are therefore receiving excitatory synaptic input from cells which do not share a similar place field. In order that a CA1 cell does not fire diffusely throughout the environment, local interneurones (see Chapter 1, Chapter 2) must be providing inhibitory input to that cell when the animal's position is not in the place field.

Inhibitory interneurones have also been incorporated into some ANN models of the hippocampus. An important issue in all models using recurrent connections is

how to avoid runaway activation of the cell population, therefore introducing the need for an inhibitory component. Hasselmo *et al* (1995) introduced a dynamic attractor network (restricted to CA3), with a biologically realistic model of cholinergic inhibition at the excitatory recurrent synapses. Interestingly, when the network is presented with new stimuli, the extent to which these are generalised as partial versions of familiar stimuli, or encoded as new patterns, depends on the degree of cholinergic activity in the system. According to this model, therefore, modulation from the medial septum could affect the way in which the hippocampus treats novel stimuli (see also Hasselmo *et al*, 1996).

The Hippocampus as an ANN: Spatial Function and Place Fields

The models outlined above all treat the hippocampus as a storage site for general memory. They investigate the ability of the hippocampus to store and retrieve patterns of information, without specifying the sensory basis of that information. There have also been attempts to describe the spatial function of the hippocampus, in particular the formation of place fields, using an ANN model. It is important to note that all these models use a different variant of the ANN to that described above; models of general memory use fixed point attractors, while models of place cell activity use a set of continuous attractors. The difference between these will be explained in more detail below (see "ANN Models and Remapping").

Samsonovitch & McNaughton (1997) modelled the firing of place cells as a continuous attractor on an arbitrary two-dimensional surface. This study was motivated by McNaughton *et al*'s (1996) model of the hippocampus as a path-integration navigation system. In the model, a sub-set of place cells are connected such that they constitute an arbitrary two-dimensional surface, where short distances are defined by strong connections. This 2D surface defines a path integration reference frame, or 'chart'. Due to its extensive recurrent connections, the anatomical site of the chart is presumed to be CA3. The position of a cell's place field within an environment is assumed to be arbitrary. When all cells in a chart are plotted on a surface, according to the position of maximum place firing, cell activity appears as a 'peak', localised to a restricted region of the chart. (The position of the activity peak corresponds to the position of the animal). Due to the connectional properties of the

chart, the place cell activity peak forms a set of continuous attractors, meaning that the mobility threshold for the activity peak moving to a neighbouring location is negligibly small, compared to a large threshold for the peak moving to elsewhere on the chart. This activity peak is then 'pushed around' on the chart by a set of path integration cells, i.e. the peak moves in the direction of the animal's heading, by an amount related to the animal's current velocity.

This model was used by Samsonovitch & McNaughton (1997) to reproduce experimental results including place fields in distorted environments (see O'Keefe & Burgess, 1996; Gothard *et al*, 1996), slow rotation of place fields (Knierim *et al*, 1995) and place fields during exploration of a novel space (Wilson & McNaughton, 1993). This study does not, however, address the issue of remapping. In the model of McNaughton *et al* (1996), the hippocampus stores a large number of independent charts, defined by different sets of connections. Remapping corresponds to switching between different charts. There are several weaknesses, however. There is no formal analysis of how multiple maps could be stored, and how this would affect the model (though this issue was later addressed by Treves & Battaglia, 1998). There is no detail on how remapping would be initiated, in response to sensory or behavioural change. Finally, the model does not seem to account for partial remapping (see Chapter 3).

Redish and Touretzky (Touretzky & Redish, 1996; Redish & Touretzky, 1997; Redish & Touretzky, 1998; Redish, 1999) produced a model of rat navigation which includes multiple maps ('reference frames') in the hippocampus. Similarly to Samsonovitch & McNaughton (1997), the connectional properties of CA3 create an attractor-dynamic peak of activity. However, the formation and movement of this peak are influenced not only by path integration, but also by sensory information (local view). Unlike Samsonovitch & McNaughton (1997), CA3 connections are not pre-set, but are learnt as the rat explores the environment, in a similar way to the cognitive graph model. Pattern separation in the dentate gyrus is responsible for activating a new map on entry into a novel environment.

Neither of the above models used the ANN to model the formation or behaviour of actual place fields in the hippocampus. By contrast, Kali & Dayan (2000) attempted to use the pattern separation/completion attractor model to explain how place fields form, and how they depend upon entorhinal input. The inputs to the attractor network were a set of feature detector cells, broadly tuned to the walls of the environment (c.f. Quirk *et al*, 1992; Frank *et al*, 2000; Hartley *et al*, 2000). The

dentate gyrus decreases the similarity of input representations, and CA3 acts as a recurrently connected auto-associator. The model can produce tightly specific place fields in CA3, and can reproduce experimental data including task-dependent directionality (see Markus *et al*, 1995) and place cell response to distorted environments (O'Keefe & Burgess, 1996). The model can also reproduce remapping, demonstrating that different sets of place cell representations can be stored in CA3. Remapping was only produced, however, by completely changing the entorhinal input to the system. The model does not, therefore, address the issue of why some sensory changes produce remapping while others do not, or how partial remapping occurs. Furthermore, the discovery of highly spatially specific cells in the entorhinal cortex (Fyhn *et al*, 2004a; Hafting *et al*, 2005), which may not remap (Fyhn *et al*, 2004b), invalidates an assumption of the model.

Touretzky *et al* (2004) also used a combination of feature detectors and attractor dynamics, in this case to model the experimental data of Fenton *et al* (2000a). Feature detectors were tuned to the distance and bearing of the animal from the two cue cards. Attractor dynamics in CA3 were then used to model how input signals from different feature detectors were integrated into an activity 'bump', representing the place field. The model successfully reproduced the experimental results, that the amount and direction of place field displacement was determined by the position of the place field relative to the cue cards. Attractor networks can therefore also model the topological distortion of a coherent representation of the environment.

ANN Models and Remapping

The major theoretical difference between the fixed point and continuous attractor models is that, in fixed point models hippocampal activity evolves towards a fixed state and, in the absence of changing input, stays in that state. In continuous attractor models, by contrast, the activity pattern of cells is always changing, as the animal moves around the environment, and the "activity bump" moves around in the CA3 network (though each bump position is, in itself, an attractor).

The continuous attractor model best describes the activity of non-remapped place cells. It does not, however, describe remapping well. Remapping is presumed to

correspond to a switch to a different functional network of CA3 pyramidal cells, but the models do not describe in detail how or why this switch would occur. Fixed point attractors can model remapping in terms of a switch between independent active cell subsets representing an environment, but do not describe how cell activity, within these subsets, changes as the animal moves around the environment. A complete attractor model of remapping would need to account for both global representations of space, and place cell discharge in particular locations.

Questions to be Addressed in this Thesis

The following questions summarise the issues arising from the Introduction which will be addressed in the experimental and Discussion sections of this thesis.

1) Can place cell remapping between environments of different shapes occur on a shorter time scale than that seen in Lever *et al* (2002)? What manipulations of the training protocol would be needed to achieve this? If faster remapping does occur, is it best characterised as complete or partial remapping, as defined in Chapter 3?

2) What is the nature of remapped place cell representations created during this training? In particular, are they coherent representations of space? For example, are individual cells responding, discretely, to different stimuli, or do groups of place cells represent the environment in a holistic manner? Is it possible to observe place cell representations which are intermediate between the existing remapped ones, or must there be an all or none switch between them?

3) Attractor Neural Networks (ANNs) are often postulated as models of memory storage and retrieval. Some features of the anatomy of the hippocampus have lead to its being proposed as the neural substrate of an ANN. Is there any evidence that remapped place cells are representing the environment in a manner consistent with a hippocampal Attractor Neural Network?

Chapter 5

Methods

Subjects

5 male Lister hooded rats were used in the experiments described in this thesis. Rats weighed between 280 and 400g at time of surgery, were housed singly in Perspex cages, and maintained on a 12:12 hour light:dark schedule, with lights off at 3 pm. Rats were maintained at 85% of their free feeding weight. Rats were implanted with electrodes before the various experiments and no pre-implant selection procedure was used.

Microelectrode Implants

Electrodes and Microdrives

The electrodes were made from microwire (90% platinum, 10% iridium, H-ML insulated), 17μm in diameter (California Fine Wire). All electrodes used were tetrodes. These were constructed by twisting four individual pieces of wire together, approximately 2 turns per mm.

Electrodes were attached to a moveable microdrive. Figure 5.1 shows a diagram of the standard microdrive. Part of the microdrive, consisting of the two metal posts, is stationary with respect to the brain of the animal. This structure is attached to the head of the animal using dental cement. One of the posts (right hand side in figure 5.1) carries a fine-threaded screw. Fitted over this screw is a nut (consisting of heat shrink plastic), attached to which, via dental cement, is the electrode cannula. When the screw turner (right, top, figure 5.1) is used to rotate the threaded post, the portion of the microdrive attached to the nut, including the electrodes, moves up or down. One 360° turn moves the electrodes 200 μm.

Figure 5.1

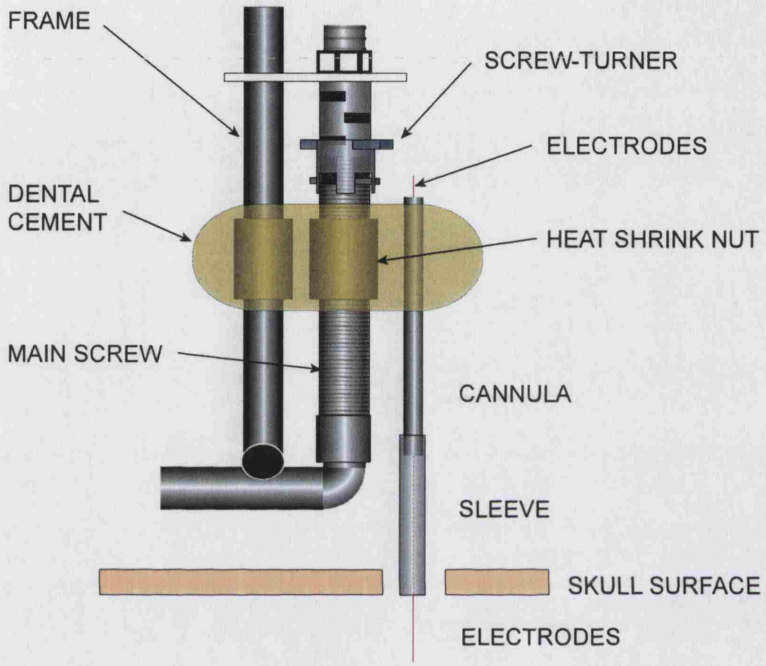

Figure 5.1. Diagram showing the main features of the microdrive. Microdrive is fixed with respect to the skull surface, using dental cement (not shown). Turning the screw-turner causes the cannula to move up and down relative to the main screw. The cannula was loaded with up to four tetrodes. 0.5 mm solid-core steel wire, mounted in dental cement, carried the signal between the tetrodes and the headstage connection (not shown). Original version of this drawing by John Huxter.

Ends of tetrode wires were stripped of insulation (exposure to naked flame), wrapped around microdrive wires, and the junction sealed with conductive silver paint.

Four tetrodes were attached to each microdrive. These were glued together so that the ends of the tetrodes formed a closely spaced 'cluster'. The distances between tetrode tips in the cluster were approximately 300-600μm. All tetrodes in the cluster were cut to the same length (with an error of approximately 50-100μm).

Surgery

The animals were removed from the animal house and placed in individual cages in a holding room close to the operating theatre at least one week prior to surgery.

The animals were first anaesthetised as follows: oxygen at 3 litres per minute, with isofluorane at 3% of the gas volume. The animal's head was then shaved using electric clippers. Before the animal was fitted with the ear bars, nitrous oxide was introduced at 3 litres per minute, and the oxygen flow was reduced to 1.5 litres per minute. At this point, analgesic (Buprenorphine (Vetergesic), 45μg, I.M.) and prophylactic antibiotic (Enrofloxacin (Baytril), 2.5mg, S.C.) were administered. The percentage of isofluorane was gradually decreased throughout surgery, stabilising at 0.5 to 1.2 %. Once the animal was stably anaesthetised, it was fitted with ear bars and mounted in the stereotaxic frame.

Seven holes for screws were drilled using a 1.2 mm burr drill. Two holes were drilled over the occipital, two over the frontal bone. Two further holes were drilled over the parietal bone contra-laterally to the implant side, and one over the parietal bone rostral to the implant site. Stainless steel screws were screwed into each hole. One screw served as the ground attachment for unit recording.

The implant co-ordinates, for every animal, were AP –3.8 to -4.0 mm; ML 2.4 to 2.7 mm, (both AP and ML relative to bregma); DV 1.5 to 1.7 below pial surface. The hole for the electrodes was drilled using a 2.3 mm diameter trephine drill. The pial surface of the brain was exposed, and the dura mater removed before wires were implanted. The sleeve around the electrode cannula was then lowered so that its lower

surface rested on the brain surface. The exposed brain around the sleeve was covered with sterile vaseline.

The tetrode-microdrive assembly was then fixed to the skull by applying dental cement around the sleeve, the feet of the microdrive, the screws and the skull. Plastic screws were cemented to the skull, to provide attachment for the headstage and to protect the drive from grooming by the animal, during recording. At all other times, the whole implant site was protected with micropore surgical tape.

Histology

After completion of the experiments, each rat was killed with an overdose of sodium pentobarbital (Euthatal, 10mg) and perfused transcardially with saline followed by 4% paraformaldehyde. The brain was extracted and stored in 4% paraformaldehyde, and later sliced coronally into 40 μm thick sections, which were mounted and Cresyl-Violet Nissl-stained to aid visualisation of the electrode track and tip relative to CA1 pyramidal cell bodies.

Electrode Placement

Table 5.1 lists the placements of tetrode clusters (Anterior-Posterior and Medial-Lateral co-ordinates only), from which all place cell data in the following results chapters was recorded. All electrode tips were in the CA1 pyramidal cell layer at the time of the recording. This was confirmed histologically, and by using physiological markers of the CA1 pyramidal cell layer during recording (see below).

Table 5.1

Anterior-Posterior and Medial-Lateral positions of tetrodes during place cell recording.

	Hemisphere	AP (mm)	ML (mm)
Rat 1	Left	-3.8	2.2
Rat 2	Left	-4.4	2.6
Rat 3	Right	-3.2	1.8
Rat 4	Left	-4.6	3.2
Rat 4	Right	-3.0	1.6
Rat 5	Left	-3.6	2.4

All positions are in mm, rounded to the nearest 0.2mm, relative to Bregma. Note that place cell data was obtained from both left and right hemisphere implants in Rat 4.

Unit recording

Screening

Approximately one week after surgery, screening for cell activity began. Screening took place while the rat was on the holding platform (see laboratory layout, figure 5.2). The main physiological marker used for CA1 was the high-frequency "ripples" state, seen when the animal is still and at low arousal levels (see chapter 2). The electrodes were moved down towards CA1 in multiples of 50 or 100 micron steps until signs of low amplitude ripples were seen. When ripples were seen, the electrodes were moved down in 25 micron steps, until complex spike activity was detected.

Unit recording apparatus

Each rat was connected to the recording equipment via a headstage amplifier which fitted onto the plug of the microdrive. These headstage amplifiers were unity-gain buffers, which served to isolate the electrodes from the wires carrying their signals to the recording system. The implanted electrodes were AC-coupled to these

amplifiers. Lightweight hearing-aid wires 2 to 3 metres in length connected the headstage to a preamplifier (gain 1000).

Signals were amplified (15-50 thousand times) and bandpass filtered (500 Hz-7 kHz). The signals were recorded differentially, meaning that a reference signal (a channel on a different tetrode) was subtracted from the target signal. This technique is designed to remove noise and artefact from the signal. Each channel was continuously monitored at 20-μs intervals and potentials were captured using 50 time sample points (200 μs pre-threshold and 800 μs post-threshold) whenever the signal from any of the pre-specified recording channels exceeded a given threshold set by the experimenter.

Two infrared LEDs were attached to the head of the rat, in order to track position and orientation with a video camera (position sampling rate 46.875 Hz). The two LEDs were positioned symmetrically to the left and to the right of the rat's head, approximately in line with ears along the anterior-posterior axis, and approximately 5 cm above the top of the rat's head. They were separated by 5-7 cm, and identified on the basis of their differential brightness.

All unit recording apparatus was custom built (O'Keefe lab, Axona).

Cluster cutting

Isolation of single units from multi-unit data (cluster cutting) is based on the premise that an action potential from an individual cell will be recorded on more than one wire of the tetrode. As the amplitude of the signal decreases in proportion with 1/(distance from neurone)^2, the amplitudes of the action potential on the four wires of the tetrode depend on their position with respect to the cell. A group of action potentials with the same set of amplitudes (over all four wires of the tetrode) is assumed to originate from one neurone.

For all the data used in this thesis cluster cutting was performed using custom software (TINT, Neil Burgess). No automatic cluster cutting algorithms were used: definition of single units was performed manually. A series of scatter plots are created, plotting peak-to-trough amplitudes for all action potentials. The series contains all possible combinations of comparison. (Six scatter plots for four amplitude values). A set of action potentials that share the same amplitude profile should form a coherent "cluster" on every one of the scatter plots. In order to reduce error, only

clusters well separated from other action potentials in 4-D amplitude space are considered. Although cluster cutting is conducted mainly on the basis of Peak-to-Trough amplitude, other parameters used include voltage at an arbitrary time, time-of-peak and time-of-trough.

Experimental Protocols

Exact details of the trials in each experiment are given in the relevant results chapters. This section will describe laboratory set up and experimental protocols common to all experiments.

Laboratory Layout

The general laboratory layout is shown in figure 5.2. During all screening for cell activity and all Inter-Trial Interval (ITI) periods the animal was placed on the holding platform and the curtains were closed around the recording environment. For all experiments, the only exposure the animal had to the recording environment is that which is detailed in the running order of trials.

Within the recording environment, the animal was placed in an open-topped box, 50 cm high and 60 – 80 cm across. The shape, colour and material of the box were the major independent variables in all experiments: details of these are given below. The box was placed on a black, Trespa floor, which was washed using soap and hot water before every trial. The only deliberate cue within the curtained environment and external to the recording box was a A1 sized plain white cue card, illuminated with a 60W desk lamp. The position of the cue card was always held constant, on the West of the recording environment. This was designed to create stability in the head direction system.

Figure 5.2

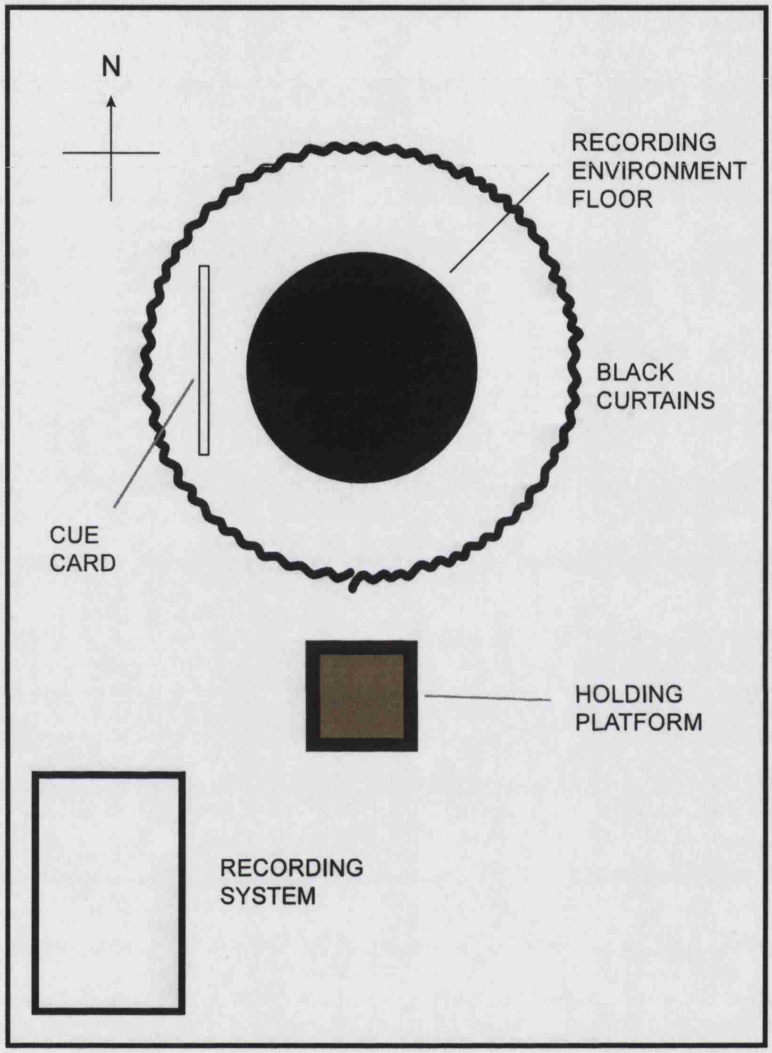

Figure 5.2. Plan view of laboratory, showing general set up of recording environment. All recording sessions took place within black curtains, on black trespa floor (black circle). The rat was always restricted to within a recording environment, walls 50cm high, which was placed on this floor. The shape, colour and material of the recording environment varied according to the experiment being conducted (see results chapters). At all other times, rat was placed on the holding platform.

Behavioural Task

In all the experiments recording took place while the rat was foraging for sweetened rice grains scattered randomly by the experimenter in the recording environments. This behavioural task is very similar to the pellet-chasing paradigm developed by Muller and Kubie (1987). Unless stated otherwise, all recording trials were 10 minutes in length, all ITIs were 20 minutes. To ensure stability in the head direction system, the animal was always carried directly from the holding platform to the recording environment, facing in the same direction (north) and placed down in the centre of the environment.

Recording Environments

To create an environment whose shape could be changed without affecting other modalities such as olfaction, texture or colour, a "morph box" was constructed. Each morph box consisted of 32 pieces of interlocking plastic tubing, all 50cm high. To hide the joints, a layer of plastic wrapping tape was stuck to the inner surface of the walls, and then another layer of masking tape was stuck onto the plastic wrapping tape. The final colour was light greyish-brown. The morph box could then be arranged in various shapes, the most commonly used of which were a square 62 x 62 cm, and a pseudo-circle (actually a 32-sided regular polygon) 79 cm in diameter. More complex arrangements of the morph box will be described later, with their relevant experiments.

Lever *et al* (2002) showed that training animals in two environments that differ only in their shape, such as the morph box square and circle described above, results in a slow and gradual remapping. One aim of this study was to induce remapping in a shorter time. The method used to achieve this was to create more sensory contrasts between the environments: in addition to their shape, the environments also differed in the colour and material of their walls. One of these environments was the morph box configured as a square. The other recording environment was a wooden circle, of the same dimensions as the morph circle. The

inner surface was painted with matt-finish white paint, therefore this environment is referred to as the "white circle".

The rotational alignment of all recording environments was maintained throughout all trials.

Data analysis

Derivation of firing rate maps

There is no standard protocol for constructing and presenting place fields. The procedures used in this thesis follow very closely the protocols used recently in the O'Keefe laboratory (O'Keefe and Burgess, 1996; Jeffery and O'Keefe, 1999; Lever *et al*, 2002). The software used was TINT.

The total possible camera viewing area is 768 x 574 pixels. Within this viewing area, it is possible to create an experimenter-defined co-ordinate frame, which was always set to 500 x 500 pixels. The environment was always placed in a standard position with respect to this frame. One pixel in the firing rate maps therefore always represented 2.5 mm^2 of space on the floor of the recording environment.

In order to construct firing rate maps, the raw pixel data were first binned. All data in this thesis was binned into 8 x 8 pixel bins. Firing rate maps were then derived by calculating the number of spikes from a cell in each bin, divided by the rat's dwell time in that bin. However, following previous work (O'Keefe and Burgess, 1996; Jeffery and O'Keefe, 1999), a box-car averaging, or 'smoothing', was also applied to the map. The rate of a particular bin is therefore derived from the total number of spikes fired in that bin and surrounding bins, divided by the total dwell time in that bin and the same surrounding bins. In this thesis the number of bins used for smoothing was 25, meaning that a square with 5-bin-long sides, whose centre is the current bin, was used to smooth the rate of that bin. Only visited bins are considered during smoothing, therefore at the edge of the environment, less than 25 bins would be used.

The firing rate in each bin is represented by colour. 5 colours are used, the rates they represent auto-scaled so that each represents 20% of the peak firing rate. In

descending order, bins with the highest rates are shown in red, then yellow, then green, then light blue, then dark blue for the lowest rates. A white bin represents an area that is unvisited. As previously (O'Keefe & Burgess, 1996), trials in which the peak firing rate fails to exceed 1.0 Hz are deemed not to express a spatial field and are shown as dark blue in all bins.

Quantifying Remapped Representations

The analyses described below are all designed to measure the similarity or difference of two firing rate maps, and therefore assess the degree of remapping in a single place cell. The focus of investigation in this thesis, however, is the behaviour of the place cell population, in particular, is there a coherent place cell representation of space in the hippocampus? The most important level of analysis is, therefore, the individual animal. What are the levels of remapping within each animal, and do each animal's place cell responses react to environmental change in a coherent way? In all Results chapters, individual cells will first be scored for remapping using the methods below, but the nature of the place cell representation will then be assessed by looking at the whole population of simultaneously recorded cells.

Topological transformations

To compare place fields in differently shaped environments it is necessary to transform the data topologically, so that all bins in one map have a spatially corresponding bin in the other. Points in one shape were mapped onto the other by shifting each point along the radius defined by that point, by an amount equal to the ratio of the circumferences of the two shapes at that radius (see also Quirk *et al*, 1992; Sharp, 1997; Lever *et al*, 2002). In order to compare two maps, A and B, positions of bin centres from map A were transformed into the shape of map B. Firing rate values were then assigned, from map B, to the transformed bin positions, by nearest neighbour linear interpolation. The resulting map contained the firing rates of map B, spatially corresponding to the untransformed map A. This procedure avoided systematic changes in firing rate when transforming shapes of different areas.

Comparison of firing rate maps

In order to quantify whether place cells are remapped (see chapter 3), a method of assessing firing rate maps for similarity or difference is required. In this thesis, this is done by correlating the firing rates of spatially corresponding bins from two firing rate maps. Only visited bins, and bins with rate > 0Hz in at least one map, were considered. The resulting correlation coefficient (Pearson's r) is taken as a measure of the similarity of the maps. This method gives a good indication of the similarity or difference of spatially specific firing when a place field is present in at least one map. However, it does not work well when both firing rate maps have no place field (peak rate < 1Hz), giving essentially random values (due to background noise), rather than scoring the maps as similar. For these comparisons, therefore, a peak rate comparison measure was used instead:

R(A,B) = min(peak rate A, peak rate B) / mean(peak rate A, peak rate B)

The correlation coefficient and the peak rate comparison were treated equally in all further analyses described below. For convenience, the raw data on map comparisons will be referred to only as correlation coefficient, r, but this data will also contain peak rate comparisons, for trial pairs both with peak rate < 1 Hz.

Quantifying Remapping: R-Difference

The correlation coefficient, r, gives a measure of the similarity or difference of two maps. In this thesis, however, for a cell to be considered remapped, it must have both a) differing responses to two different environments, and b) similar responses to repeated trials of the same environment. Stability of response to an environment is required to distinguish between place cells that are remapped (i.e. different representations for different environments) and those that simply change firing patterns in different trials. (See chapter 3 for further background on remapping). To combine both of these aspects of cell response, a measure termed "r-difference" was introduced. R-Difference for each cell was calculated as

$$\text{r-difference} = r_{(within)} - r_{(across)}$$

where $r_{(across)}$ was the correlation coefficient derived from comparing firing in different environments, $r_{(within)}$ from comparing firing in repeated trials of the same environment. Cells with larger r-difference were considered more remapped.

In remapping training experiments (chapter 6), in order to investigate temporal trends in remapping, r-difference was calculated for each pair of temporally adjacent trials of different shapes (3 times for 6 trials). $r_{(across)}$ was therefore derived from correlation of this trial pair. $r_{(within)}$ was the maximum of all $r_{(within)}$ scores derived from within-shape comparisons that included one of the $r_{(across)}$ trial pair. The maximum value was used, rather than the mean of all $r_{(within)}$ scores, as changing cell responses were often observed during remapping training, and, to be considered remapped, a cell only had to show a stable response in one environment.

In octagon probe and chimeric shape experiments (chapters 7 and 8, respectively), for ease of interpretation of effects in probe trials, a cell needed to show stable and remapped responses in all baseline trials, in order to be considered for further analysis. For these experiments, therefore, $r_{(across)}$ was the mean r from all correlations between baseline trials of different shapes (square and circle for octagon probe, square and octagon for chimeric shapes). $r_{(within)}$ was the mean r from all comparisons of baseline trials, within shapes.

For all experiments, a threshold value, r-difference ≥ 0.5, was used to classify cells as remapped or non-remapped. This value was chosen on the basis of two considerations. First, it matched well with judgement by eye of whether cells were remapped, in the sense of showing stable, unrelated firing responses (see chapter 3). Second, it was consistent with the observed correlation values for repeated trials of the same shape ($0.7 < r < 0.8$), and unrelated fields ($-0.2 < r < 0.2$). In order to be considered remapped, therefore, a place cell needed to show clearly stable responses within an environment, and clearly divergent responses to a different environment.

Statistical Analysis of Remapping

In order to investigate levels of remapping in the recorded cell population, Analysis of Variance (ANOVA) was used to compare $r_{(within)}$ and $r_{(across)}$ during remapping training, and compare r-difference between different trials. However, it is not always valid to use parametric tests on Pearson's r data: samples with consistently high correlations produce skewed distributions of r-values. Before using ANOVA, therefore, Fisher's z-transform was applied to all r-values:

$$z = (\ln[\ (1 + r) / (1 - r)\ ]) / 2$$

ANOVA analysis of r-difference was not applied to 'raw' r-difference ($r_{(within)} - r_{(across)}$), but, rather, r-difference derived from the z-transform values of $r_{(within)}$ and $r_{(across)}$.

Note that z-transform data were only used for statistical analyses. All data shown in figures is untransformed r or r-difference.

Similarity Score

In the octagon probe and chimeric shapes experiments, probe trials consisted of environments intermediate between the two familiar baseline environments. It was of interest to what extent the place cell response to the probe trial was similar to the responses in either of the baseline environments. This was quantified as the similarity score of the cell on that probe trial. If baseline environments are defined as A and B, the similarity, s, to baseline A on probe trial P is

$$s(P, A) = (r_{(PA)} - r_{(AB)}) / (r_{(AA)} - r_{(AB)}),$$

where $r_{(PA)}$ is the correlation of the probe response and the baseline A response, $r_{(AB)}$ is the mean $r_{(across)}$ for the cell, and $r_{(AA)}$ is mean within shape correlation for baseline A. $s = 1$ indicates a firing as similar to A as repeated trials of A are to themselves. $s = 0$ indicates firing as different from that in baseline A as the firing in baseline B is

As non-similarity to A is not necessarily similarity to B, two similarity scores were calculated for each cell, similarity to baseline A and similarity to baseline B. Similarity to B, for probe trial P, would be

$$s(P, B) = (r_{(PB)} - r_{(AB)}) / (r_{(BB)} - r_{(AB)}).$$

Comparison of time-interval maps

For analysis of 10s intervals (figures 7.8, 7.9), the similarity measure is applied as above, using the firing rate map derived from the 10s interval for trial P and the full duration rate maps for baseline trials A and B (in this case, Square and Circle). The similarity score is therefore a measure of the similarity of interval firing to full trial duration firing. The correlation r is used in all cases (peak-rate similarity *R* cannot be used as the animal does not adequately sample the environment in 10s, often missing the centre of the place field). Cells that fired no spikes in the given intervals for a given shape are omitted from the similarity data for that interval and shape. Note that the similarity of a 10s interval in the Square to Square baselines is less than 1.0 (and its similarity to Circle baselines less than 0.0) due to the greater noise in these maps than in full duration maps.

The similarity-difference (SD) score was calculated as

$$s(P, A) - s(P, B),$$

for each cell, in each trial, at every time point. This gives a unitary score of whether cells display a square-like or circle-like response, ranging from 1 (square-like) to -1 (circle-like). SD = 0 indicates an intermediate representation. In order to look for trends in place cell responses over time, a linear regression was performed on SD versus time point. The regression analysis was performed for individual trials, and for data from several trials of the same shape grouped together.

Chapter 6

Results: Remapping Training

Previous studies have shown that, when presented with environments that differ only in shape (e.g. a square and a circle), place cells are non-remapped on initial exposure, and become remapped over a long period, days or weeks of daily exposure to the environments (Lever *et al*, 2002). The present study investigated the effect on remapping of initial exposure to environments that, in addition to shape, differed also in colour and material.

Experimental Design

The experimental protocol is shown in Figure 6.1. On each day, the rat was given six 10 minute long trials, three in the square and three in the circle, in alternating order. The square environment was constructed using the morph box ('morph square') for all trials on all days. For the first three days of training, the circular environment was made of wood, with a smooth interior surface painted white ('white circle'). During these days, therefore, visual, tactile and olfactory cues differentiated the walls of two environments, in addition to their shape. For rats 2, 3, and 4, the remapping training described here was the first exposure to any environment in the curtained arena area of the laboratory (see methods). Rat 1 was pre-exposed to (only) the morph square environment, for four 10 minute trials, on the day immediately preceding the remapping training.

The next stage of the training, Days 4-6, was designed to test whether any remapping produced during Days 1-3, in response to multi-modal environmental differences, would then transfer to square and circle environments that differed only in their shape. From Trial B on Day 4 onwards, therefore, a circle constructed using the morph box ('morph circle') replaced the white circle (see Figure 6.1B).

This chapter will focus on the two most important days of this training schedule: first exposure to different environments (day 1) and transfer to morph only environments (day 4).

Figure 6.1

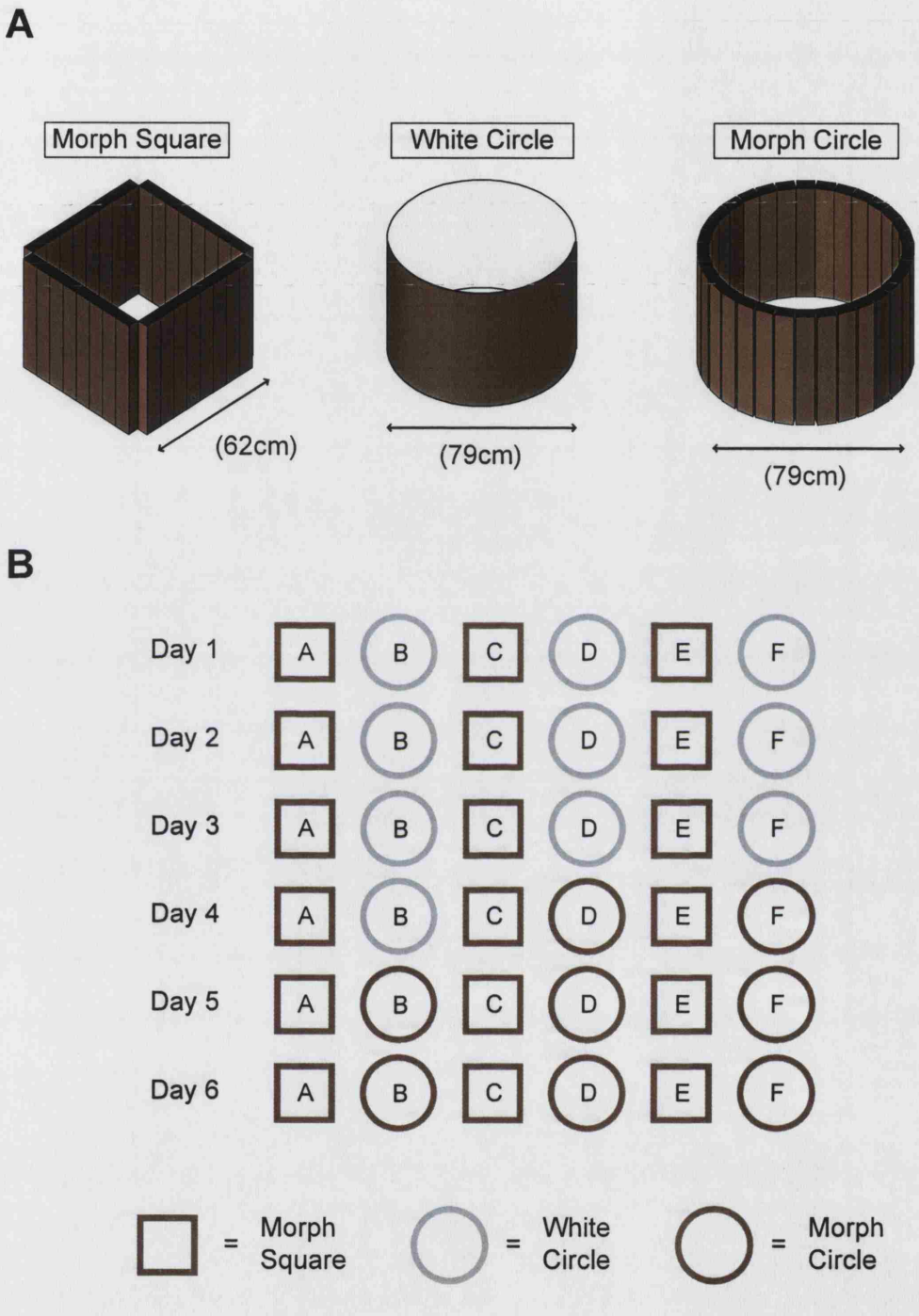

Figure 6.1. Remapping training protocol. **A)** Illustrations of environments used. Morph square and morph circle are constructed using the same morph box environment. The interior surface of the morph box is masking tape, the interior surface of white circle is matt-finish white paint. **B)** Trial running order during the 6 days of remapping training. Each shape represents a trial. Outline colour represents environment type (white vs morph), shape represents environment shape. Letters in shapes show temporal running order. All trials 10 min duration, all inter-trial intervals 20 min.

Fast remapping between environments differing in shape and colour.

Firing rate maps for Day 1 of training for each rat are shown in Figures 6.2, 6.3, 6.4 and 6.5 (rats 1, 2, 3 and 4, respectively). Inspection by eye shows that, by the end of Day 1, the majority of place cells have remapped between the morph square and the white circle.

Remapping takes different forms in different cells. Concentrating on place cell behaviour in Rat 2 (Figure 6.3), for example, it can be seen that some cells, such as cell 6 and cell 9, appear remapped from the first exposure to the white circle. Place fields are already different between trial A and trial B. These remapped place fields are then relatively stable throughout the rest of Day 1. The place fields of other cells change over the course of the day. Some, for example cell 2 and cell 4, are not remapped between trials A-B but become remapped through the day. Others, for example cell 3, are already different on trials A-B and continue to change through the day. A minority of cells do not remap, for example cell 12. Of those cells not remapped by the end of day 1 training, some are remapped at the beginning of training, but converge onto a common representation (for example, cell 11). This heterogeneity in place cell remapping responses can also be seen in the other three rats (see Figures 6.2, 6.4, 6.5).

The proportion of cells remapped by the end of day 1 training varies across animals, but, generally, a majority of cells are remapped. The lowest proportion of remapped cells is 50%, in rat 3. Rats 1, 2 and 4 have 83%, 69% and 77% of cells remapped by the end of day 1, respectively. (Criteria to consider a cell remapped is $r_{(within)} - r_{(across)} > 0.5$, where $r_{(within)}$ is correlation between rate maps in the same shape, and $r_{(across)}$ is the correlation between rate maps in different shapes, see below and Methods for details).

Presented with environments differing in shape and colour, therefore, place cells show heterogeneous responses. The majority of cells remap after six trials of 10 minutes each, much faster than the remapping previously seen in response to differing shape alone. Within the category of remapped cells, there are differing degrees of plasticity or learning, with some cells showing the same responses to square or circle for all trials, while others change throughout the day.

Figure 6.2

Figure 6.2. Firing rate maps for all cells recorded from rat 1 during day 1 remapping training. All cells simultaneously recorded. Each row shows one cell, each column shows one trial. Shape diagrams at the top of each column represent environment shape and colour. Letters within shapes show temporal running order. Firing rate maps are false-colour coded, blue = lowest rate, red = highest rate, auto-scaled to peak firing rate. Peak rate is shown as white text on each map (see methods). 10 cells were remapped by the end of day 1; 4 with changing place responses (cells 1-4), 6 with constant place responses (5-10). 2 cells did not reach the criterion for remapping (11-12) (see methods).

Figure 6.3

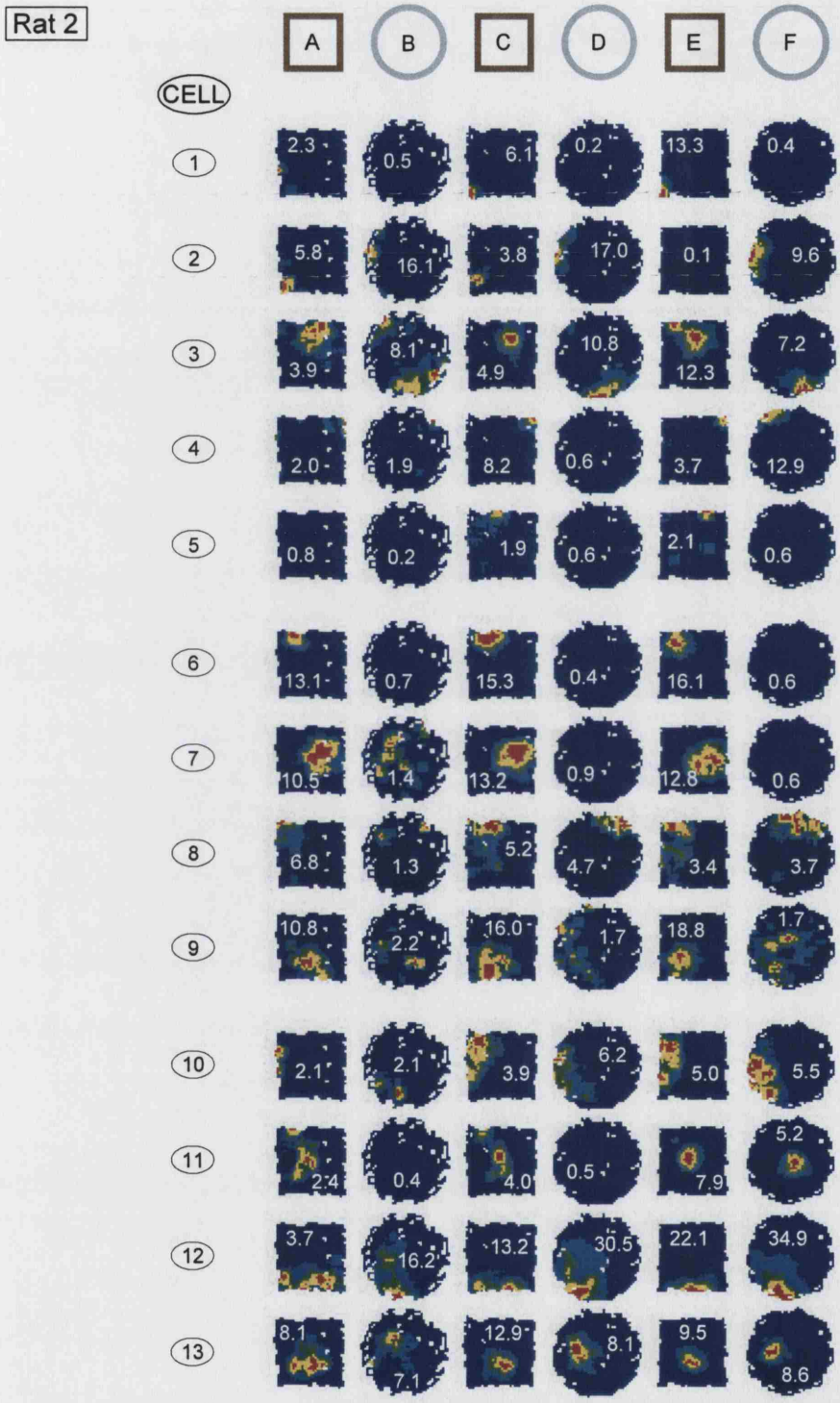

Figure 6.3. Firing rate maps for all cells recorded from rat 2 during day 1 remapping training. All cells simultaneously recorded. Details and layout of firing rate maps as for figure 6.2. 9 cells were remapped by the end of day 1; 5 with changing place responses (cells 1-5), 4 with constant place responses (6-9). 4 cells did not reach the criterion for remapping (10-13) (see methods).

Figure 6.4

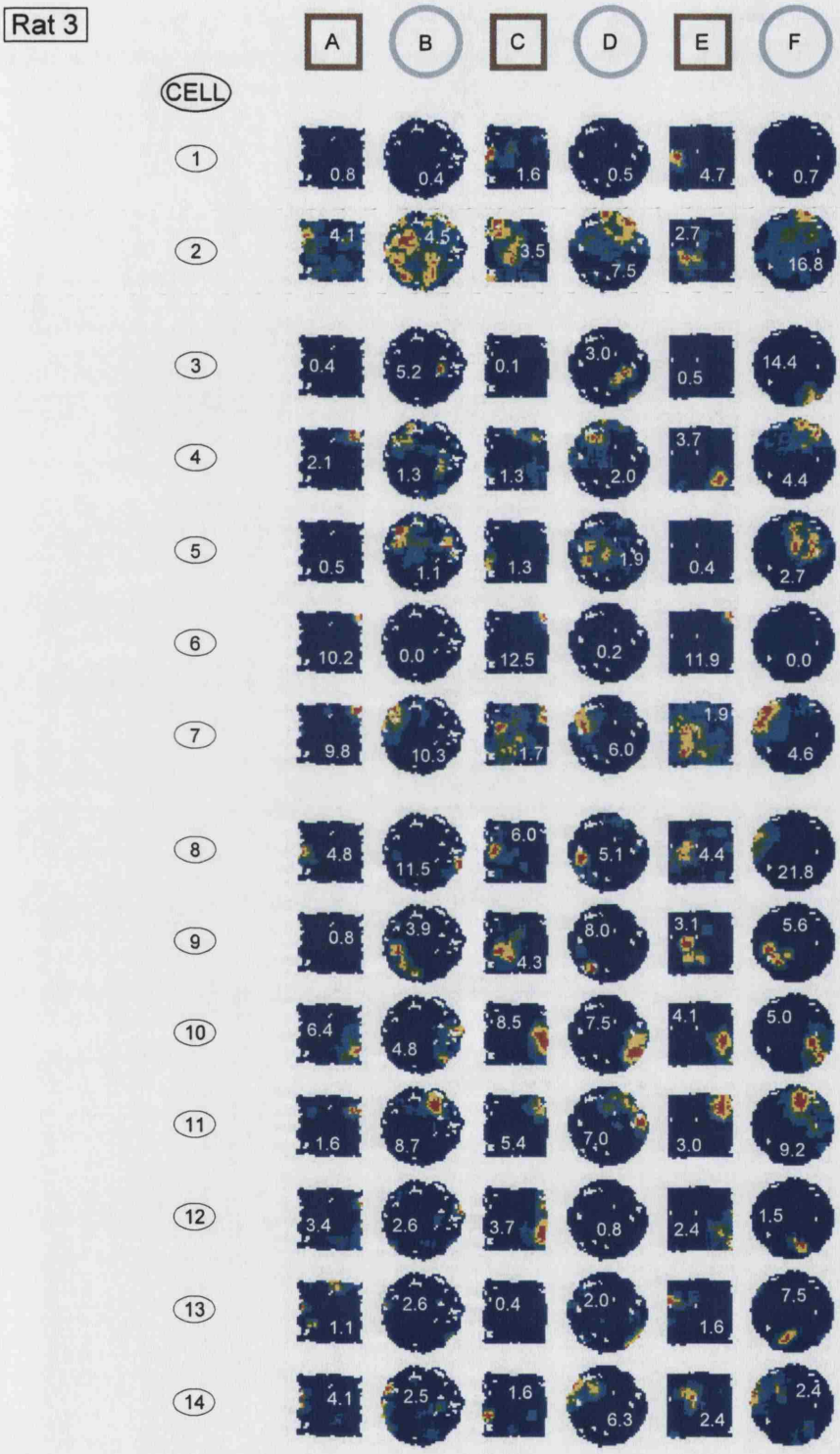

Figure 6.4. Firing rate maps for all cells recorded from rat 3 during day 1 remapping training. All cells simultaneously recorded. Details and layout of firing rate maps as for figure 6.2. 7 cells were remapped by the end of day 1; 2 with changing place responses (cells 1-2), 5 with constant place responses (3-7). 7 cells did not reach the criterion for remapping (8-14) (see methods).

Figure 6.5

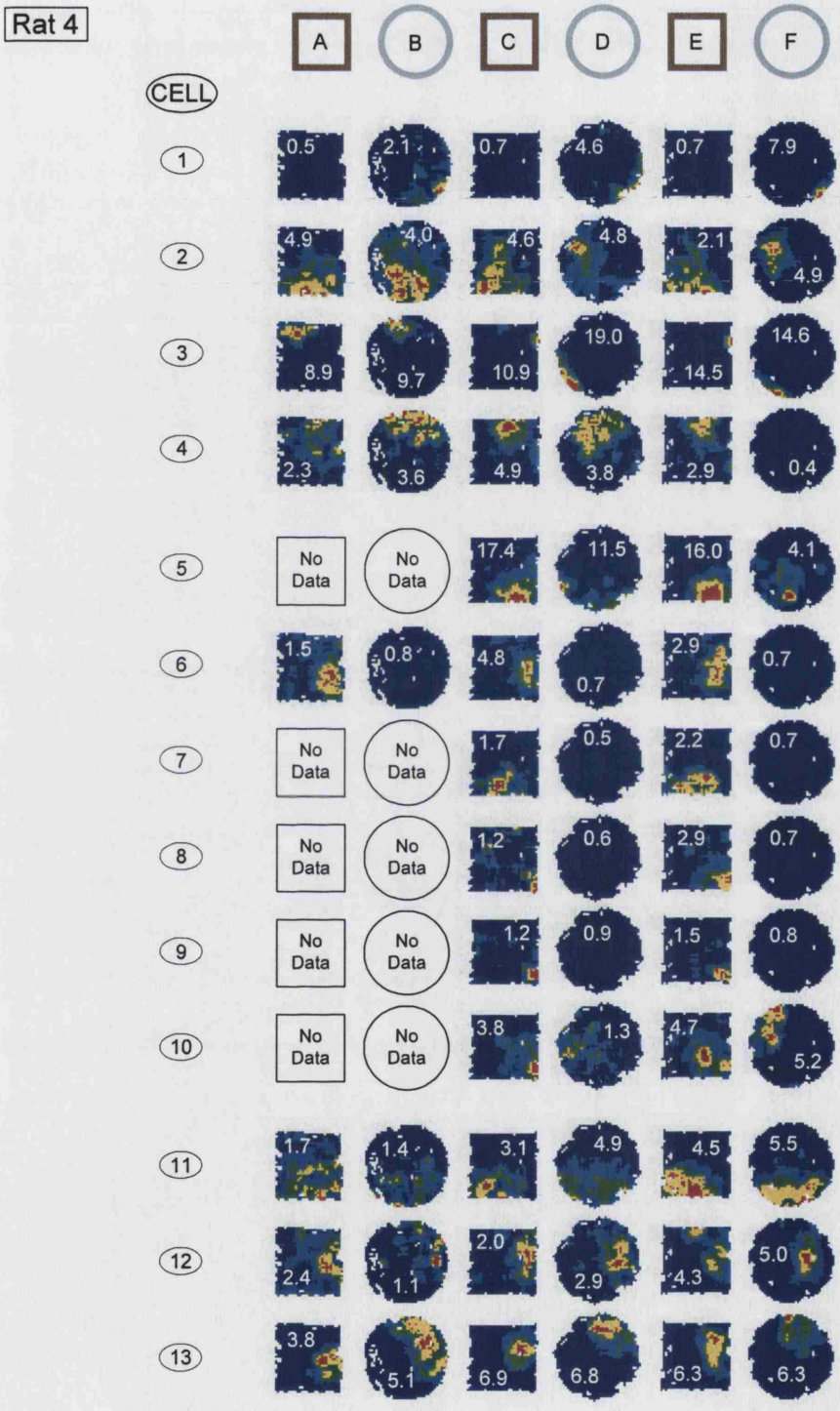

Figure 6.5. Firing rate maps for all cells recorded from rat 4 during day 1 remapping training. All cells simultaneously recorded. Details and layout of firing rate maps as for figure 6.2. Where blank outline maps are shown, no data was available (due to tetrode drift). 10 cells were remapped by the end of day 1; 4 with changing place responses (cells 1-4), 6 with constant place responses (5-10). 3 cells did not reach the criterion for remapping (11-13) (see methods).

Correlation of place fields, within shape and across shape

In order to quantify place cell remapping, a measure of the similarity or difference of place fields is needed. The measure used in this thesis will be correlation of spatially corresponding firing rate values (see methods for details). High correlation co-efficients (Pearson's-r) indicate similar place fields, low r values indicate different fields.

The first measure considered is the across shapes correlation index (referred to as r-across). This measures the similarity of firing between square and circle rate maps. For each cell recorded during Day 1, three r-across values were calculated, for each of the three pairs of square-circle trials (trials A vs B, trials C vs D, trials E vs F). Comparing the three values gives a measure of the dynamics of remapping during the day. The r-across values for individual cells, together with the mean and ± standard error of the mean (±SEM), over all cells, are plotted in Figure 6.6 (separate plots are shown for each rat).

Figure 6.6 illustrates, in a quantitative way, the divergence of place field responses described above. First, it is clear that the r-across values are low by the end of the day (trials E vs F). The mean r-across values, for each rat, never exceed 0.2, indicating a high level of divergence between the square and circle firing rate maps. Looking at the cell-by-cell r-across values (following individual colour coded lines in Figure 6.6) it can be seen that each cell responds differently to the manipulation (some cells differentiate immediately between square and circle, while for some others this occurs during the course of training). In the case of Rat 1 and Rat 4 a clear downward trend in the mean r-across values can be seen, confirming that even at a population level, divergence is increasing during the course of the day. (Note, however, that in rat 4, most cells stable over trials C-F are missing data for trials A-B, which could be the cause of an artefactual downward trend in the mean).

The r-across values only show the degree of divergence between the square and circle representations. However, high divergence across shapes does not discount the possibility that cellular responses are divergent even within shape, with no consistent square or circle hippocampal representation emerging. In order to quantify the degree of stability of firing patterns within shapes, an r-within correlation measure was calculated. The r-within measure is the Pearson's r value derived from the

Figure 6.6

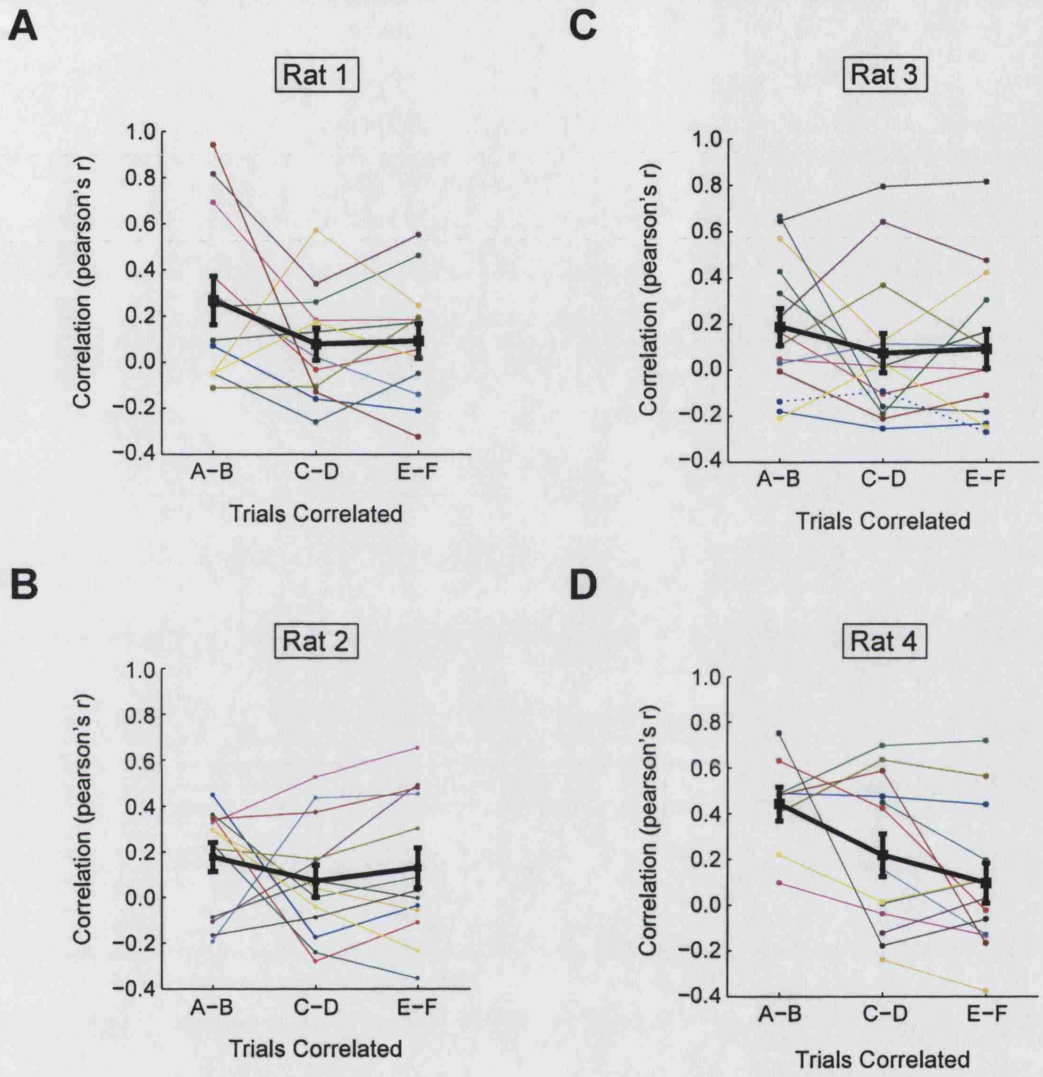

Figure 6.6. Correlation between square and circle firing rate maps, day 1. Pearson's-r is calculated for three different trial-to-trial comparisons for each cell; trial A vs B, trial C vs D, trial E vs F (see methods for details). Thin, coloured lines show r values for individual cells. Bold, black lines show mean r value and ±SEM for each comparison. Each plot shows correlations for all recorded cells in a rat. **A**) Rat 1, **B**) Rat 2, **C**) Rat 3, **D**) Rat 4.

correlation between the firing rate maps of all temporally adjacent same shape trials (trials A vs C, trials C vs E for the square; trials B vs D, trials D vs F, for the circle). Figure 6.7 shows the r-within values for individual cells together with their mean and SEM values, in separate plots for each rat. For each plot the two leftmost values refer to the square-square correlations, the rightmost to the circle-circle correlations.

The plots in Figure 6.7 show a clear pattern for rats 1, 2 and 4, whereby the overall intra-shape stability is higher for the square-square comparisons, than for the circle-circle ones. The highest r-within values for square-square comparisons are those for rat 1, possibly reflecting the more extensive experience this rat had in the square morph environment (pre-exposure day, see above). Another clear trend, common to these three rats, is that the r-within values for the first circle-circle comparison (trials B vs D) are lower than those for the second comparison (trials D vs F). This reflects the fact that the majority of any change in place cell representations seems to happen between first and second exposure to the wooden circle (see also Figure 6.2, 6.3 and 6.5 for the firing rate maps).

Rat 3 shows a different pattern of results, with a wide spread of r-within values across cells, and average r-within values lower than those shown by the other three rats. Moreover, for rat 3, no difference between the circle and square intra-shape stability is observed. Place cells in rat 3 therefore show less stable responses to repeated trials of the same shape.

To investigate differences between correlations, both within shape vs across shape, and changes over time, a two-way repeated measures ANOVA was run. The groups compared were; across correlations from the beginning and end of training (A vs B and E vs F, respectively), mean within correlations from the beginning and end of training (mean of A vs C, B vs D and mean of C vs E, D vs F, respectively). As Pearson correlation coefficients may not be normally distributed, the ANOVA was run on the z-transform of the r values (see Methods). The results are summarised in Table 6.1, below. All four rats showed a highly significant difference between within and across correlations ($p < 0.005$), but 3 showed no effect of time. Only rat 4 also showed a significant interaction of time and within *versus* across correlations. r-within increased during training, while r-across decreased (see Figures 6.6D and 6.7D for plots of r-values).

Figure 6.7

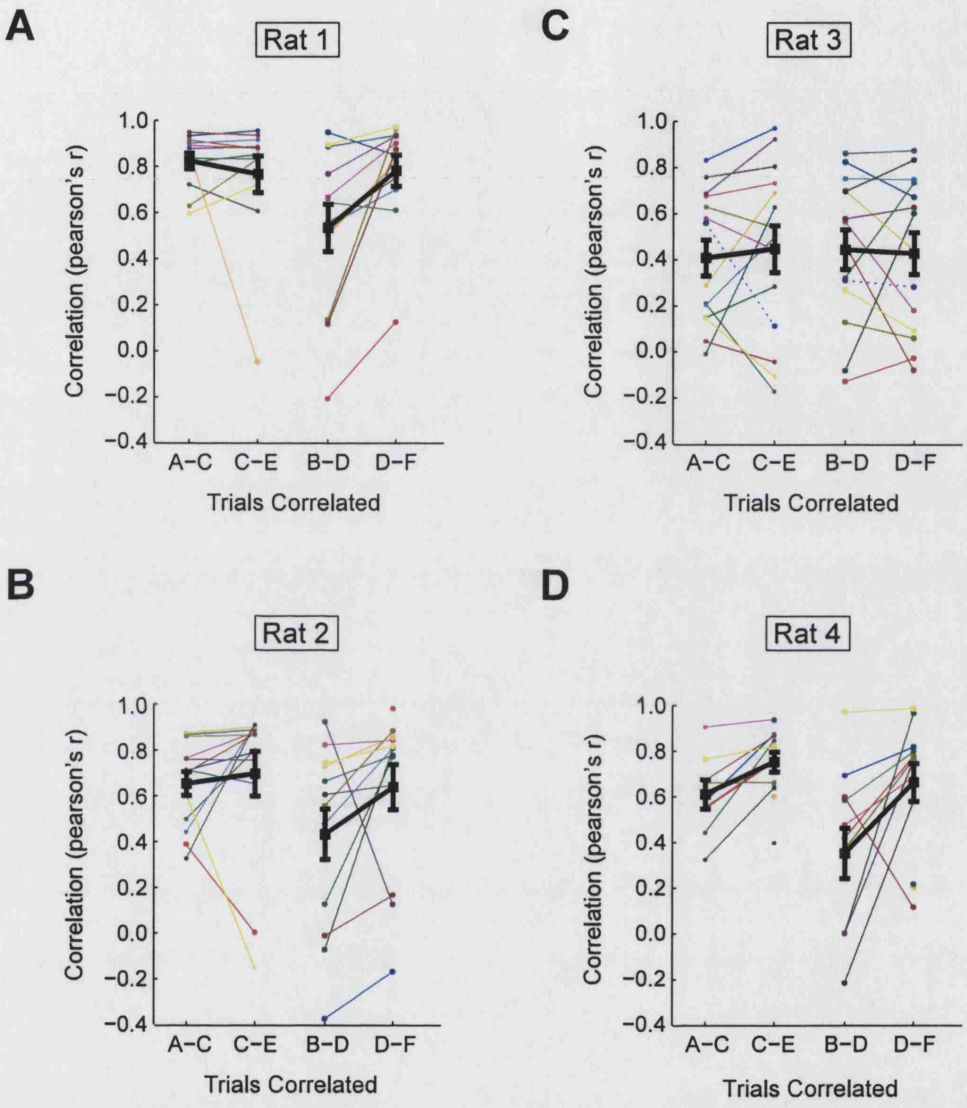

Figure 6.7. Correlation between firing rate maps, within shapes, during day 1. Pearson's-r is calculated for two square-to-square comparisons (trial A vs C, trial C vs E, left-hand side of each plot) and two circle-to-circle comparisons (trial B vs D, trial D vs F, right-hand side of each plot). Thin, coloured lines show r values for individual cells. Bold, black lines show mean r value and ±SEM for each comparison. Each plot shows correlations for all recorded cells in a rat. **A**) Rat 1, **B**) Rat 2, **C**) Rat 3, **D**) Rat 4.

Table 6.1

ANOVA summary, effect of within-across shape comparisons and time on Z-transform of correlation coefficient.

	Effect	Degrees of Freedom (Trials, Error)	F	p
Rat 1	Within-Across*	2,11	18.01	0.001
	Time	2,11	2.47	0.144
	Interaction	2,11	1.49	0.247
Rat 2	Within-Across*	2,12	22.0	0.001
	Time	2,12	0.1	0.979
	Interaction	2,12	0.1	0.916
Rat 3	Within-Across*	2,13	9.91	0.009
	Time	2,13	1.23	0.290
	Interaction	2,13	2.30	0.157
Rat 4	Within-Across*	1,7	9.69	0.021
	Time	1,7	0.52	0.497
	Interaction*	1,7	8.10	0.041

* Effect significant at $p > 0.05$ level

Quantification of overall remapping: r-difference

In order to give an overall score of remapping to each cell, the r-across and r-within measures were combined. This measure, named r-difference, is calculated as (r-within) - (r-across) for each cell, for each comparison of trials. The motivation for this measure is that, to be considered remapped, a place cell must have both a stable response within repeated trials of a particular environment, and a divergent response to the dissimilar environment. R-difference was calculated at three different points during day 1 training. For each of these, r-across was r(A vs B), r(C vs D) and r(E vs F), for the first, second and last comparisons respectively. For each comparison, r-

within was taken as the maximum of all r-within scores relating to the trials of the r-across pair (see Methods for further details).

Figure 6.8 shows the r-difference plot for each rat. The r-difference measure reiterates the pattern of results visible in the firing rate maps. Scores for individual cells show a heterogeneity of responses, with some cells showing constant r-difference scores through the course of training, and others increasing (or decreasing) over the day. In order to quantify numbers of cells remapped, all cells with an r-difference greater than a 0.5 threshold were considered remapped (for details of threshold selection, see methods). The division of cells into remapped and non-remapped categories in Figures 6.2 - 6.5 was determined by whether the r-difference of cells for trials E vs F was greater than this threshold.

All rats have a cell population mean r-difference of greater than the 0.5 threshold by the end of training. Population mean r-difference scores, by the end of training, are highest in rats 1, 2 and 4. The lower mean score for rat 3 reflects the overall lower levels of remapping. Interestingly, lower levels of remapping in rat 3 appear primarily due to a lack of within shape stability: r-across values are as low as for other rats, but r-within values are spread over a much wider range, with a lower mean (see Figures 6.6C, 6.7C). This is reflected in the firing rate maps (Figure 6.4) for non-remapped cells 8, 12 and 13. Representations are divergent between square and circle, but there is a lack of intra-shape response stability.

The r-difference score also highlights the fact that some cells become more remapped during training. Those cells classified as changing their responses during training, in Figures 6.2 - 6.5, were those whose r-difference score for trials A vs B was 0.4 greater than that for E vs F. (Three exceptions were made; cell 3 (rat 1), cell 1 (rat 2), cell 1 (rat 4). These cells were classified changing their responses despite r-difference not increasing. All three increased firing rate in the place field, not well detected by correlation measures).

Despite some individual cells becoming more remapped, the only clear upward trend at the population level is in rat 4. This was confirmed by a one-way repeated measures ANOVA, results of which are summarised in Table 6.2, below. (As r may not be normally distributed, ANOVA was run on an r-difference composed of the z-transformed r-within minus the z-transformed r-across scores. See Methods). The effect of trials compared on the mean difference was significant only for rat 4. When the three conditions were compared using related samples t-tests, and a

Figure 6.8

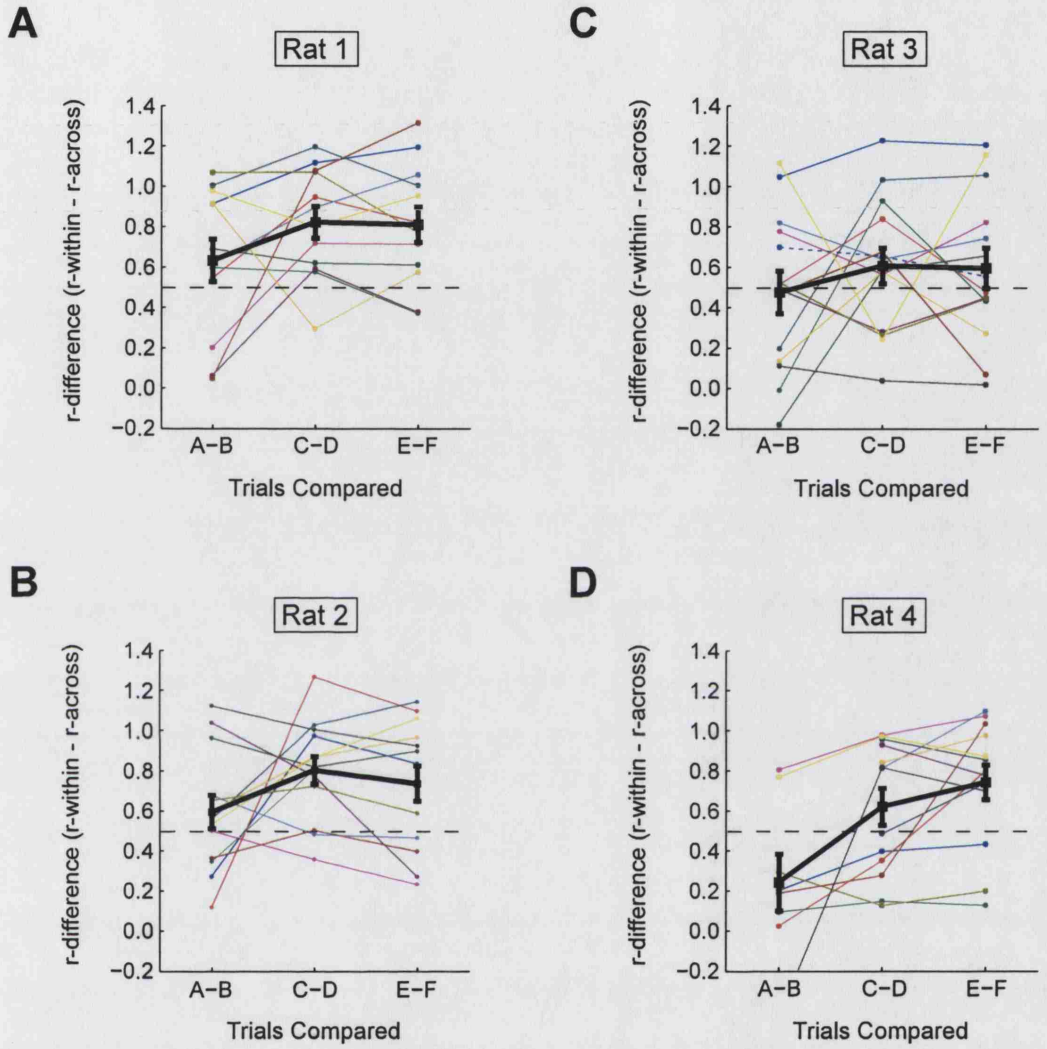

Figure 6.8. R-difference score (r-within - r-across) for all cells for each rat, day 1. R-difference is calculated for three different trial-to-trial comparisons for each cell; trial A vs B, trial C vs D, trial E vs F (see methods for details). Thin, coloured lines show values for individual cells. Bold, black lines show mean r-difference and ±SEM for each comparison. Black dashed line at r-difference = 0.5 indicates threshold for classifying cells as remapped. Each plot shows correlations for all recorded cells in a rat. **A**) Rat 1, **B**) Rat 2, **C**) Rat 3, **D**) Rat 4.

Bonferroni correction applied, the only significant difference was found between r-difference(A vs B) and r-difference(E vs F) ($t = -2.6$, $df = 7$, $p = 0.035$).

Table 6.2

ANOVA summary, effect of trials compared on r-difference score, day 1.

	Degrees of Freedom (Trials, Error)	F	p
Rat 1	2,22	2.17	0.160
Rat 2	2,24	1.86	0.195
Rat 3	2,26	0.69	0.76
Rat 4	2,14	6.43*	0.01

* Effect significant at $p > 0.05$ level

Proportions of Cells Active in Each Environment

It has been reported that approximately 40% of all CA1 cells are active in any environment (Wilson & McNaughton, 1993; Guzowski *et al*, 1999). Although in this study estimates of the total number of cells were not taken (e.g. by recording during slow-wave sleep), it is possible to compare the proportions of recorded cells active in each environment. However, it should be noted that the proportions of recorded cells will be higher than the proportions of total cells. If two subsets, each comprising an independent 40% of all cells, are active in each environment, 16% should be active in both (as $0.4 \times 0.4 = 0.16$). However, only 64% of cells will fire in either environment at all ($0.4 + 0.4 - 0.16 = 0.64$). In each environment, therefore, 63% (0.4/0.64) of all recorded cells would be expected to be active.

Table 6.3 shows the counts and proportions of cells active in each environment. These data are taken from the trials A and B of day 4 remapping training, after 3 days of training in morph square and white circle.

Table 6.3

Proportions of remapped cells firing in each environment.

	Total Cells	Total active in Square	Total Active in Circle
N Cells			
Rat 1	10	10	5
Rat 2	16	11	13
Rat 3	12	9	9
Rat 4	11	9	9
As % of Total			
Rat 1		100	50
Rat 2		69	81
Rat 3		75	75
Rat 4		82	82
Overall Mean		**81**	**72**

It can be seen that the proportions of recorded cells active in each environment are greater than the 63% predicted if 40% of all cells were to be active in each environment. (81% in the square, 72% in the circle). It is possible, therefore, that more than 40% of all cells are active in each remapped representation. It is also possible, however, the active subsets in each environment are not independent, and overlap by more than $p_{(active)}^2$ (where $p_{(active)}$ is the probability of each cell being active in an environment). This would result in less of the whole cell population being recorded in either of the two environments, and therefore a higher proportion of the recorded cells being active in each environment.

Almost All Remapping Occurs During Day 1

In some circumstances, remapping involves a learning process, in the sense that place cells change their responses some time after first presentation of the novel stimulus (Bostock *et al*, 1991; Lever *et al*, 2002). In this study, learning has been shown, in some cells, over the course of day 1. It is also possible to ask whether there is further learning over repeated days of training. Full data sets for days 2 and 3 will

not be presented here, as, in many cases, place cell data does not exist, or consists of few cells. However, a rough estimate of changes in the amount of remapping can be given by comparing the last trials of day 1, and the first trials of day 4 (transfer test day, see below for details). Table 6.4 shows the proportions of recorded cells remapped on day 1, trials E and F, and on day 4, trials A and B. It can be seen that, for rats 1, 2 and 4, the proportions of cells remapped are almost the same at these times. Only rat 3 shows a small increase, from 50% to 67%. Almost all remapping that occurs, therefore, happens during training on day 1.

Table 6.4

Proportions of place cells remapped on Trials E-F, Day 1 and Trials A-B, Day 4

	Day 1			Day 4		
	N Cells Recorded	N Cells Remapped	%	N Cells Recorded	N Cells Remapped	%
Rat 1	12	10	**83**	10	8	**80**
Rat 2	13	9	**69**	16	11	**69**
Rat 3	14	7	**50**	12	8	**67**
Rat 4	13	10	**77**	11	9	**82**

Remapping persists when only environmental shape differs.

The two environments used in the remapping training during days 1 to 3 (morph square and wooden circle) differ in several ways: shape, wall material, texture and smell. In order to investigate which of these is responsible for producing or maintaining the divergent hippocampal representations, on the fourth day rats were exposed to the morph circle (referred to as "transfer test"). If environmental shape were to be responsible for inducing, or at least maintaining, the remapping observed during days 1-3, then one would expect that the white circle and morph circle place cell representations would be similar (referred to as "transfer"). If, on the other hand, environmental features other than shape are maintaining remapping, firing patterns in white and morph circle should be dissimilar. Morph square and morph circle place cell firing patterns would be expected to converge to a common representation.

Figures 6.9 - 6.12 show the firing rate maps for the transfer test day for each rat. The overall pattern observed is that, in the majority of remapped cells, white and morph circle firing patterns are similar (compare trial B with trials D and E): place cell representations did transfer between white circle and the morph circle. Differing environmental shape is, therefore, sufficient to maintain the remapping between the place representations.

Looking in more detail at the data for each rat, it can be seen that in the case of rats 2 and 4, almost complete transfer occurred. Place cells for each rat have been classified into four groups; stably remapped, becoming remapped during training (diverging), becoming non-remapped during training (converging), and stably non-remapped (classification based on r-difference for each cell, see below). Within these two rats, only one cell was classified as converging (cell 9, rat 4) - all other remapped cells transferred their remapped firing patterns from white circle to morph circle. Furthermore, the only cells from rat 2 to change firing pattern during transfer test training became more remapped (cell 12, 13). Within these two rats, therefore, overall high levels of remapping (81% and 88% cells remapped from rats 2 and 4, respectively) were maintained during white to morph transfer test.

A more complex set of results was apparent for rats 1 and 3. In these animals, although a majority of remapped cells remained remapped during training, a substantial proportion converged to a non-remapped representation. (3/8 remapped cells converged in both rat 1 and rat 3; cells 7, 8 and 9 in rat 1, cells 7, 8 and 9 in rat 3). The overall proportion of remapped cells at the end of training was lower in these two animals, rat 3 having the lowest proportion of all, due to a larger number of stably non-remapped cells. (60% and 50% cells remapped from rats 1 and 3, respectively). In these two animals, therefore, replacing the white circle with the morph circle induced a partial convergence of the place cell representation.

Transfer of remapping: quantification

In a manner similar to the quantification of day 1 remapping training, r-across and r-within values were calculated for each cell during transfer test training. Figure 6.13 shows the r-across values for individual cells, along with the mean and SEM

Figure 6.9

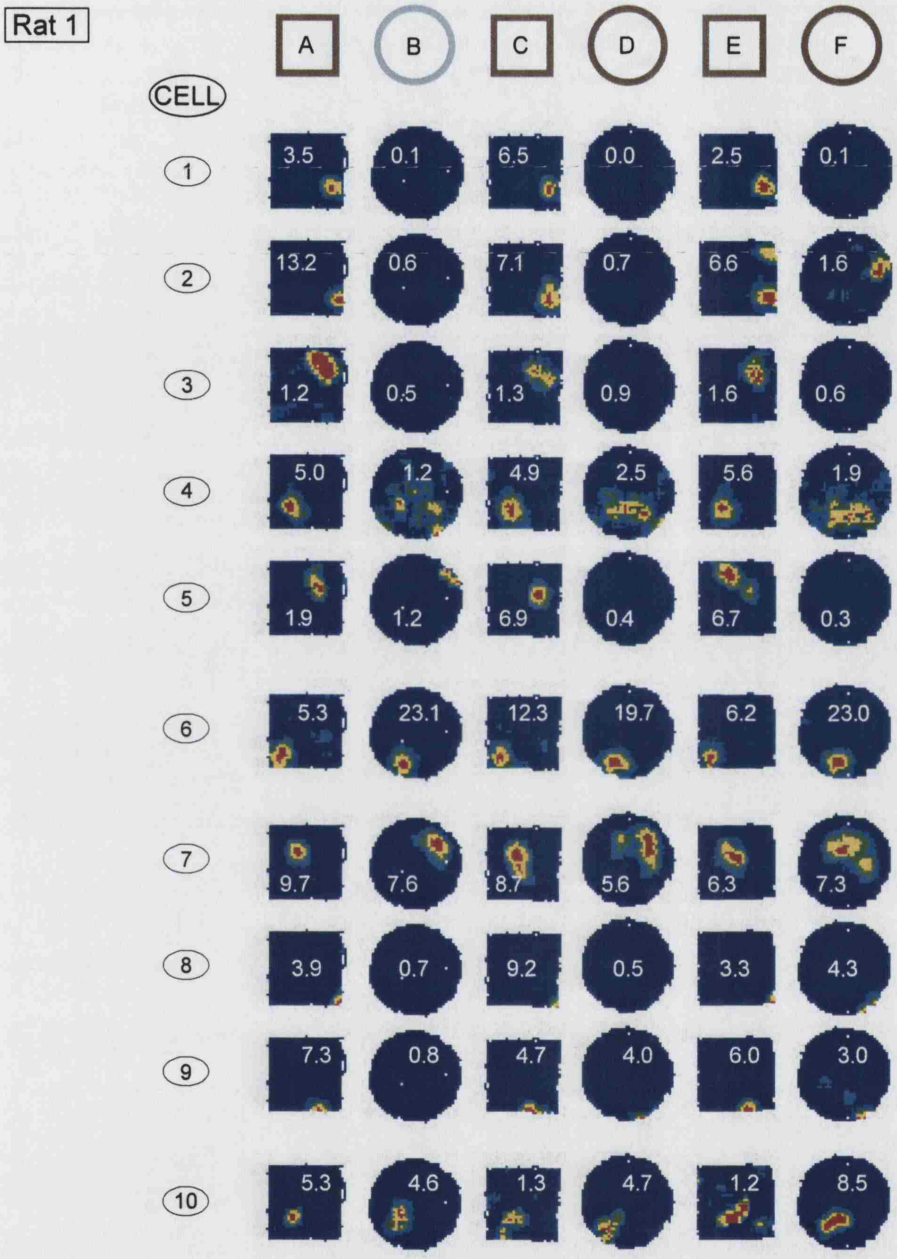

Figure 6.9. Firing rate maps for all cells recorded from rat 1 during transfer day of remapping training. All cells simultaneously recorded. Details and layout of firing rate maps as for figure 6.2. Note switch from white circle to morph circle, between trials B and D. 6 cells were remapped by the end of training; 5 remapped throughout the day (cells 1-5), 1 remapping during the course of training (cell 6). 4 cells were non-remapped by the end of training; 3 converging to a non-remapped response during training (7-9), 1 non-remapped throughout the day (cell 10). For details of classification criteria, see main text and methods.

Figure 6.10

Figure 6.10. Firing rate maps for all cells recorded from rat 2 during transfer day of remapping training. All cells simultaneously recorded. Details and layout of firing rate maps as for figure 6.2. Note switch from white circle to morph circle, between trials B and D. 13 cells were remapped by the end of training; 11 remapped throughout the day (cells 1-11), 2 remapping during the course of training (12-13). 3 cells were non-remapped by the end of training; all were non-remapped throughout the day (14-16). For details of classification criteria, see main text and methods.

Figure 6.11

Figure 6.11. Firing rate maps for all cells recorded from rat 3 during transfer day of remapping training. All cells simultaneously recorded. Details and layout of firing rate maps as for figure 6.2. Note switch from white circle to morph circle, between trials B and D. 6 cells were remapped by the end of training; 5 remapped throughout the day (cells 1-5), 1 remapping during the course of training (cell 6). 5 cells were non-remapped by the end of training; 3 converging to a non-remapped response during training (7-9), 3 non-remapped throughout the day (10-12). For details of classification criteria, see main text and methods.

Figure 6.12

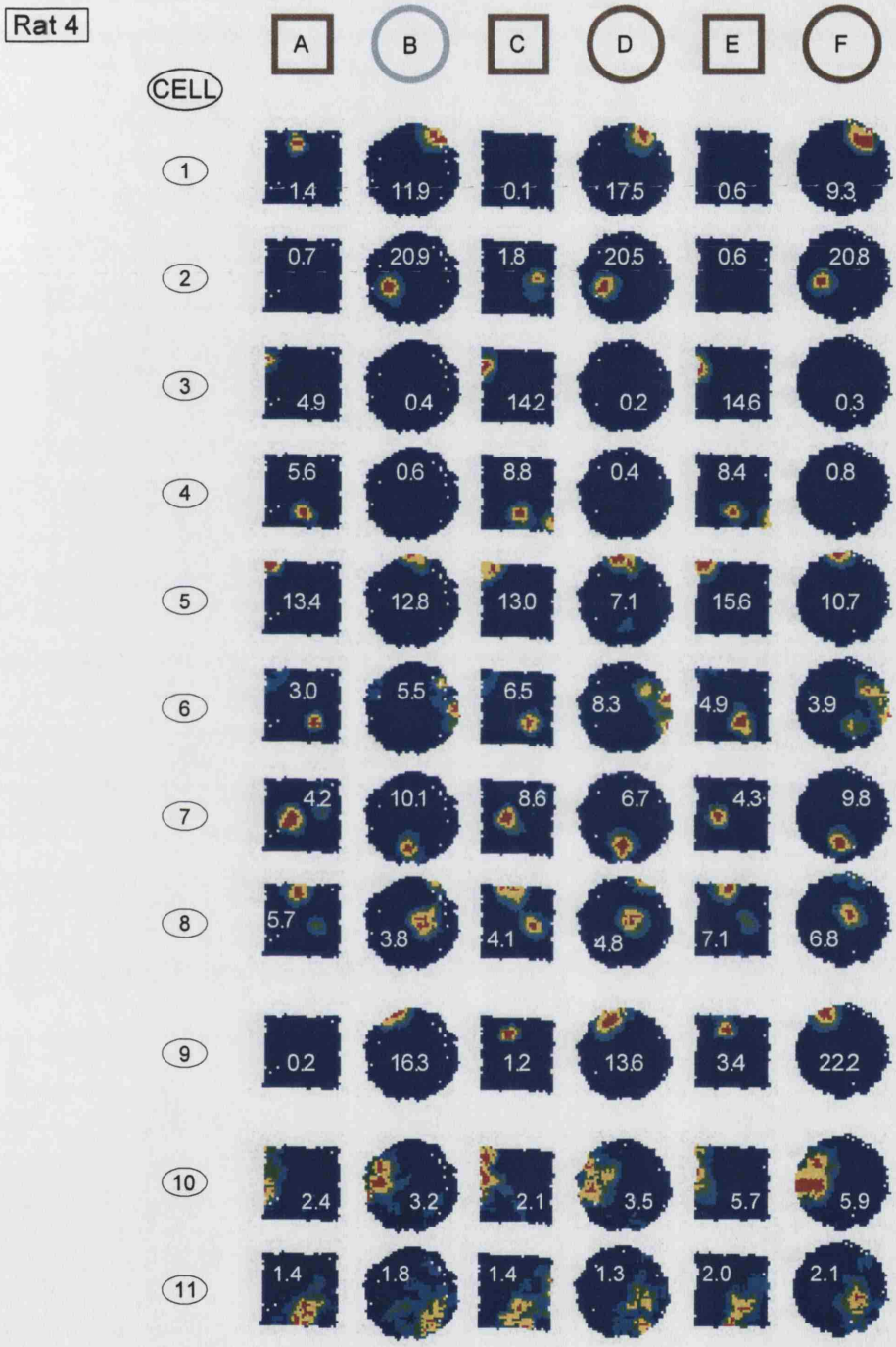

Figure 6.12. Firing rate maps for all cells recorded from rat 4 during transfer day of remapping training. All cells simultaneously recorded. Details and layout of firing rate maps as for figure 6.2. Note switch from white circle to morph circle, between trials B and D. 8 cells were remapped by the end of training; all were remapped throughout the day (cells 1-8). 3 cells were non-remapped by the end of training; 1 converging to a non-remapped response during training (cell 9), 2 non-remapped throughout training (cells 10-11). For details of classification criteria, see main text and methods.

Figure 6.13

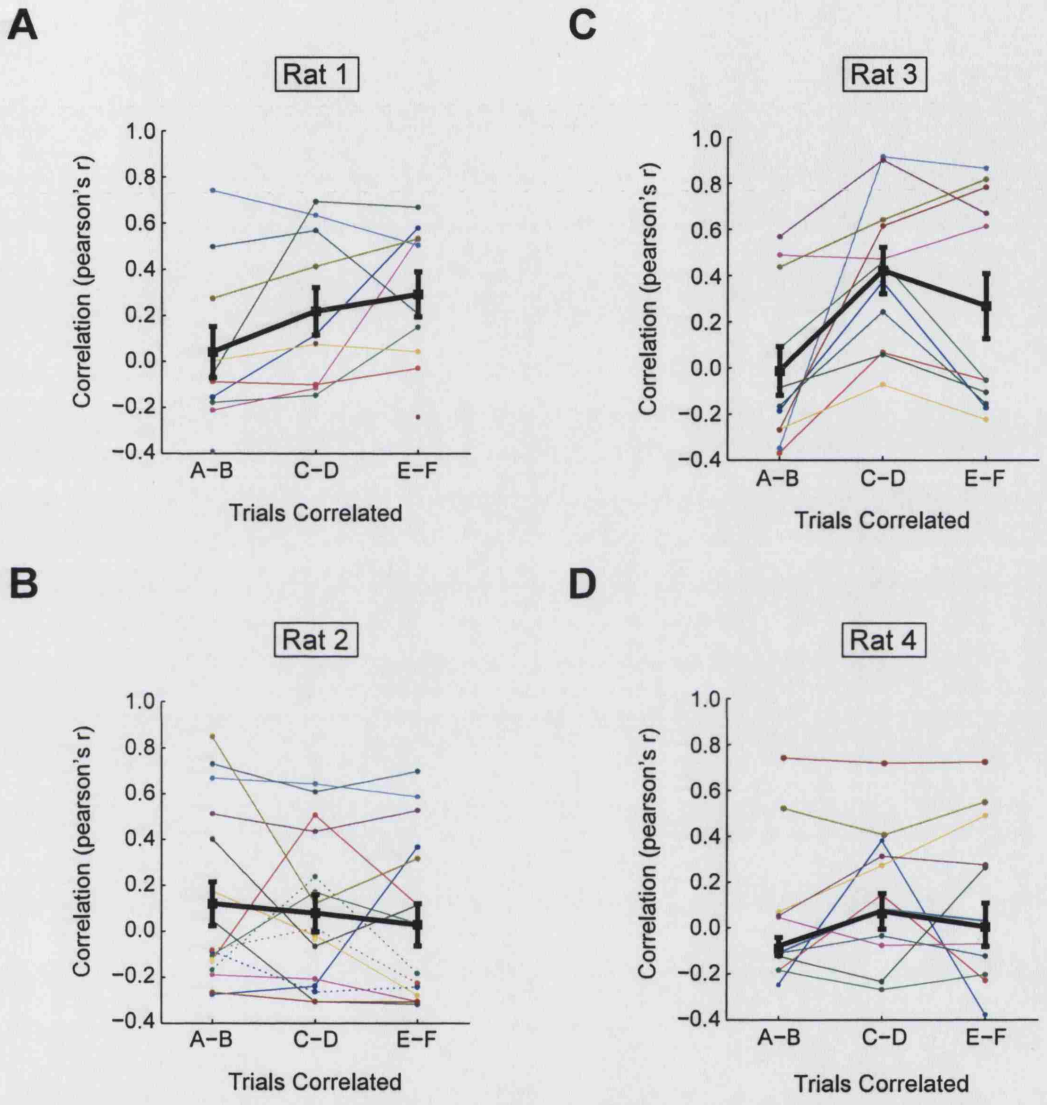

Figure 6.13. Correlation between square and circle firing rate maps, transfer day. Pearson's-r is calculated for three different trial-to-trial comparisons for each cell; trial A vs B, trial C vs D, trial E vs F (see methods for details). Thin, coloured lines show r values for individual cells. Bold, black lines show mean r value and ±SEM for each comparison. Each plot shows correlations for all recorded cells in a rat. **A**) Rat 1, **B**) Rat 2, **C**) Rat 3, **D**) Rat 4.

Figure 6.14

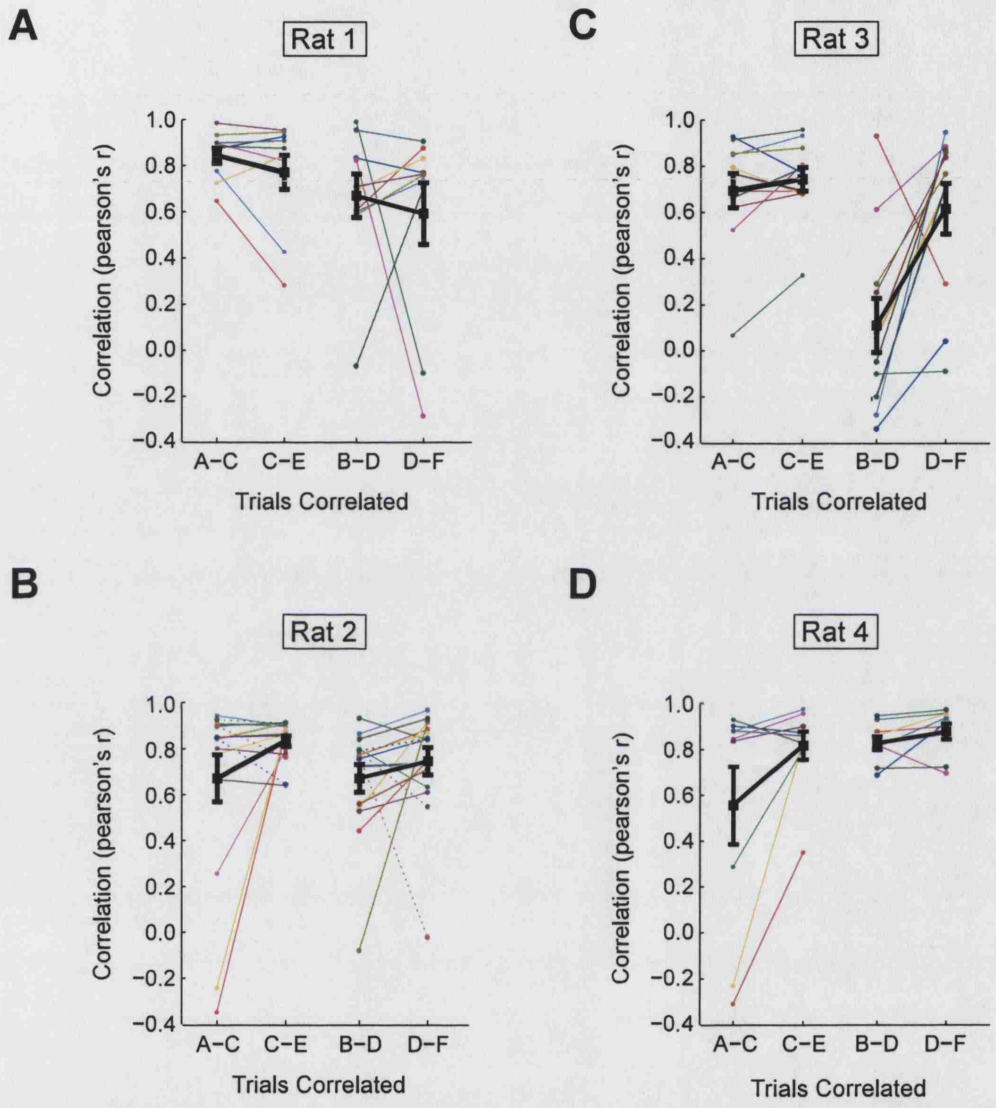

Figure 6.14. Correlation between firing rate maps, within shapes, during transfer day. Pearson's-r is calculated for two square-to-square comparisons (trial A vs C, trial C vs E, left-hand side of each plot) and two circle-to-circle comparisons (trial B vs D, trial D vs F, right-hand side of each plot). Thin, coloured lines show r values for individual cells. Bold, black lines show mean r value and ±SEM for each comparison. Each plot shows correlations for all recorded cells in a rat. **A**) Rat 1, **B**) Rat 2, **C**) Rat 3, **D**) Rat 4.

values, plotted on separate graphs for each rat. The values for r-within are shown in Figure 6.14.

Correlation results for rats 2 and 4 are similar, and consistent with the conclusions reached from examining firing rate maps: remapped representations transfer from white circle to morph circle. The r-within scores for circle-circle comparisons (Figure 6.14B, 6.14D, right-hand side of plots) are high for the whole cell population, for both rats. Mean r for the cell population is approximately 0.7 or above. There is very little difference between the white-morph circle correlation (trial B vs trial D), and the morph-morph circle correlation (D vs F). Furthermore, both circle-circle correlations are similar or higher than square-square correlations. The transfer test did not disrupt intra-shape firing patterns in these rats, therefore. The across shape correlations are low, and remain low throughout transfer test training (population means < 0.2 for all comparisons), indicating that place fields remain divergent between square and circle.

Despite sharing the general result of partial place representation convergence, rats 1 and 3 show different correlation results, reflecting different underlying place cell behaviour. For rat 1, circle-to-circle r-within values (Figure 6.14A, right-hand side of plot) are reasonably high for both comparisons. R-across scores rise gradually throughout training, with the population mean approximately $r = 0.3$. These results suggest a gradual process of convergence, with high place field stability in other, non-converging cells. This is confirmed by examining the firing rate maps (Figure 6.9), which show cells 7, 8 and 9 converging at different times during training, and high stability in other cells.

By contrast, the r-within values for rat 3 (Figure 6.14C, right-hand side of plot) drop sharply for the white-morph correlation (trials B vs D). Figure 6.11 shows that almost all cells show different firing patterns on trials B and D. For this animal, therefore, replacing the white circle with the morph circle does disrupt the circle representation. Mean r-across values for morph square vs morph circle are high (Figure 6.13C), indicating low divergence (high similarity) of hippocampal representations across these two environments. Interestingly, there is a peak in the similarity for trials C vs D, when the morph circle is first introduced, but then a decrease for trials E vs F. The r-across and r-within results together suggest that, in this animal, the transfer test initially caused a large convergence of place

representations, which, subsequently, diverged again. Clear examples of cells showing this behaviour are cells 1, 4, and 6 (Figure 6.11).

As for day 1 of remapping training, the r-difference measure was used to give an overall quantification of remapping for each cell. R-difference scores, for three trial comparisons (A vs B, C vs D and E vs F), and for each animal, are shown in Figure 6.15A-D. As previously, an r-difference score of 0.5 or greater was taken as the threshold for classifying a place cell as remapped. Those cells with r-difference > 0.5 for both first and last comparisons were classified stably remapped, those < 0.5 for both stably non-remapped. Cells which moved from > 0.5 to < 0.5 between the first and last comparisons were classified as converging, those whose scores moved in the opposite direction as diverging.

The r-difference plots reiterate the results already described. For rats 2 and 4, r-difference levels are constant, or increasing, throughout training, indicating that remapped representations are maintained despite replacing the white circle with the morph circle. Mean r-difference is slightly lower in rat 2, due to a the presence of stably non-remapped cells. Rats 1 and 3 both show convergence, with the mean r-difference decreasing over the day. However, rat 1 shows a gradual decrease over the course of training, while rat 3 has a large, sharp decrease for comparison C vs D (first exposure to morph circle), which partially recovers on the last (E vs F) comparison. The larger number of stably non-remapped cells in rat 3 reduces the population mean r-difference, which, at the end of training, is only just greater than the r-difference = 0.5 threshold.

To investigate the effects of the transfer test on r-difference, a repeated measures ANOVA was used to compare r-difference scores for the three different trial comparisons (A vs B, C vs D, E vs F), for each rat. (For the purposes of ANOVA, r-difference was composed of z-transformed r-within and r-across. See Methods). The results are summarised in Table 6.5, below. It can be seen that the only significant effect of trial group on r-difference is for data from rat 3. For rat 3, when the three r-difference groups were compared using related samples t-tests, the only significant difference, after a Bonferroni correction, was between the means of r-difference(A vs B) and r-difference(C vs D) ($t = 3.0$, $df = 11$, $p = 0.036$). The white-morph transfer test therefore had no significant effects on remapping for 3 out of the 4 animals described here. For rat 3, the transfer test caused a significant drop in the population

Figure 6.15

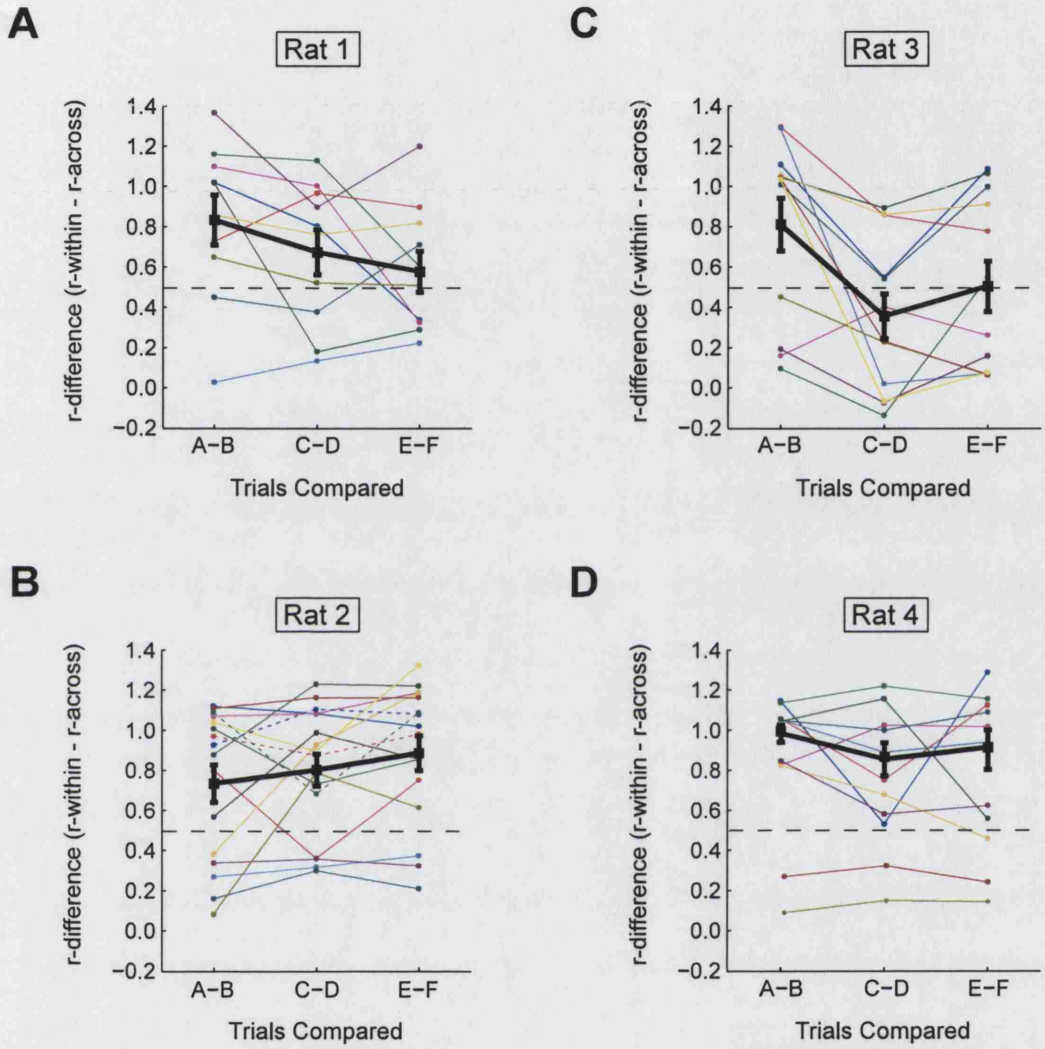

Figure 6.15. R-difference score (r-within - r-across) for all cells for each rat, transfer day. R-difference is calculated for three different trial-to-trial comparisons for each cell; trial A vs B, trial C vs D, trial E vs F (see methods for details). Thin, coloured lines show values for individual cells. Bold, black lines show mean r-difference and ±SEM for each comparison. Black dashed line at r-difference = 0.5 indicates threshold for classifying cells as remapped. Each plot shows correlations for all recorded cells in a rat. **A**) Rat 1, **B**) Rat 2, **C**) Rat 3, **D**) Rat 4.

remapping score, when comparing remapping on trials A and B (morph square vs white circle) and C and D (morph square vs morph circle).

Table 6.5

ANOVA summary, effect of trials compared on r-difference score, transfer test day.

	Degrees of Freedom (Trials, Error)	F	p
Rat 1	2,18	2.14	0.147
Rat 2	2,30	1.97	0.165
Rat 3	2,20	6.54*	0.006
Rat 4	2,16	0.58	0.943

* Effect significant at $p > 0.05$ level

Summary

When exposed to environments differing in shape, colour, texture and odour, rapid remapping was observed. By the end of the first day of training, at least 50% of cells were classified as remapped in all animals, and a greater proportion than this in most rats. Individual cells showed heterogeneous responses, some stably remapped from the first exposures to environments onwards, some changing responses during the course of training. Only one animal showed a statistically significant increase in remapping at the level of the cell population, though.

The remapping observed during day 1 of training could have been caused by the differing shape, colour, texture or odour of the environments. Substituting the morph circle for the white circle, on day 4 of training, showed that shape alone was capable of at least maintaining remapped representations. In two animals, complete transfer of remapped representations occurred. In two other animals, partial convergence occurred, but, in both cases, at least 50% of cells were still remapped by the end of training.

Chapter 7

Results: Octagon Probe

After remapping training (see chapter 6) rats were subjected to a series of probes, in order to investigate the relationship between the shape of the environment and place cell responses. This chapter describes the results of a probe in which rats were exposed to environments incrementally intermediate between square and circle. This experiment was designed to ask whether, faced with incremental changes to sensory input, place cell responses would also change incrementally, or, rather, jump abruptly from one representation to the other. It was also designed to investigate whether a population of place cells would respond in unison to changes in environmental shape, suggesting they were representing shape as a coherent population, or whether each cell individually would have a different response, suggesting that shape was encoded as a collection of independent features.

Experimental Design

The shapes intermediate between the square and the circle were all octagons, constructed using the morph box (see Methods). The series of incremental steps between the square and the circle were produced by changing the ratio of adjacent sides, one morph box section at a time (see Figure 7.1A). The most square-like of the octagons therefore had an adjacent side ratio of 1:7, whereas the most circle-like was a regular octagon, with adjacent side ratio 4:4. The two octagons intermediate in between these two had adjacent side ratios 2:6 and 3:5.

Figure 7.1B shows the running order of trials for the octagon probe experiment. Each octagon shape was presented twice, in two series, each series consisting of one of each shape. (1^{st} series: C,D,E,F; 2^{nd} series: H,J,K,L). The two repeats of each shape were run as far apart in time as possible, to avoid the occurrence of potentially confounding time dependent effects. Moreover, trials were run in a pseudo-random order, in order to avoid systematic hysteresis effects. For instance, the

Figure 7.1

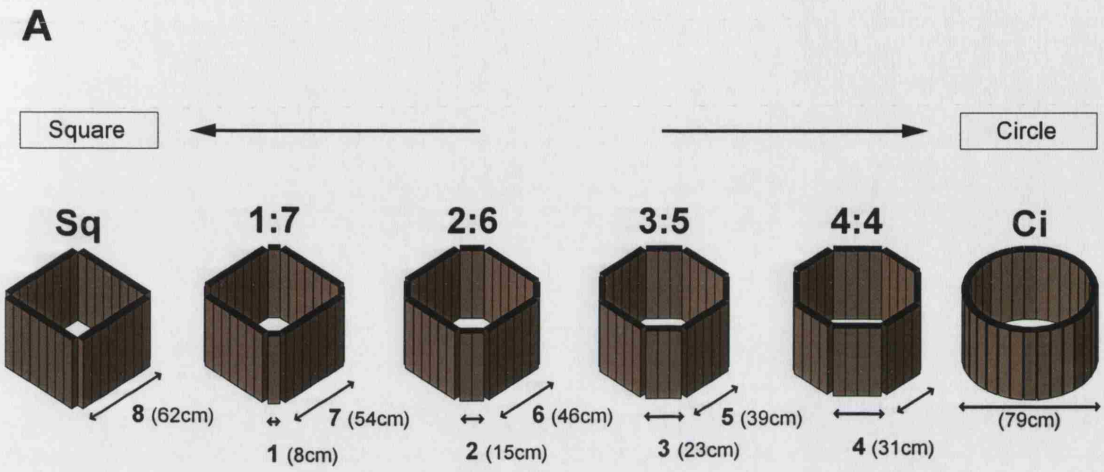

Figure 7.1. Octagon probe protocol. **A**) Illustrations of environments used. A series of square-like to circle-like intermediate shapes are constructed by changing the relative lengths of adjacent sides, one morph section at a time. Numbers in bold above each shape refer to the lengths of adjacent sides, in morph sections. Sq = square, Ci = circle. All shapes constructed using the same morph box deformable environment. **B**) Trial running order. Each outline shape represents a trial. Environment shape shown by shape of outline, and by the adjacent side ratio, above each shape. Letters in shapes show temporal running order. All trials 10 min duration, all inter-trial intervals 20 min.

two most intermediate octagons (2:6 and 3:5) were preceded by a square-like shape in one series and a circle-like shape in another. Three pairs of square-circle trials ('baselines') were run at the beginning (A,B), in the middle (G,I), and at the end (M,N) of the experimental series.

All cells abruptly and simultaneously shift between square and circle representations.

Firing rate maps for the octagon probe experiment on Rat 4 are shown in Figure 7.2. In this Figure, the trials are arranged by order of shape, from square (left) through to circle (right). Note, however, that this is not the running order of the trials (see above). The letters in the shapes at the top of each column show the temporal running order. Two important results are shown in Figure 7.2.

Firstly, almost all individual cells show an abrupt jump between the square and circle representations. They do not show responses intermediate between those of square and circle. Furthermore, no cells show a wholly new response, similar to neither square nor circle. For example, Cell 4 shows a strong place field in the southern part of the circle (mean rate approximately 8 Hz), but does not fire in the square. In all 4:4 and 3:5 octagons, the cell displays a place field in the same position and with approximately the same firing rate as in the circle. In all 1:7 and 2:6 octagons, the cell does not fire. A minority of cells show intermediate firing on some trials, in that a place field is present in the same location as in the baseline trial, but the peak rate is much reduced (for example, Cell 9, trial J). For the majority of cells, though, a small change in sensory input produces an abrupt jump between the two representations.

Secondly, almost all recorded cells jump between representations simultaneously. All cells fire as if in response to the square in the 1:7 and 2:6 octagons, and as if in response to the circle in the 3:5 and 4:4 octagons. On any given trial, therefore, all recorded cells constitute a coherent representation, either square or circle. They do not show a heterogeneous set of responses.

This phenomenon can be quantified as seen in Figure 7.3, in which firing rate maps for all shapes are assessed for similarity to square or circle. Scores are based on

Figure 7.2

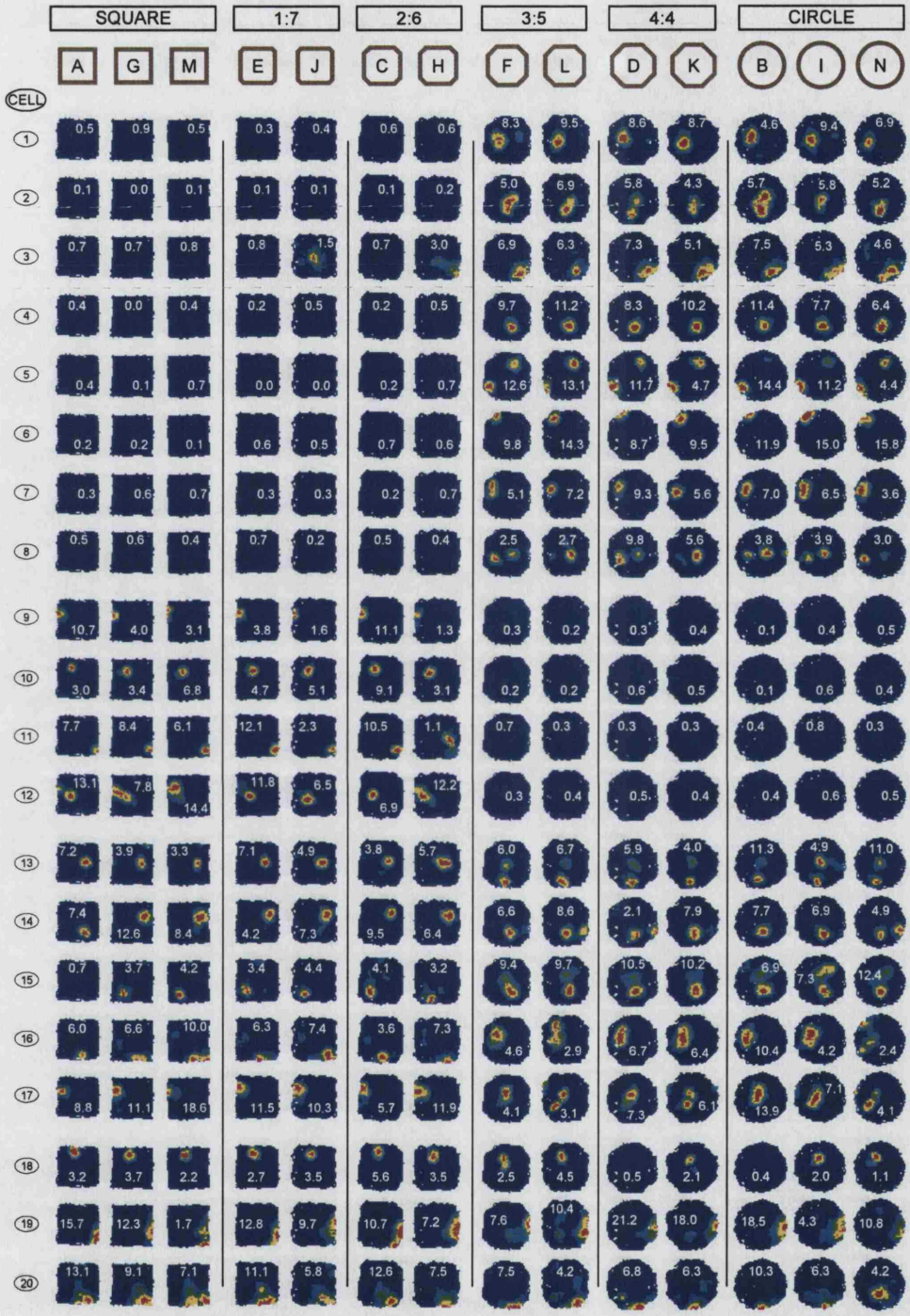

Figure 7.2. Firing rate maps for all cells recorded from rat 4 during the octagon probe. All cells simultaneously recorded. Details of firing rate maps as for figure 6.2. Each row shows one cell, each column shows one trial. Trials are arranged from square-like (left) to circle-like (right). Vertical black lines group trials into repeats of the same shape. 8 cells had a field in the octagon but not the square (cells 1-8); 4 in the square but not the octagon (8-12); 5 fired in both but in different places (13-17), and 3 did not did not reach the criterion for remapping (18-20) (see methods).

firing rate correlation and adjusted, so that, for each cell, the average correlation of squares to other squares equals 1, and the average correlation of squares to circles equals 0. (See Methods for details). This adjusted r-value will be referred to as the 'similarity' score. A similarity-to-square score of 1 indicates that a place cell is responding to a shape as if that shape were a square, a score of 0 indicates that the place cell is responding as differently from a square as the cell responds to a circle. As non-similarity to square is not necessarily similarity to circle, there are two lines on each graph, similarity-to-square (red) and similarity-to-circle (blue).

Figure 7.3A shows the mean similarity scores for all remapped cells from Rat 4, the 1st series octagons on the left, the second series on the right. In both cases, the abrupt jump in representations can clearly be seen, shown by the step function profile of the similarity scores. Squares, 1:7 octagons and 2:6 octagons all have a similarity-to-square score of approximately 1, and a similarity-to-circle score of approximately 0. Conversely, circles, 4:4 octagons and 3:5 octagons all have a similarity-to-circle of approximately 1, and a similarity-to-square of approximately 0. Figure 7.3B shows the same data, for each remapped cell. The same step-function profile can be seen even on the level of individual cells.

The same result can also be observed in the next largest data set, from Rat 1 (Figure 7.4, Figure 7.5A & B). Figure 7.4A shows the firing rate maps for Rat 1. As with Rat 4, it can be seen that: a) the majority of remapped cells show an abrupt switch between square and circle responses, and b) this switch happens at the same point for all remapped cells. The switch point for Rat 1 is the same as for Rat 4, i.e. between 2:6 and 3:5 octagons. Figures 7.5A and B show, respectively, the mean and cell-by-cell similarity scores for this data. Again, the step-like profile of the curves clearly shows the abrupt jump between representations.

Different representations can be elicited by the same octagon shape

The octagon probe trial series included two exposures to every intermediate octagon. This was in order to test whether place cell representations of intermediate shapes would display hysteresis or, rather, be constant over repeated exposures. Place cells from rats 1 and 4, described above, showed constant responses over two trials in

Figure 7.3

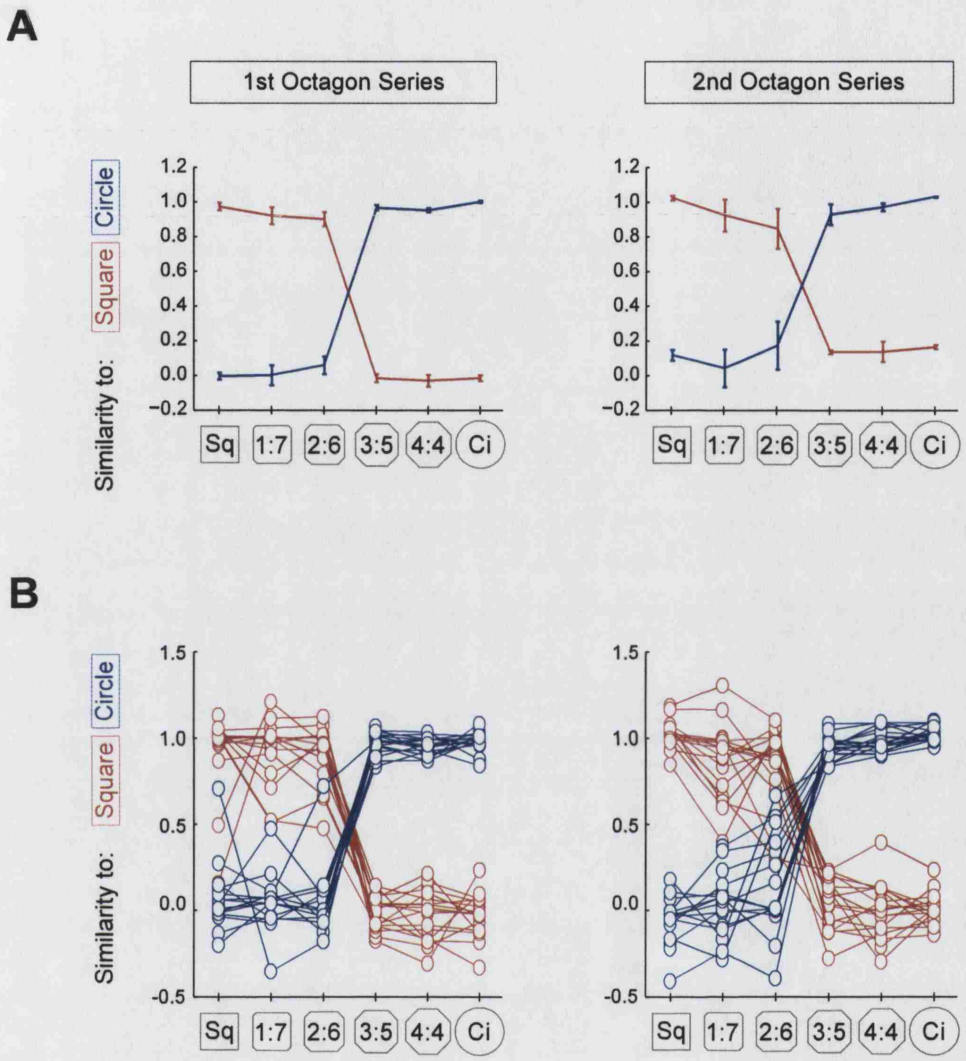

Figure 7.3. Octagon probe similarity scores for rat 4. For each plot, x-axis shows shape, arranged in order from square-like to circle-like. Y-axis shows similarity score. Similarity score is based on spatial correlation of firing rate maps, normalised such that similarity(X-to-X) = 1 and similarity(X-to-Y) = 0, where X and Y are baseline shapes square and circle (see methods). Red line = similarity-to-square, blue line = similarity-to-octagon. Left column shows similarity scores from the first series of intermediate shapes (C, D, E, F). Baseline data for these plots are the means of first (A, B) and second (G, I) baseline trials. Right column shows similarity scores from the second series of intermediate shapes (H, J, K, L). Baseline data for these plots are the means of second (G, I) and third (M, N) baseline trials. **A)** Mean similarity for cell population. Error bars show ±SEM. **B)** Data by cell, for all remapped cells.

Figure 7.4

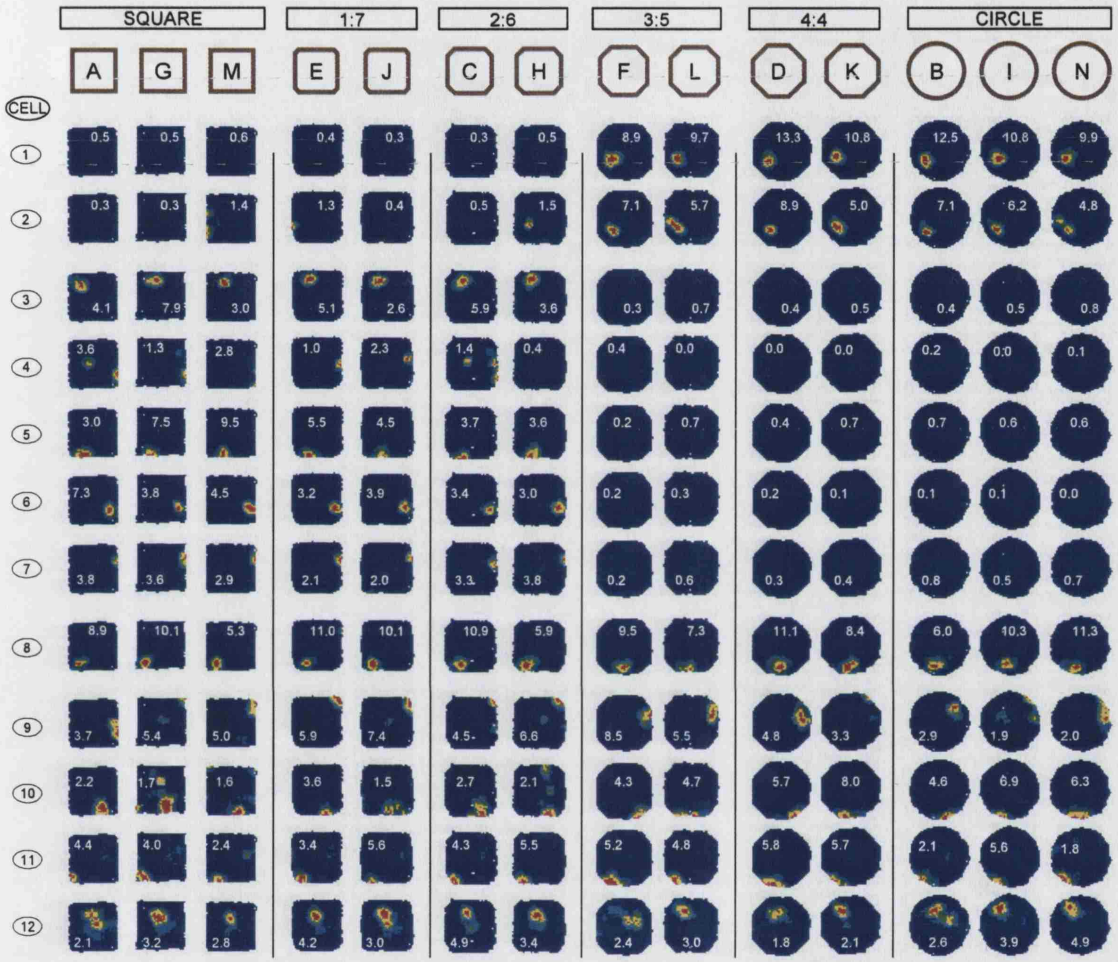

Figure 7.4. Firing rate maps for all cells recorded from rat 1 during the octagon probe. All cells simultaneously recorded. Details of firing rate maps and layout as for figure 7.2. 2 cells had a field in the octagon but not the square (cells 1-2); 5 in the square but not the octagon (3-7); 1 fired in both but in different places (cell 8), and 4 did not did not reach the criterion for remapping (9-12) (see methods).

Figure 7.5

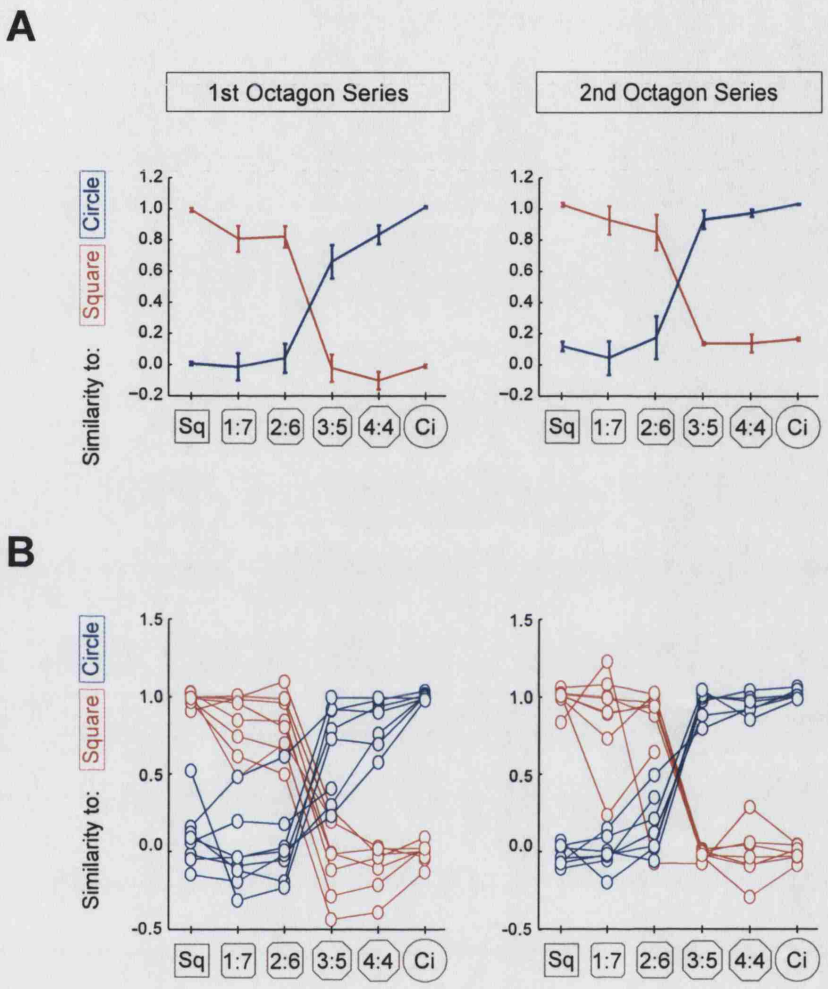

Figure 7.5. Octagon probe similarity scores for rat 1. For each plot, x-axis shows shape, arranged in order from square-like to circle-like. Y-axis shows similarity score. For details of similarity score, see figure 7.3 legend, methods. Data plotted in left column and right column are as for figure 7.3. **A**) Mean similarity for cell population. Error bars show ±SEM. **B**) Data by cell, for all remapped cells.

the same intermediate shape. In the two other animals, however, place cell responses to intermediate shapes changed between the first and second octagon series.

Figure 7.6A shows firing rate maps for rat 2. In this Figure, trials are arranged by series as well as by shape, with the octagons separated into first and second series. Within each octagon series, square-like octagons are shown to the left and circle-like octagons to the right. The baseline trials are shown as three pairs, first (left), middle (between octagon series) and last (right). This dataset shows two interesting features. Firstly, rat 2 shows the same pattern of results as the previous two rats (Rats 1 and 4), insofar as all remapped cells jump abruptly and simultaneously between square and circle responses. Secondly, it can be seen that, in the first octagon series the representation switch occurs between octagons 2:6 and 3:5, while during the second series, the switch takes place between the square and the 1:7 octagon. It follows, therefore, that the representations elicited by octagons 1:7 and 2:6 are square-like in the first octagon series, but circle-like in the second octagon series. The same sensory input elicits different place cell representations.

These results are also evident when looking at the similarity scores for these data. (Figure 7.6B, trial mean scores, 7.6C, individual cell scores). The first octagon series shows a step function profile switch from square-like at 2:6 to circle-like at 3:5. On the second series, however, it can be seen that the switch point between representations has moved, so that the major change in place cell responses occurs between Square and 1:7 octagon.

Figure 7.7A shows the firing rate maps for Rat 3. The results for this rat are similar to those observed for Rat 2, the only difference being that with this animal, it is only the 2:6 octagon that elicits different representations on the two octagon series. The direction of the change in representations is the same as in Rat 2, with more octagons eliciting the circle response on the second series than on the first series. The phenomenon is also shown as similarity scores in Figures 7.7B and 7.7C.

The fact that place cell responses to an intermediate octagon can change can be interpreted in different ways. It may be due to plasticity in place cell responses, possibly induced by the first exposure to the octagon series. Being exposed to stimuli intermediate between environments with remapped representations may be sufficient to alter how stimuli map onto those representations. Alternatively, changing responses may reflect the fact that, presented with intermediate input, an attractor network

Figure 7.6

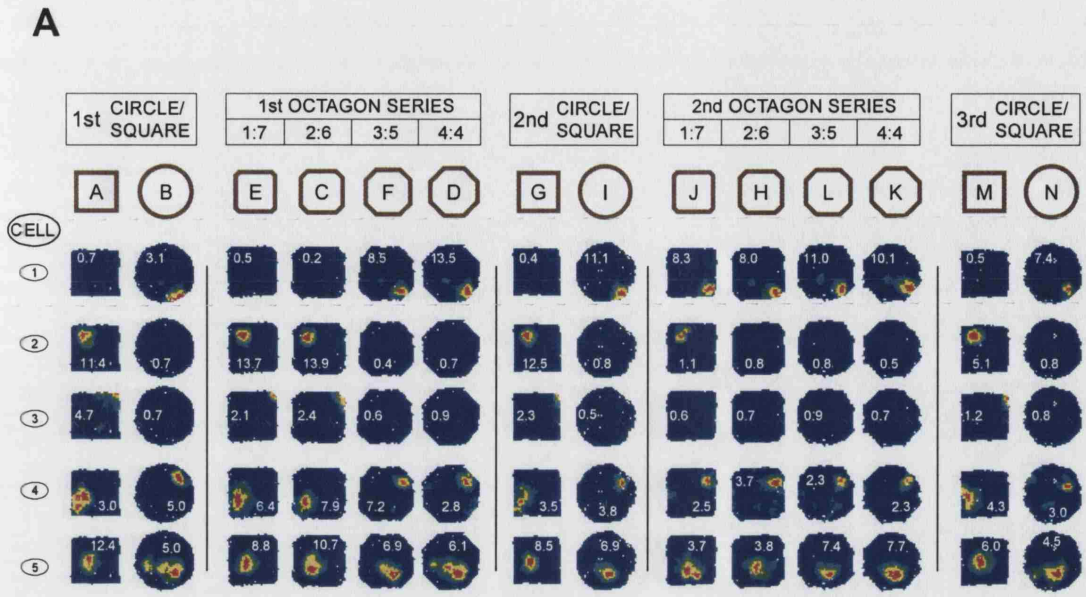

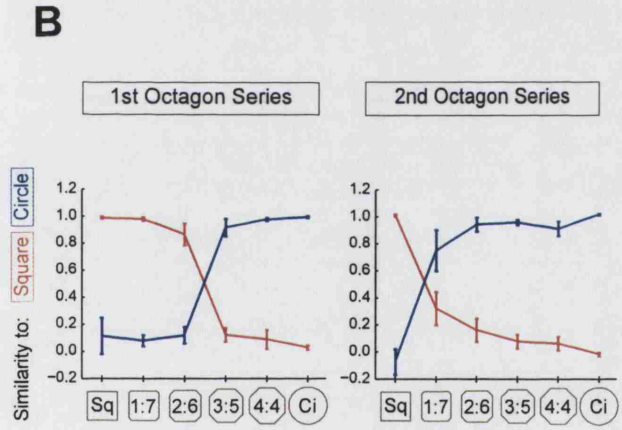

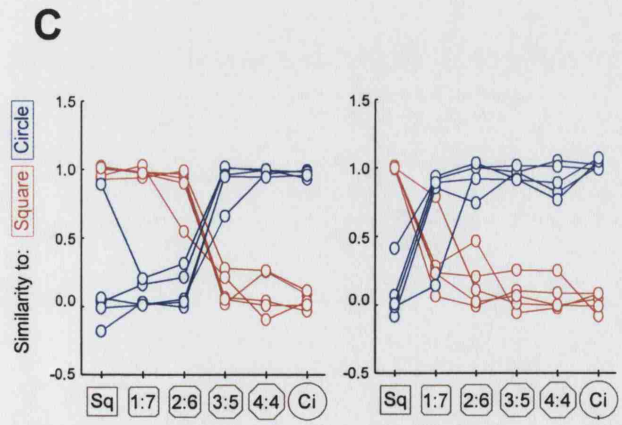

Figure 7.6. Octagon probe data for rat 2. **A)** Firing rate maps for all cells recorded during the octagon probe. All cells simultaneously recorded. Details of firing rate maps and layout as for figure 7.2. 1 cell had a field in the octagon but not the square (cell 1), 2 cells had a field in the square but not the octagon (2-3), 2 cells had fields in both but in different places (4-5). **B, C)** Similarity scores for octagon probe data. For each plot, x-axis shows shape, arranged in order from square-like to circle-like. Y-axis shows similarity score. For details of similarity score, see figure 7.3 legend, methods. Data plotted in left column and right column are as for figure 7.3. **B)** Mean similarity for cell population. Error bars show ±SEM. **C)** Data by cell, for all remapped cells.

Figure 7.7

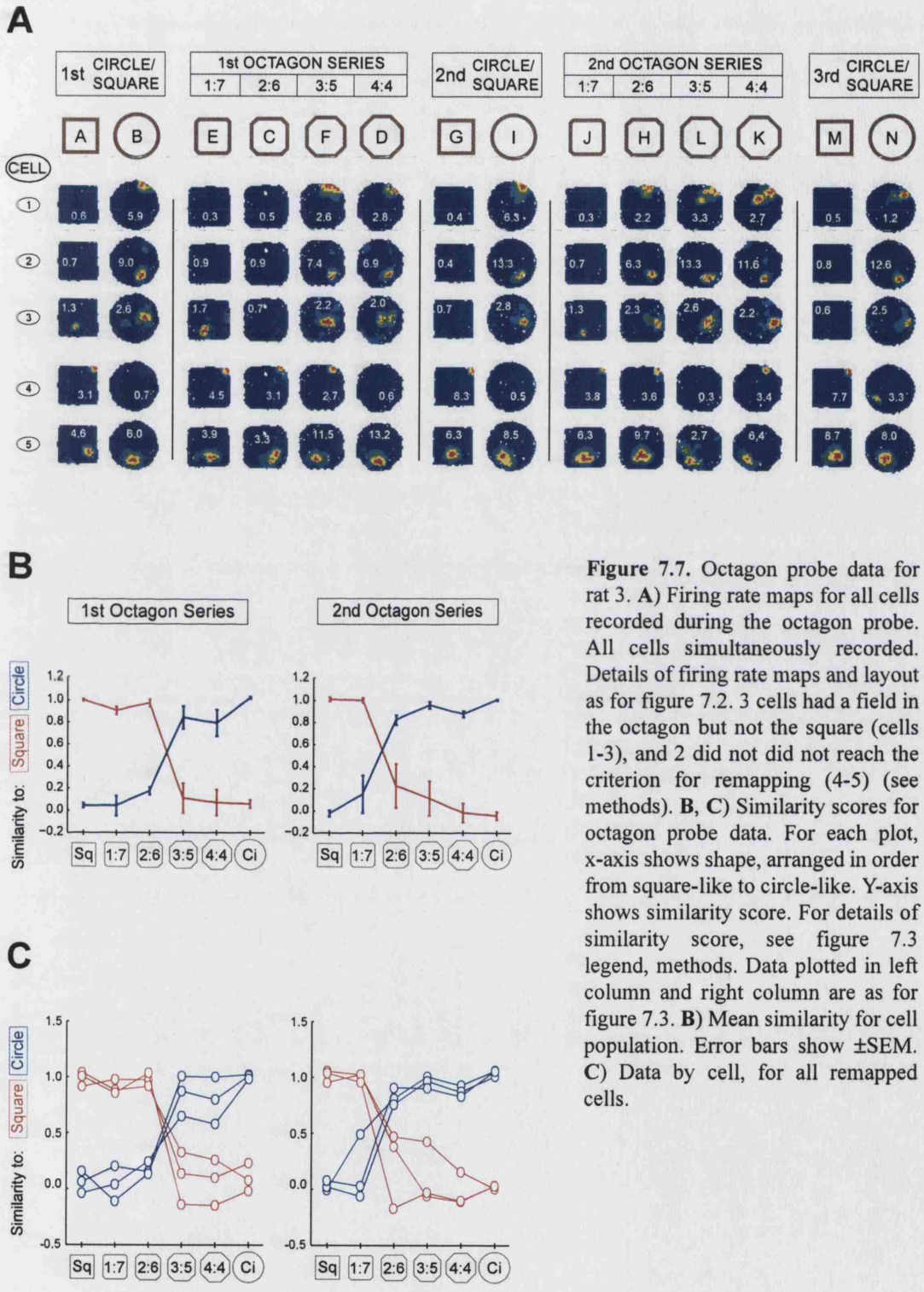

Figure 7.7. Octagon probe data for rat 3. **A**) Firing rate maps for all cells recorded during the octagon probe. All cells simultaneously recorded. Details of firing rate maps and layout as for figure 7.2. 3 cells had a field in the octagon but not the square (cells 1-3), and 2 did not did not reach the criterion for remapping (4-5) (see methods). **B, C**) Similarity scores for octagon probe data. For each plot, x-axis shows shape, arranged in order from square-like to circle-like. Y-axis shows similarity score. For details of similarity score, see figure 7.3 legend, methods. Data plotted in left column and right column are as for figure 7.3. **B**) Mean similarity for cell population. Error bars show ±SEM. **C**) Data by cell, for all remapped cells.

system may chose a final state in a noisy and probabilistic manner (see Discussion for further details).

Attractor dynamics in the place cell representation.

If the place cell population is representing the environment in a coherent fashion, possibly as an auto-associative network, is it possible to see any dynamics present in that representation? For example, do place cells in the more ambiguous, intermediate octagon trials take longer at the beginning of the trial to fire than in the square or circle representation? Attractor network dynamics are generally thought to operate on a time scale of milliseconds (see Chapter 9 for further discussion). These effects are difficult to investigate in place cells due to sampling problems. Using the current data, it is possible, however, to investigate whether there are any slow changes (on the scale of tens of seconds) in the place cell representation of the environment.

To investigate whether the place cell representation becomes more square-like or circle-like over the first two minutes of each trial, twelve 10-second slices of data, between 0 and 120 seconds, were used to construct firing rate maps for each cell. This map was then correlated to the whole trial rate map for that cell. The resulting r-value was then adjusted to produce a similarity score, as described in the preceding section. Importantly, the r-values for the baseline-to-baseline correlations on which the adjustment was based were derived from whole trial firing rate maps. As a consequence, the similarity scores indicate how similar (or different) each time slice map is to whole trial baseline maps. As 10-second long firing rate maps are very noisy (containing frequent spurious high rate bins), a large sample of cells is needed to discern any effect. This analysis was therefore run only for rats 1 and 4, as they provided the largest number of remapped cells (Rat 1: 8 cells, Rat 4: 17 cells).

Figure 7.8A shows the shape mean similarity scores for each 10 second time slice between 0 and 120 seconds. The shape mean similarity score is the mean of the 1st and 2nd series similarity scores for each shape. Looking at the similarity-to-square scores (red line) over different time slices, it can be seen that the place cells take some time to display the square representation. In the first three time slices, from 0-30 seconds, it can be seen that the similarity-to-square is low for all octagons. At 30-40 seconds, the similarity to square is now higher in the 'square' octagons, 1:7 and 2:6

Figure 7.8

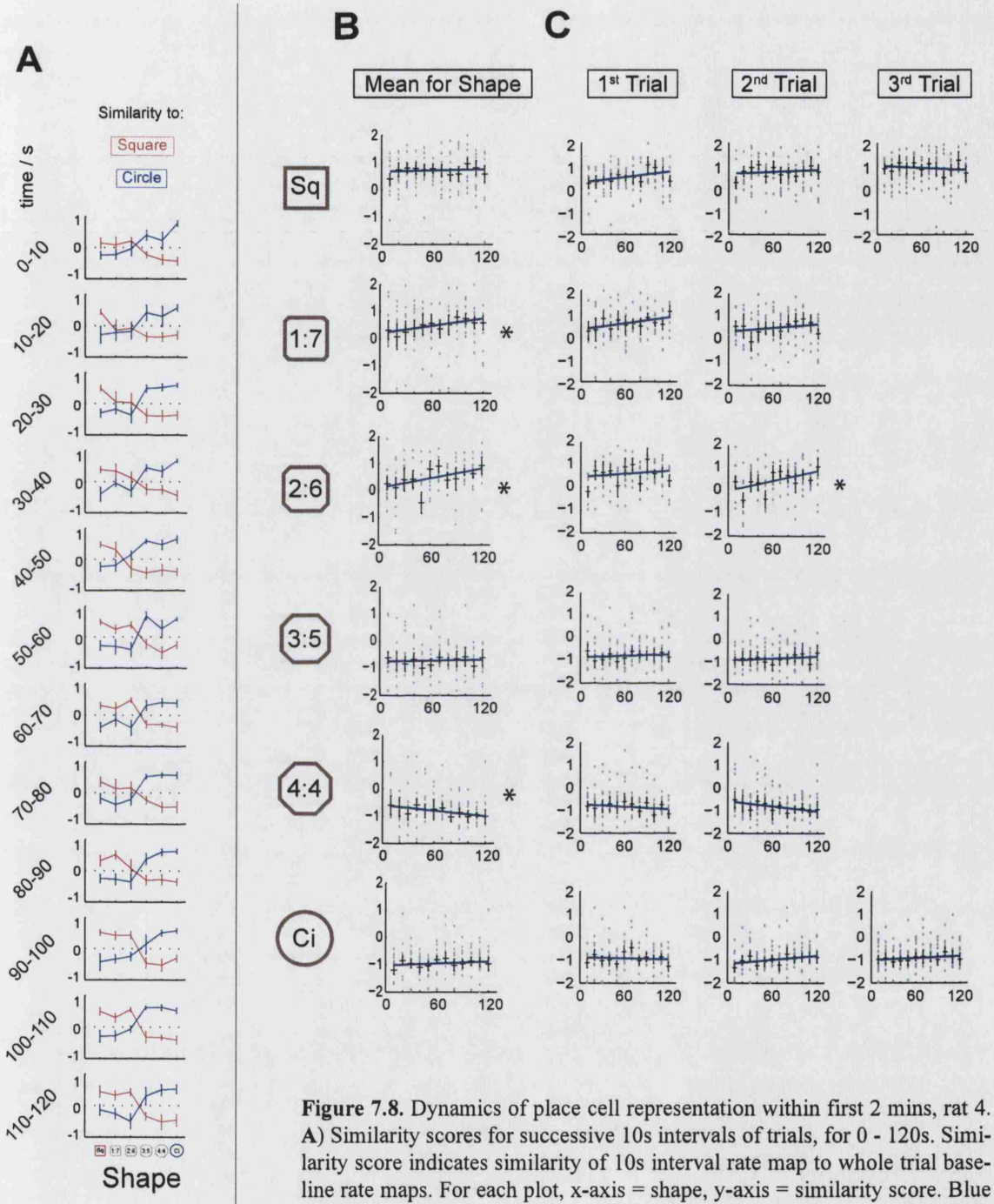

Figure 7.8. Dynamics of place cell representation within first 2 mins, rat 4. **A**) Similarity scores for successive 10s intervals of trials, for 0 - 120s. Similarity score indicates similarity of 10s interval rate map to whole trial baseline rate maps. For each plot, x-axis = shape, y-axis = similarity score. Blue line shows similarity-to-circle, red line shows similarity-to-square. **B**) Mean Similarity Difference (SD) scores for each shape. Grey dots show SD scores for each cell. Black crosses show mean SD and ± SEM for all remapped cells. Blue line shows regression fit to this data. **C**) SD scores for each trial. Format for each plot as for (B). Row = shape, column = n^{th} repeat of shape.
* Regression significant at $p > 0.05$ level.

Figure 7.9

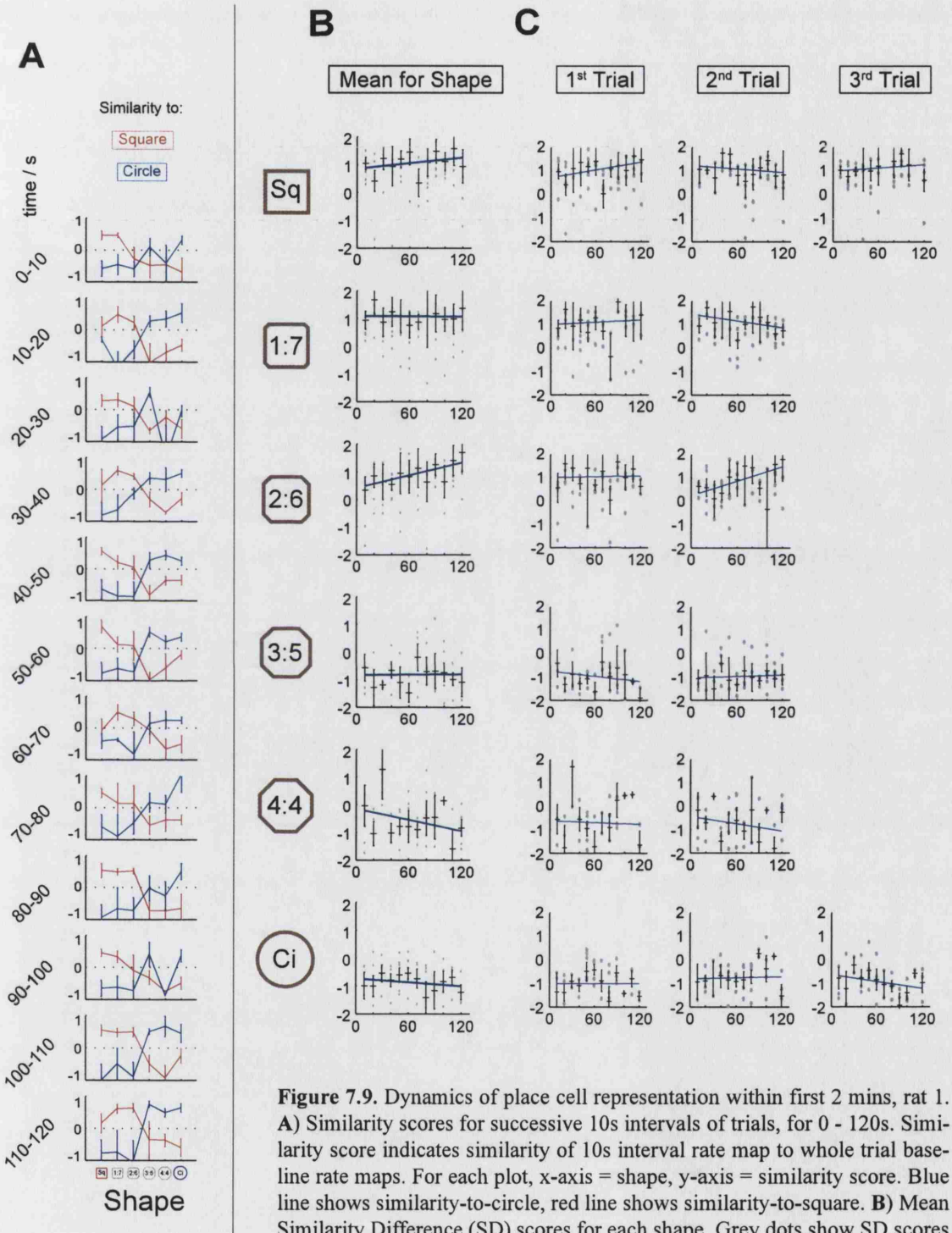

Figure 7.9. Dynamics of place cell representation within first 2 mins, rat 1. **A**) Similarity scores for successive 10s intervals of trials, for 0 - 120s. Similarity score indicates similarity of 10s interval rate map to whole trial baseline rate maps. For each plot, x-axis = shape, y-axis = similarity score. Blue line shows similarity-to-circle, red line shows similarity-to-square. **B**) Mean Similarity Difference (SD) scores for each shape. Grey dots show SD scores for each cell. Black crosses show mean SD and ± SEM for all remapped cells. Blue line shows regression fit to this data. **C**) SD scores for each trial. Format for each plot as for (B). Row = shape, column = n^{th} repeat of shape.

(the octagons that elicit a square response). However, the curve does not show a step-function profile, but rather a smooth gradient between square and circle. Only by 90-120 seconds does the curve consistently show a step-function profile, indicating an abrupt switch in the mean place cell response. A strong square-like representation in all 1:7 and 2:6 octagons takes some time to appear, therefore. Changes in the similarity-to-circle score are less pronounced, but a strong step-function shape still does not appear until 20-30 seconds.

In order to quantify these changes in the similarity scores, (similarity-to-square) - (similarity-to-circle) was calculated for each shape at every time point. This score is referred to as the similarity difference (SD), and is a unitary measure of whether place cells show the square or circle representation. An SD of 1 indicates a square representation and an SD of -1 indicates a circle representation. A linear regression between the SD score and time was then performed for each shape.

Figure 7.8B shows the mean SD plotted against time for each shape. The blue line represents the regression line fitted to these data. For the 1:7 and 2:6 octagons, the SD shows a clear increase over time (indicating place cell responses becoming more square-like). Likewise, for the 4:4 octagon, the mean SD shows a decrease over time, indicating place cell responses becoming more circle-like. All these trends are significant at the $p < 0.05$ level (one-tailed). A slow dynamic response, with the place cell representation taking time to reach its final state, is clearly visible in these shapes. Are these trends due to a non-specific 'warming-up', such that place cells take time to reach a stable representation of the environment? The results for square and circle argue against this, as these SD scores are stable over the time period being looked at. This suggests that, in this experiment, the dynamic responses seen are specific to the octagon shapes. The only anomalous result, which does not fit into this interpretation, is the 3:5 octagon, whose SD scores are stable over time. Place cells in this octagon displayed a circle-like response from the very beginning of the trial.

The results described so far relate to the mean SD for each shape. It is also possible to ask whether any particular trial is responsible for creating the dynamic trends observed. For instance, are the trends more pronounced in the first series of octagons, when the trials constitute exposures to novel stimuli? Figure 7.8C shows the SD trends for each trial individually. (Row = Shape, Column = n^{th} Repeat). There is no clear difference between 1^{st} and 2^{nd} series octagons. For 1:7, the 1^{st} exposure seems to show the strongest trend, but for 2:6, the 2^{nd} exposure is stronger, the only trend to

reach significance ($p < 0.05$, one-tailed) among individual trials. There is, therefore, no clear trend as to which trial shows the strongest dynamic effects.

The same analysis was also run on the next-largest data set, Rat 1. In this case, it is harder to see a consistent pattern in the similarity score plots (Figure 7.9A). Many time slices, both early and late, do not show a clear step function profile. This may be due to an insufficiently large sample of remapped cells. In the SD scores, however, it is possible to see trends over time in some shapes (Figure 7.9B, C). In particular, the 2:6 square becomes more square-like over time, and the 4:4 octagon more circle-like over time. However, none of these trends are significant at the $p < 0.05$ level. The data from this animal is, therefore, suggestive of a general slow dynamic effect, in response to the octagon probe, but the number of remapped cells is to too small to allow definite conclusions to be drawn.

Non-simultaneous response switching, after slow remapping training.

All the results presented so far relate to animals trained using the remapping protocol described in chapter 6. Octagon probe experiments were also run, however, on one rat (Rat 5) trained on a protocol that produces slow remapping, on a time scale of days or weeks. The results from this rat are different from those from the rats trained on the fast remapping protocol.

Experimental Protocol

The training protocol shared the same laboratory setup, behavioural task and morph box apparatus as the fast remapping training protocol (see chapter 6, Figure 6.1). Each day of training consisted of six trials of 10 minutes each, three squares and three circles in alternating order. Unlike the fast remapping protocol, both circle and square were always constructed using the morph box. The rat was trained in this manner for 21 consecutive days.

Place cell data were not recorded during the remapping training of this animal. However, rats trained using this protocol have been shown to remap over a long period of training. The overall level of remapping in the population increases

gradually, and individual cells remap at different points during the training (Lever *et al*, 2002). By the end of training, remapping can be shown to respond to environmental shape alone: substituting the morph square and circle with environments of the same shapes, but made of different material, preserves the remapped representations.

Different cells jump abruptly between representations at different points in the octagon series

Figure 7.10A shows the firing rate maps for Rat 5 on the octagon probe. Trials are arranged by shape, with the square on the left and the circle on the right, as for Figure 7.2. It can be seen that most remapped cells (cells 1-7) show an abrupt switch between responses. For example cell 2 fires in the south-east corner of the circle, but does not fire in the square. The south-east place field is present in all trials ranging in shape from 2:6 octagon to circle, but the place cell does not fire in the square or 1:7 octagon. Cell 7 changes field position between square and circle, south-east in the square, north in the circle. The cell fires with a north field in 4:4 trials and one 3:5 trial (trial F), and south east in all others. Rat 5, therefore, shows abrupt place cell response switching, in the same manner as for rats 1-4.

The important contrast with results described above, however, is that different cells jump between square and circle responses at different points in the octagon series. In Figure 7.10A, the red lines between maps highlight where the response switch points appear to be for each cell. It can be seen that the red lines are distributed approximately evenly from between octagons 1:7 and 2:6, to between octagons 3:5 and 4:4. On exposure to 2:6 and 3:5 octagons, therefore, place cells show a heterogeneous set of responses, some firing as if exposed to square, others firing as if exposed to circle. This set of heterogeneous responses is also biased towards a square or circle representation, depending on environmental shape. On the 2:6 octagon trials (C and H), respectively 5/7 and 4/7 remapped cells fire as if in response to a square. On the 3:5 octagon trials, 5/7 remapped cells (in both trials) fire as if in response to the circle. The place cell representation therefore appears to be incrementally shifting between square and circle.

Figure 7.10

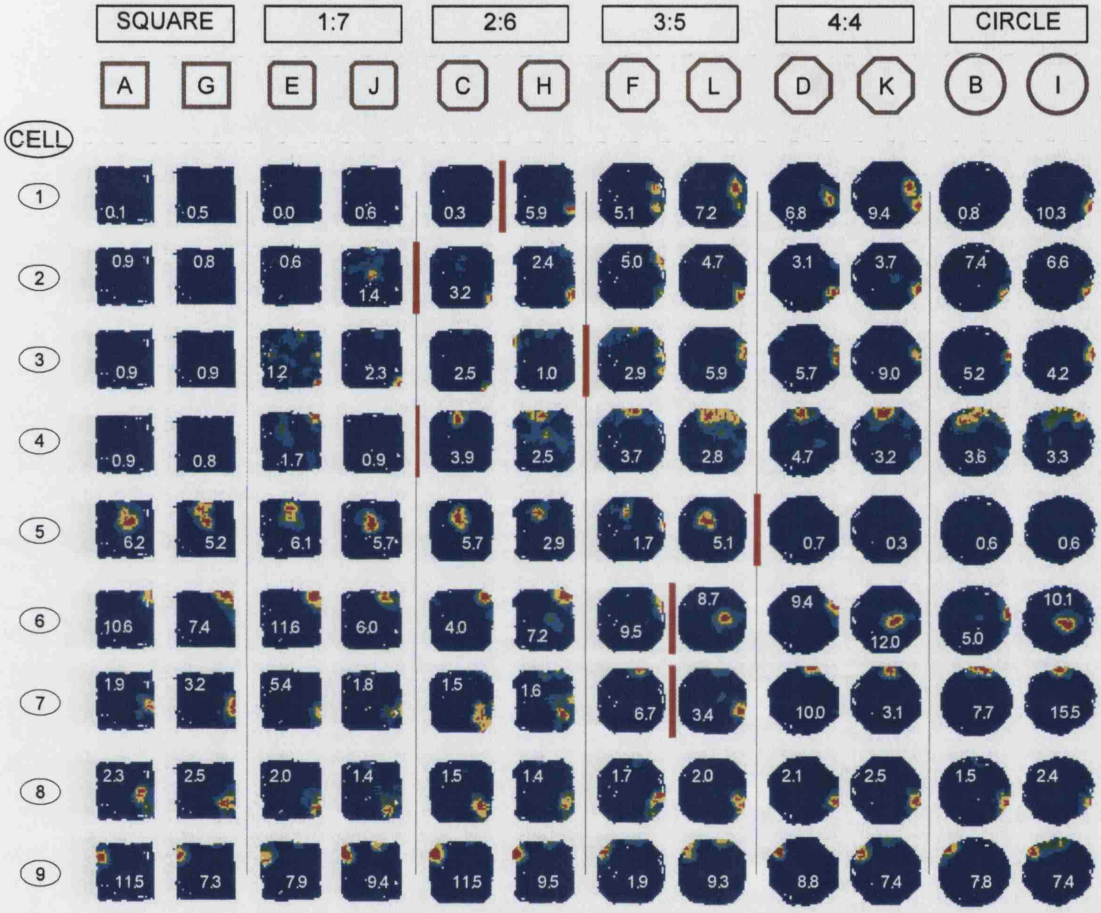

Figure 7.10. Firing rate maps for all cells recorded from rat 5 during the octagon probe. All cells simultaneously recorded. Details of firing rate maps and layout as for figure 7.2. Bold red lines between firing rate maps indicate the square-like to circle-like switch point for each cell. Note that different cells switch at different points in the series. 4 cells had a field in the octagon but not the square (cells 1-4); 1 in the square but not the octagon (cell 5); 2 fired in both but in different places (6-7), and 2 did not did not reach the criterion for remapping (8-9) (see methods).

Figure 7.11

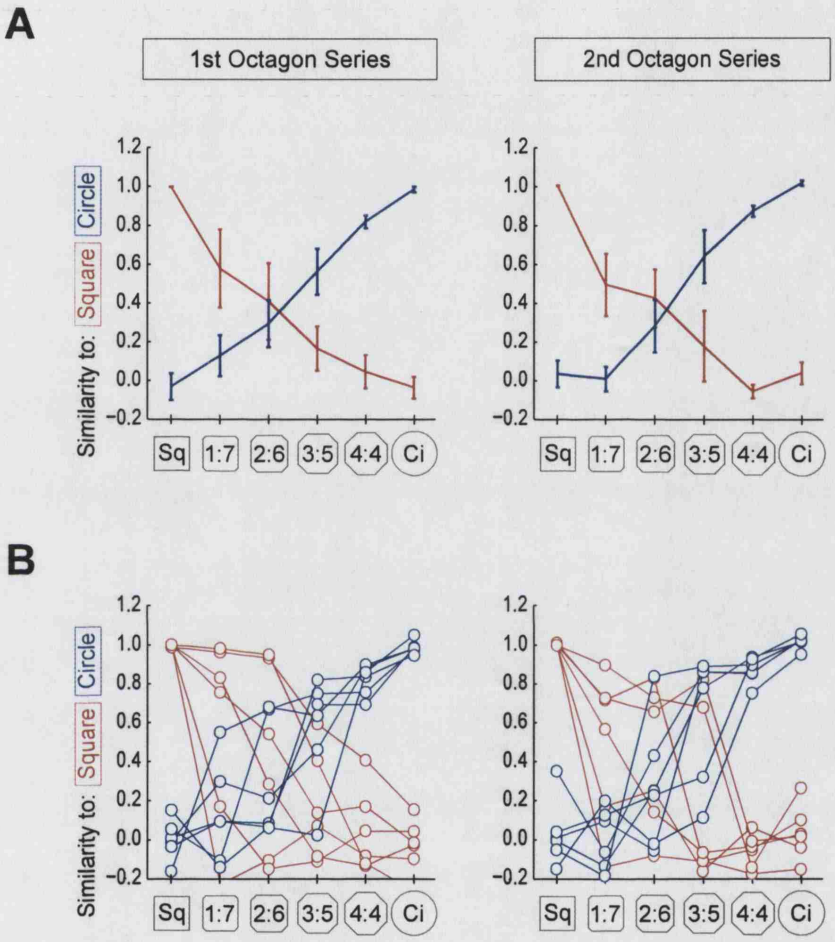

Figure 7.11. Octagon probe similarity scores for rat 5. For each plot, x-axis shows shape, arranged in order from square-like to circle-like. Y-axis shows similarity score. For details of similarity score, see figure 7.3 legend, methods. Data plotted in left column and right column are as for figure 7.3. **A**) Mean similarity for cell population. Error bars show ±SEM. **B**) Data by cell, for all remapped cells.

This incremental change can be more clearly seen in the similarity scores. (Figure 7.11A, B). The mean similarity scores for each trial (7.11A) show an approximately smooth gradient, changing incrementally with each octagon. In contrast to the fast remapping rats, there is no step function-like jump in the mean similarity score at any point. The heterogeneous nature of the place cell responses can also be seen when looking at the individual cell similarity scores (7.11B). The scores for single cells diverge over the intermediate octagons, and are tightly clustered only in the square and circle. This is in contrast to the fast remapping rats, where individual cell scores were tightly clustered on all shapes, including intermediate octagons.

In a manner similar to the fast remapping rats, individual cells can show different place fields in response to the same environmental shape. This is seen clearly for cell 7, for example, where the place field is in the south-east of the environment in the trial L 3:5 octagon, but in the north of the environment in the trial F 3:5 octagon. A similar pattern is also seen for cell 1, where the place field is only present in one of the two 2:6 octagon trials. It is possible, therefore, that even though place cells do not switch representations simultaneously, individual cell responses are not solely determined by straightforward sensory input.

Summary

The octagon probe experiment was designed to test the behaviour of remapped place cell representations, when presented with a series of environments incrementally intermediate between the familiar environments eliciting remapping. In the main experimental group (rats 1-4), two crucial results were observed. First, individual place cells switch abruptly between representations. For the vast majority of cells, firing on each trial was either square-like or circle-like: intermediate firing patterns were not observed. Individual cells, therefore, show a dissociation between the incremental change in environment stimuli, and the abrupt change in place-specific firing. Secondly, almost all cells switched between representations at the same point in the octagon series, demonstrating a coherent place cell representation of the environment. These two results, taken together, suggest an auto-associative, or attractor, network of place cells exists in the hippocampal representation of the intermediate shapes.

There were two further important results in this data set. First, for two animals (rats 2 and 3), a different place cell representation could be elicited by the same intermediate shape. This may reflect plasticity induced by exposure to the intermediate octagons, or, possibly, stochastic processes in the selection of attractor states (see Discussion). Secondly, changes in the place cell representation are observable over the course of the first two minutes of a trial. Place cells in the two square-like octagons show progressively more square-like representations, and, in one circle-like octagon, progressively more circle-like representations. Although much slower than predicted by attractor network theory, these changes demonstrate the presence of dynamic processes in the selection of place representations.

One animal (rat 5) showed a partially different set of results. Like rats 1-4, individual place cells abruptly switched between representations. Furthermore, different responses could be elicited, from individual cells, by the same intermediate shape. On the level of single cells, therefore, there was a dissociation between environmental stimuli and place response, possibly suggestive attractor dynamics in the place response of each cell. In contrast to rats 1-4, however, different cells switched between representations at different points in the octagon series. At the level of the place cell population, therefore, there is no coherent representation. One possible cause for this difference is the different remapping training protocol used for this rat.

Chapter 8

Results: Chimeric Shapes

A subset of the 5 rats exposed to the octagon probes underwent a further experiment to test the nature of the hippocampal place cell representation. In this experiment a series of chimeric environments were used. Each environment contained some environmental features of the circle and some environmental features of the square. In the octagon probe series, environments represented geometric intermediates between the circle and square. Each shape was ambiguous, but uniformly so. In the chimeric shapes probe, by contrast, rats were exposed to conflicting perceptual stimuli as they moved around the environments.

The chimeric shapes probe was designed to test the response of the place cell representation, when exposed to these conflicting stimuli. Will chimeric environments elicit a chimeric place cell representation? On the other hand, it might be possible to observe pattern completion, such that the place cell representation is either square or circle. This would suggest that place cells are acting as a coherent representation. Alternatively, a new representation may emerge for the chimeric shapes. If the chimeric shapes do elicit a chimeric representation, what are the environmental features that determine each cell's firing? For example, is the firing of place cells driven by the environmental features closest to each of their place fields?

Experimental protocol

Chimeric environments were built using the morph box. Each chimeric environment consisted of two portions: a half square and a half octagon, positioned at opposing ends of the environments (see Figure 8.1 for a diagrammatic representation of the environments used). As the place cell representation in the regular 4:4 octagon was always indistinguishable from that of the circle (see chapter 7), half octagons were used, rather than half circles, providing ease of shape construction. Baseline trials, at the beginning and end of the experimental series, were square and octagon, rather than square and circle. The chimeric environmental series consisted of four

Figure 8.1

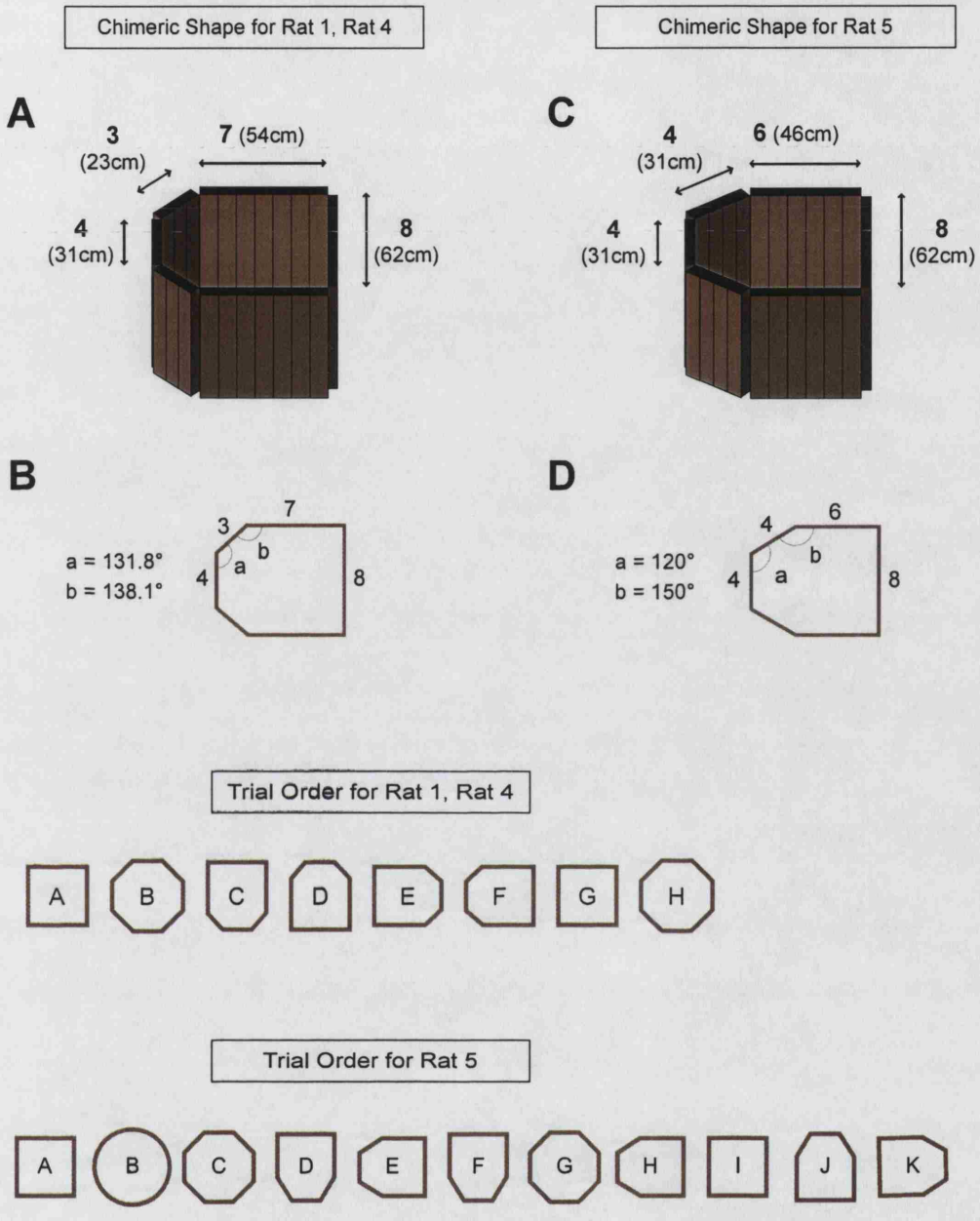

Figure 8.1. Recording environments used for chimeric shapes experiment. **A)** Morph box configuration of chimeric shape used for rats 1, 4. Numbers in bold show wall lengths in morph box sections. **B)** Plan view, showing octagon corner angles. Four chimeric shapes were used, formed by rotating configuration shown in A and B through 90°, 180° and 270°. Orientation of morph box walls with respect to laboratory remained constant. **C, D)** Chimeric shape used for rat 5. **E)** Trial running order for rats 1, 4. All environments constructed using morph box. Shape represents environment configuration. Letters inside shapes show temporal running order. **F)** Trial running order for rat 5.

different chimeric environments, each with the octagonal half positioned at a different cardinal point of the compass. This was done to ensure that all place fields would be exposed both to proximal square walls and proximal octagon walls. The environments will be named with reference to the positioning of the octagonal portion: north-octagon, south-octagon, east-octagon and west-octagon. The chimeric shapes probe was run once for each rat. All cells shown for each rat were simultaneously recorded.

The subjects for the chimeric shapes experiment were rats 1, 4 and 5 only. Rats 1 and 4 shared the same experimental protocol. There were a number of differences, however, for rat 5. For rats 1 and 4, the chimeric shapes probe was run on the day directly following the octagon probe. For rat 5, the chimeric shapes probe was run on the day directly before the octagon probe, directly after the last day of remapping training (see chapter 7 for details of remapping training). A different series of trials was used for rat 5 (see Figure 8.1). The exact shape used as the chimera was different for rat 5 (see Figure 8.1).

Chimeric shapes elicit chimeric place cell representations

Simultaneous square-like and octagon-like responses from different place cells

The firing rate maps for all recorded cells from rats 1, 4 and 5 are shown in Figures 8.2, 8.3 and 8.4, respectively. The same result is clear in all 3 rats: chimeric shapes elicit chimeric representations, that is, in each chimeric shape, some place cells show square-like responses and some cells, simultaneously, show octagon-like responses. Furthermore, almost all cells show different responses depending on the which particular chimeric shape they are exposed to.

These results can be illustrated by concentrating on rat 4 (Figure 8.3). Examining the cells 1-11, (those classified as remapped according to the standard criteria, see Methods for details) it can be seen that, in any particular chimera, different cells show different responses. For example, in trial D (north-octagon), cells 3, 4, 5, 6, 8 and 9 respond as if to an octagon (though cell 8 is missing one sub-field), while, simultaneously, cells 1, 2, 7, and 10 respond as if to a square. (Square and octagon responses for cell 11 are too close to discriminate by eye). The place cell

Figure 8.2

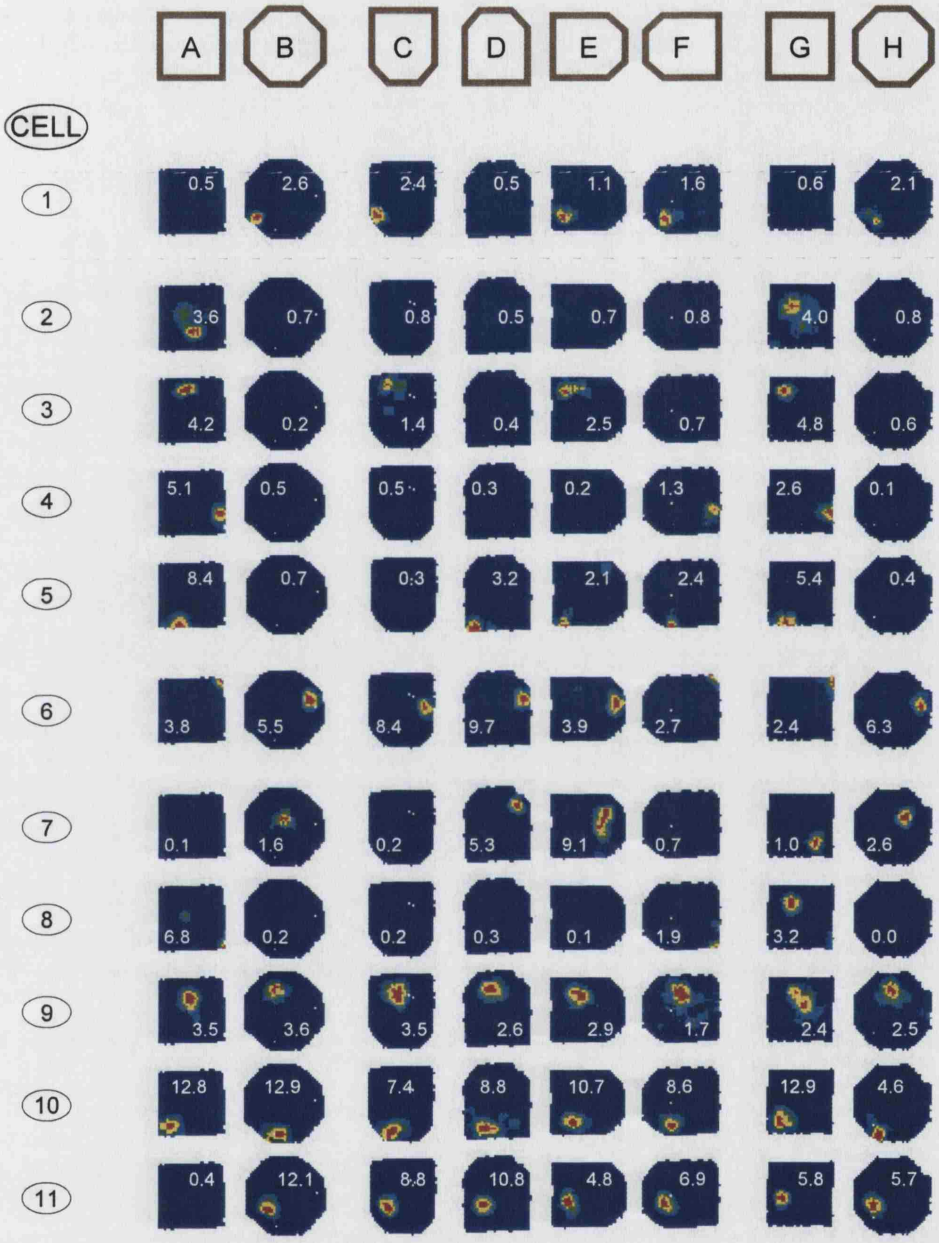

Figure 8.2. Firing rate maps, for all cells recorded during chimeric shapes experiment, for rat 1. All cells simultaneously recorded. Details of firing rate maps and layout as for figure 6.2. 1 cell had a field in the octagon but not the square (cell 1); 4 in the square but not the octagon (2-5); 1 fired in both but in different places (6), and 5 did not did not reach the criterion for remapping (7-11) (see methods).

Figure 8.3

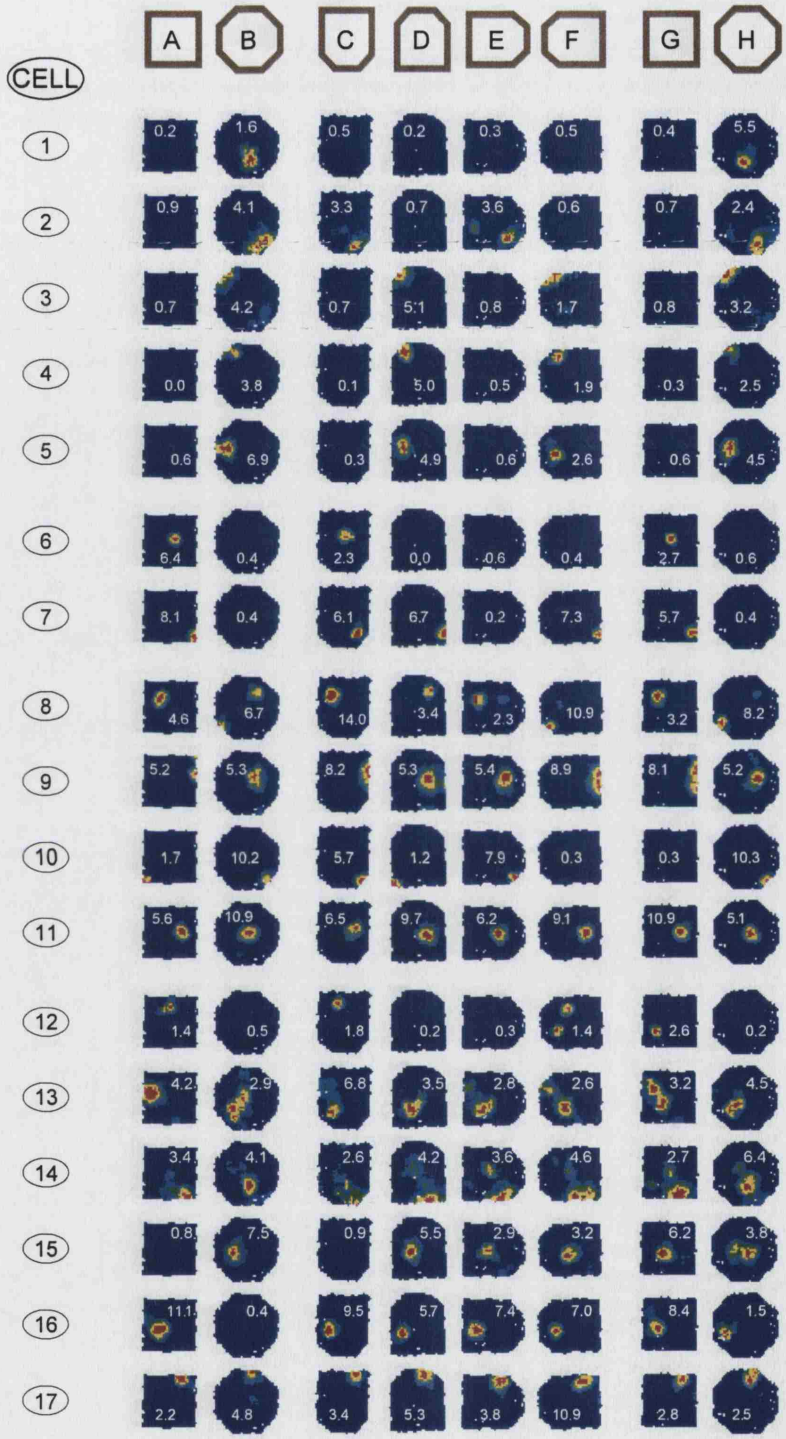

Figure 8.3. Firing rate maps, for all cells recorded during chimeric shapes experiment, for rat 4. All cells simultaneously recorded. Details and layout of firing rate maps as for figure 6.2. 5 cells had a field in the octagon but not the square (cells 1-5); 2 in the square but not the octagon (6-7); 4 fired in both but in different places (8-11), and 6 did not did not reach the criterion for remapping (12-17).

Figure 8.4

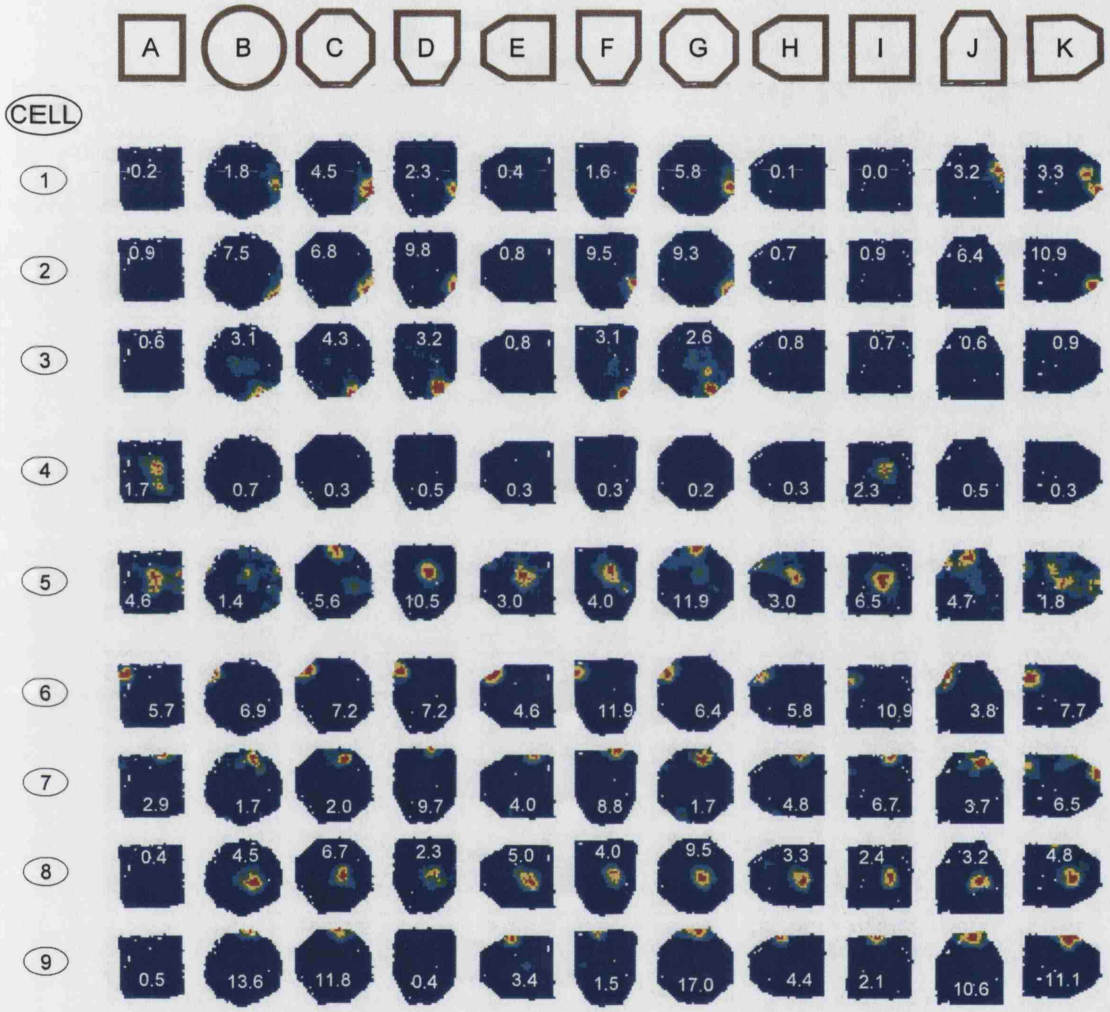

Figure 8.4. Firing rate maps, for all cells recorded during chimeric shapes experiment, for rat 5. All cells simultaneously recorded. Details and layout of firing rate maps as for figure 6.2. 3 cells had a field in the octagon but not the square (cells 1-3); 1 in the square but not the octagon (4); 1 fired in both but in different places (5), and 4 did not did not reach the criterion for remapping (6-9).

representation is therefore evenly split between square-like and octagon-like. The response of each cell does not depend on the type of remapping it exhibits. There are cells from all 3 remapping categories (square-field only, octagon-field only, field position remapped) in each of the square-like and octagon-like groups.

Cells do not have fixed responses to half-square/half-octagon shapes in general. The response seen on each trial depends on the configuration of that particular chimeric environment. In trial C (south-octagon), cells 2 and 10 respond as if to an octagon, while cells 1, 3, 4, 5, 6, 7, 8, 9, 10 and 11 now respond as if to a square. There are further permutations for trials E and F, octagon-east and octagon-west. It appears as if the walls close to the place field of the cell are important in determining response. For example, cell 2 has a field near the south-west wall of the octagon - it does not have a field in the square. The cell only has a field in those chimeric shapes (octagon-south, octagon-west) which are octagonal in the south-west quadrant. However, the relationship is not a strict one. Cell 7 has a field in the south-west corner of the square, which is also present in the octagon-south chimera (trial C). This issue will be discussed in more detail later in this chapter.

The same result can also be observed in rats 1 and 5. In all trials, there is a fairly even split between remapped cells showing square-like responses, and remapped cells showing octagon-like responses.

Individual place cells show mutually exclusive square-like or octagon-like responses

In almost all place cells recorded, the response of the each cell to the chimeric shapes was either strongly square-like or strongly octagon-like. Cells did not show intermediate firing patterns, neither did they show new responses. Particularly clear examples of this are field position-remapped cells such as cell 9 (rat 4), cell 10 (rat 4) or cell 6, (rat 1). In these cases, it can clearly be seen that in each chimera, one and only one place field is present. Cell 6 (rat 1), for example, has a place field which is in the north-east quadrant of the octagon, but tight into the north-east corner of the square. In trials C, D and E, the place field is in the north-east quadrant, but not in the corner. In trial F (west-octagon), cell firing is only directly in the north-east corner. A similar effect can be seen for rate-remapped cells (square-only and octagon-only). In

general, when these cells have a place field in a chimeric shape, the field is in the same position, and with a similar peak firing rate, as that seen in the baseline shape.

This result can be demonstrated by quantifying the similarity of place cell responses to the square or octagon firing. Figures 8.5A, B and C show plots of the similarity scores for all remapped cells, for rats 1, 4 and 5 respectively. Two similarity scores were calculated for each cell: similarity-to-square, and similarity-to-octagon. The similarity score is based on a spatial correlation between firing rate maps, and then normalized so that (for example) similarity of square to square equals 1, and similarity of square to octagon equals 0. (For further details, see Methods). In Figure 8.5, red lines show similarity-to-square, blue lines show similarity-to-octagon. Trial order in similarity plots is the same as for firing rate maps.

It can been seen from Figure 8.5 that the similarity scores (both to square and to octagon) for all cells cluster around 1 and 0. The lines plotting similarity score jump between 1 and 0 as cells switch from one representation to the other from trial to trial. Cells are therefore firing as if in response to a square or a octagon, but not in an intermediate fashion. Furthermore, it can be seen that the lines plotting similarity-to-square (red) and similarity-to-octagon (blue) are, for each cell, approximately mirror images of each other. When a cell is similar to square, it is not similar to octagon, and visa versa. At least for each individual cell, the two representations are mutually exclusive.

The tendency of cells to act as if in response to a square or to an octagon is further illustrated in Figure 8.6. This Figure shows a histogram of similarity scores, pooled over all cells from all three rats. A clear bi-modal distribution of similarity scores can be seen, with clusters around 1 and 0. There are very few intermediate similarity scores within the whole data set.

There are, however, examples of intermediate firing patterns which should be pointed out. For example cell 5 (rat 5) is field position-remapped, with a field in the centre of the square and in the northern section of the octagon. In trial H (west-octagon), the main place field is central, but there is substantial firing in the northern part of the environment. This intermediate firing is reflected in similarity scores for that trial both being below 0.5 (see Figure 8.5C). A similar example is cell 14 (rat 4) though in this case, due to overlapping fields on baseline trials, the cell was classified as non-remapped.

Figure 8.5

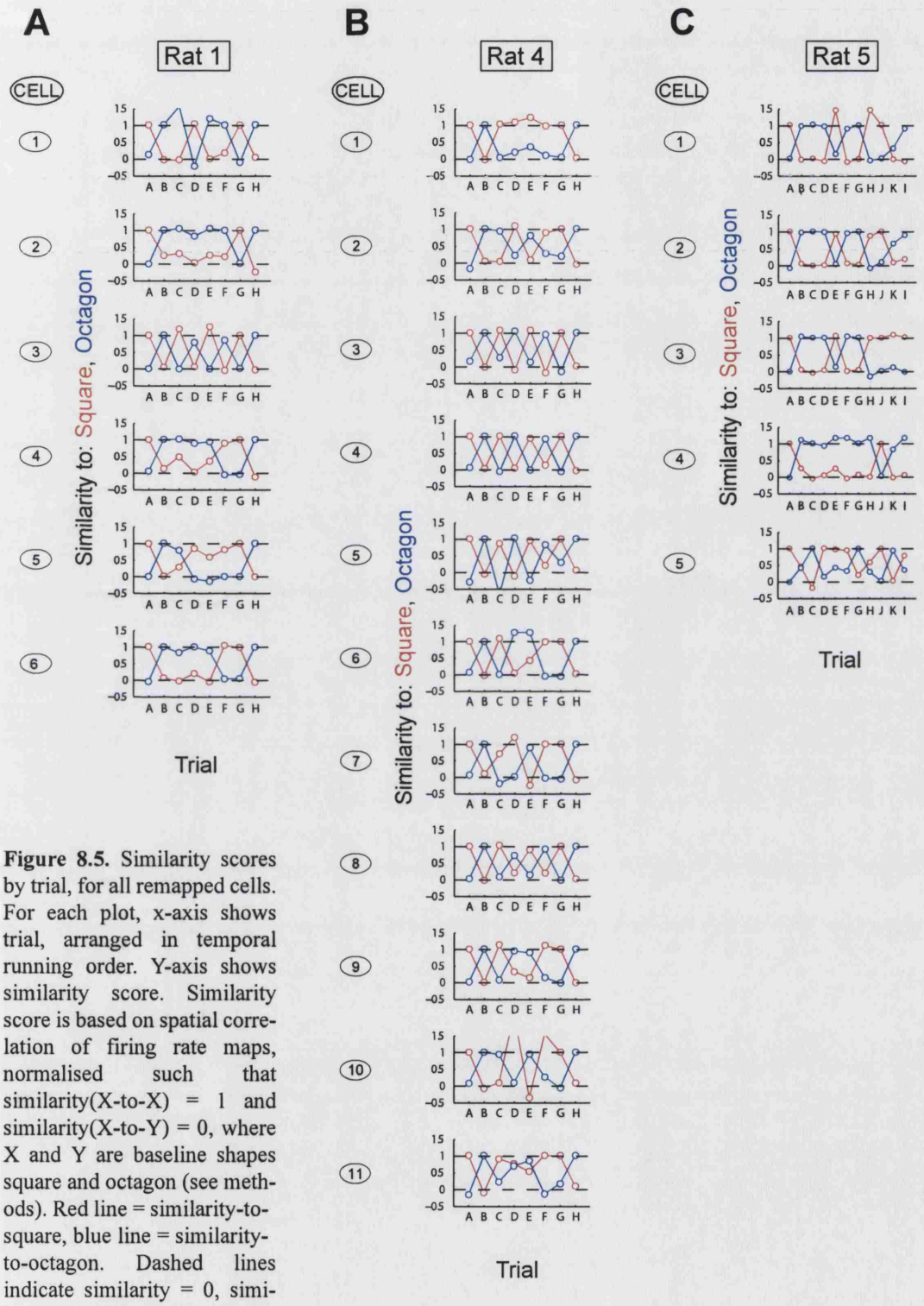

Figure 8.5. Similarity scores by trial, for all remapped cells. For each plot, x-axis shows trial, arranged in temporal running order. Y-axis shows similarity score. Similarity score is based on spatial correlation of firing rate maps, normalised such that similarity(X-to-X) = 1 and similarity(X-to-Y) = 0, where X and Y are baseline shapes square and octagon (see methods). Red line = similarity-to-square, blue line = similarity-to-octagon. Dashed lines indicate similarity = 0, similarity = 1. Cell numbers, to the left of each plot, correspond to cell numbers in figures 8.2, 8.3, 8.4. **A**) All remapped cells for rat 1, **B**) All remapped cells for rat 4, **C**) All remapped cells for rat 5. Note that all similarity scores cluster around 1 or 0, and that, in general, every trial is similar to one baseline shape, and dissimilar to the other.

Figure 8.6

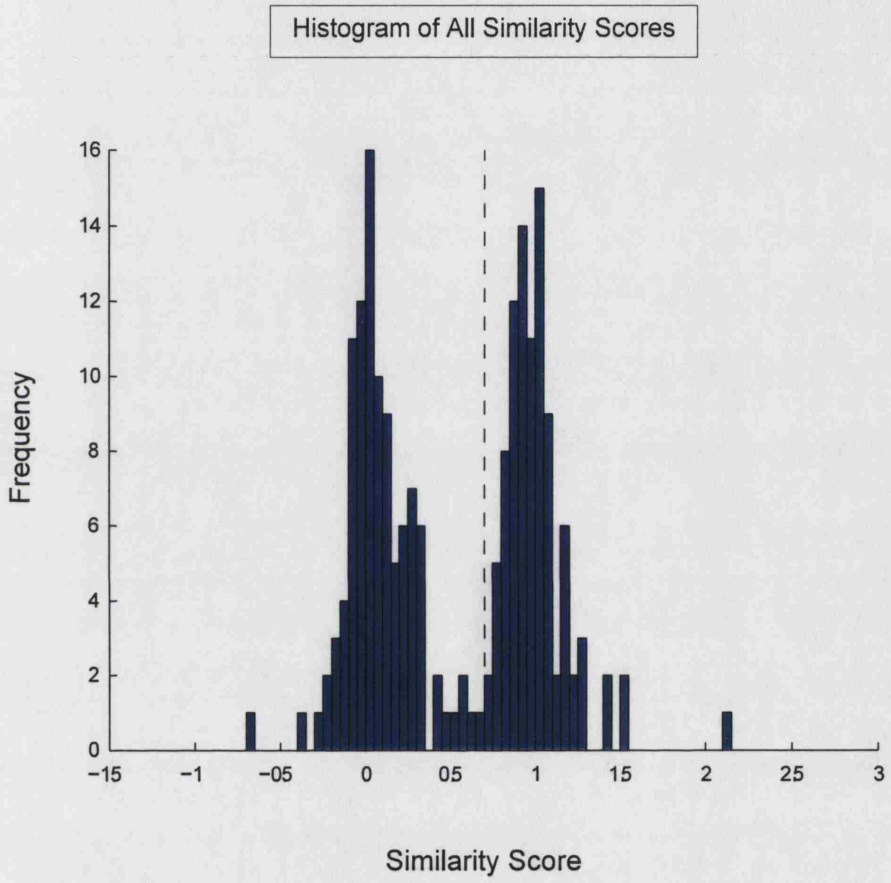

Figure 8.6. Histogram of all similarity scores, for all remapped cells, in chimeric shapes. X-axis shows similarity score, y-axis shows frequency counts over all similarity-to-square and similarity-to-octagon scores for all chimeric shapes, for all three rats. Note the clear bi-modal distribution, with similarity scores clustering around 0 and 1. The vertical dashed line shows the similarity = 0.7 threshold used to assess place cell response for the construction of diagrams in figures 8.7 and 8.9.

A further caveat to the main result is that, although no new place cell responses were seen in the chimeric shapes, altered firing in the baseline trials was often observed. Examples of new fields appearing in baselines shapes are cell 7 (rat 1) and cell 12 (rat 4). More cells showed simple 'convergence', i.e. cells were remapped on the first baseline pair but not on the second (cell 11 (rat 1), cells 15, 16 (rat 4)). In all these cases, cells were classified as non-remapped. The common occurrence of this phenomenon suggests that exposure to the chimeric shapes can disrupt the hippocampal place representation.

Place cell responses are influenced by proximal environmental features

The result that, in general, place cell response is primarily driven by environmental features close to the place field of the cell is clearly seen in all three rats (Figures 8.2, 8.3 and 8.4). For example, for the majority of remapped cells from rat 4 (cells 2, 3, 4, 7, 8, 9 and 10), the response of the cell (square-like or octagon-like) is easily predicted from whether environment wall in the quadrant closest to the place field is square or octagonal.

It is not the case, however, that cell firing is always strictly determined by the shape of the closest environment walls. Some cell responses in the chimeric shapes are directly opposite to what would be predicted on the basis of wall shape closest to the place field. For example, cell 1 (rat 1) in trial E fires as if in response to the octagon, despite the fact the two most proximal walls are configured as a square. Further examples of this behavior are cell 5 (rat 1) on trial F, and cell 7 (rat 4) on trial C. Cells with centrally placed fields in only one baseline shape generally need all walls of the environment to be configured as that baseline in order to show a field (see cell 2 (rat 1), cell 1 (rat 4), cell 4 (rat 5)). However, cell 6 (rat 4) shows a field on trial C (octagon-south) but no other chimeras. Individual cells may therefore show responses to particular chimeric shapes that do not seem influenced by the wall shape proximal to the place field.

This study will not attempt to define exactly which environmental features drive the responses of each individual place cell. The main reason is that there are not enough different shape probes to dissect exactly the influences of every wall on each cell. For instance, larger shapes would be needed to investigate how different

environment walls affect cell firing (see O'Keefe & Burgess, 1996). Furthermore, the fact that, in general, rats were exposed to each chimera only once means that hysteresis and trial order effects on cell firing are hard to rule out.

It is possible, however, to describe trends within the cell population, relating place cell response to environmental shape. Figure 8.7 shows one method of illustrating these trends. The diagrams in Figure 8.7 represent each of the four chimeric shapes, with the field peak positions of all place cells, from all animals, shown as coloured dots. The dots are colour-coded so that square-like responses are shown in red, octagon-like responses in blue. Square-like and octagon-like responses were defined as cells showing a similarity score of > 0.7 to square or octagon. This value was chosen as a threshold as it captures the upper lobe of the bi-modal distribution of similarity scores, those clustered around 1 (see Figure 8.6). Filled dots show the position of actual place fields, with peak rate > 1Hz in that shape. In addition, the diagrams also show the position of cells which did fire in baseline trials, but not in the chimera (peak rate < 1Hz). These are shown as hollow dots. A red hollow dot, for example, signifies that the cell has a place field in the octagon, in the position shown, but does not fire in this chimera. It is therefore counted as a square-like response.

The diagrams of Figure 8.7 reiterate the finding that, in general, place cell response is mainly influenced by proximal wall shape. Blue dots cluster at the octagonal end of the environment, red dots cluster at the square end of the environment. They also show that some place cell responses run counter to this general rule. In addition, they further highlight the chimeric nature of the place cell representation. Figure 8.8 shows some quantification of these results, analyzing the relationship between place cell response and field position, in terms of distance from the 'square' and 'octagonal' corners of the chimera (see Figure 8.8A). The distances between field peak position and the four corners of the chimera (two square, two octagonal) were calculated and, for each corner, whether the cell response matched the corner type (i.e. shape). Figure 8.8B shows the proportion of cells with responses matching the corner type, according to the distance from the corner to the peak, for all remapped cells from rats 1, 4 and 5. It can clearly be seen that shorter distances have a higher percentage of matching responses. Cells are, therefore, biased to fire such that cell response is appropriate to the shape of the most proximal corners. It can also be seen that the decrease in matching responses, as distance to corner increases, is

Figure 8.7

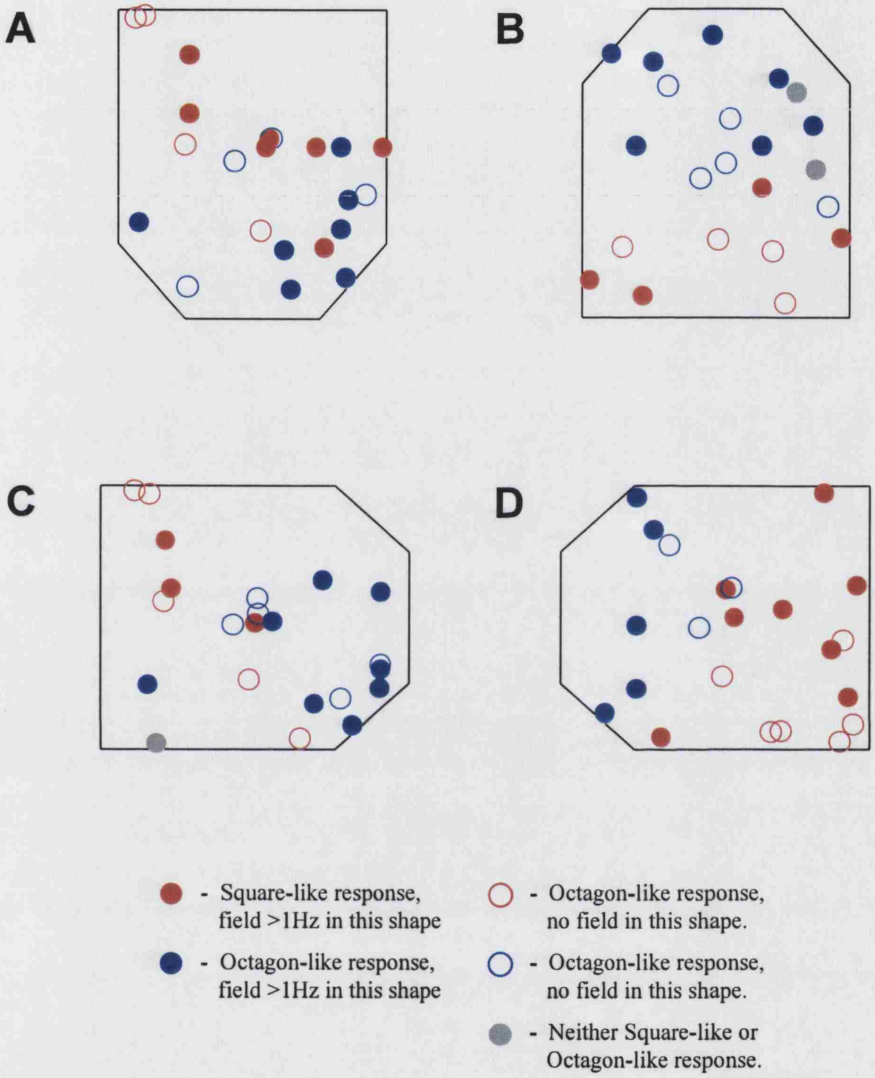

Figure 8.7. Diagrams illustrating field position and place cell response for chimeric shapes. Each shape represents a chimeric shape configuration. Coloured dots represent place field peak firing rate bin positions, for all remapped cells from rats 1, 4 and 5. Red dots = square-like responses, blue dots = octagon-like responses. To be judged showing a square-like or octagon-like response, a place cell needed similarity > 0.7 to one baseline shape, and < 0.7 to the other. Grey circles show fields of cells with similarity < 0.7 to both baselines. Filled dots represent cells with place fields in that chimera. Hollow dots represent cells which have a place field in a baseline shape, in the position shown, which do not fire (peak rate < 1Hz) in that chimera. Baseline field positions are transformed to chimera equivalents using standard shape transformation algorithms (see methods). **A**) South-Octagon, **B**) North-Octagon, **C**) East-Octagon, **D**) West-Octagon.

Figure 8.8

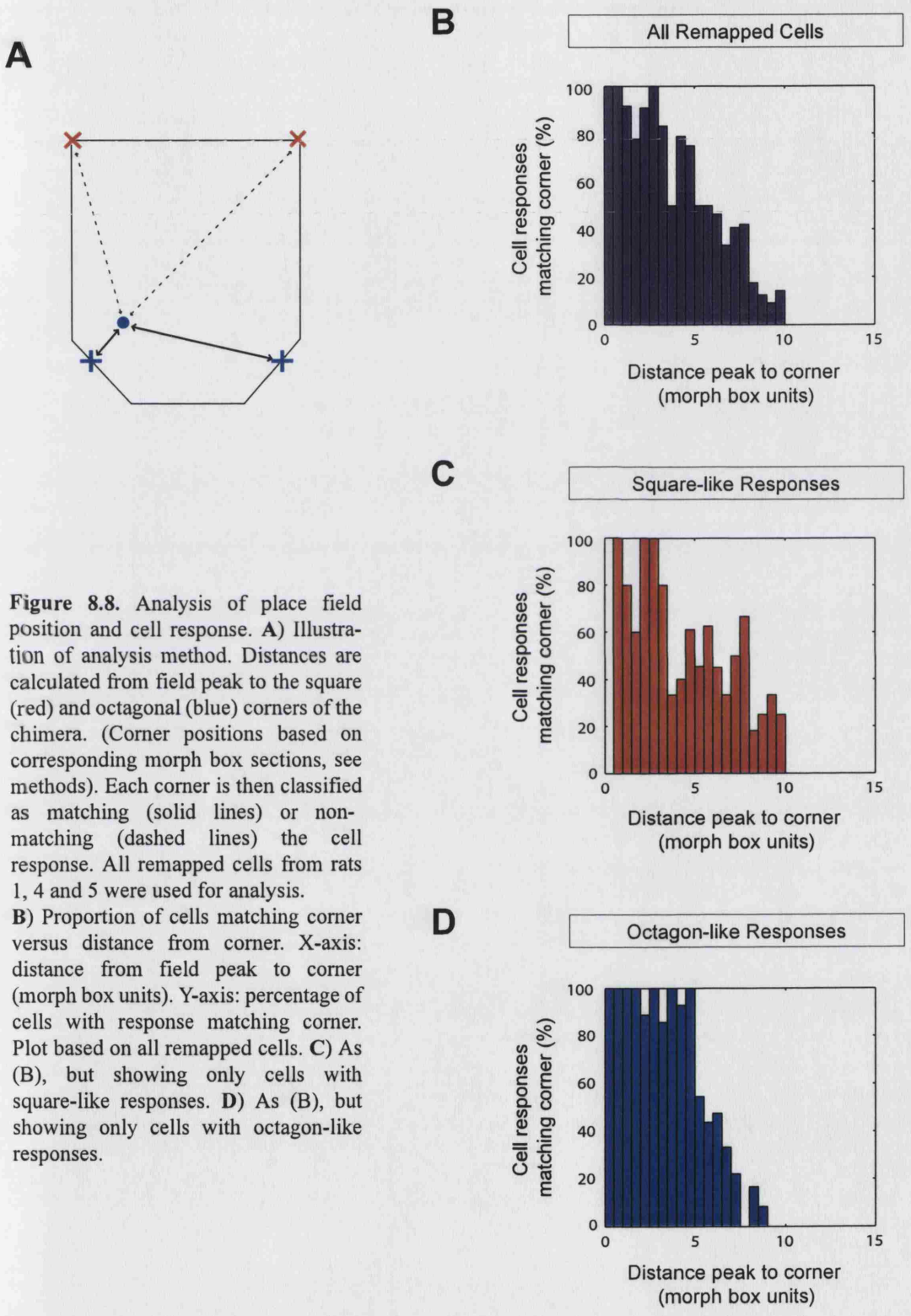

Figure 8.8. Analysis of place field position and cell response. **A**) Illustration of analysis method. Distances are calculated from field peak to the square (red) and octagonal (blue) corners of the chimera. (Corner positions based on corresponding morph box sections, see methods). Each corner is then classified as matching (solid lines) or non-matching (dashed lines) the cell response. All remapped cells from rats 1, 4 and 5 were used for analysis.
B) Proportion of cells matching corner versus distance from corner. X-axis: distance from field peak to corner (morph box units). Y-axis: percentage of cells with response matching corner. Plot based on all remapped cells. **C**) As (B), but showing only cells with square-like responses. **D**) As (B), but showing only cells with octagon-like responses.

gradual and approximately linear. Even at the longest distances (9 - 10 morph box units) 10-15% of cells' responses match the shape of the corner.

Figures 8.8C and 8.8D show the same analysis, but for only those cells with square-like (8.8C) or octagon-like (8.8D) responses. Both plots show a greater proportion of matches when the field is close to a corner. Comparing the two, however, it can be seen that for square-like cells the gradient of decrease in matching responses is flatter, and a larger proportion of distant corners match cell responses. Contrastingly, the plot for octagon-like cells shows a more abrupt drop in the proportion of matching responses, at a distance of approximately 5 morph box units. Place fields therefore show square-like responses over a larger part of the chimeric shape. Octagon-like responses, by contrast, are seen in those fields more tightly clustered in areas close to the octagonal part of the shape.

Is there flipping between different coherent representations?

Chimeric responses to chimeric shapes do not necessarily rule out a coherent place cell representation of the environment. It may be that, as the rat moves around the environment, hippocampal activity 'flips' between the square and octagon representations, switching between them being driven by whichever environmental features are close to the animal. If this were the case, one would expect to see clearly delineated areas of the environment in which there are exclusively square-like or octagon-like responses. By contrast, if square-like and octagon-like responses were to be mixed together, in the same areas of the environment, it would argue against this interpretation.

Figures 8.7 showed that square-like and octagon-like responses were, to some extent, spatially intermingled (particularly in the South-octagon, 8.7A, and the East-octagon, 8.7C). However, binning together data for all rats could be obscuring a clear delineation between square and octagon areas on individual trials. Figure 8.9, therefore, shows the same data as Figure 8.7, but showing separately the remapped cells recorded on each trial.

For rat 1 (Figure 8.9A), place cell responses do seem spatially separated into square-like and octagon-like, but there are too few remapped cells to reach a firm conclusion. Rat 4 (Figure 8.9B) offers better evidence for flipping between different

Figure 8.9

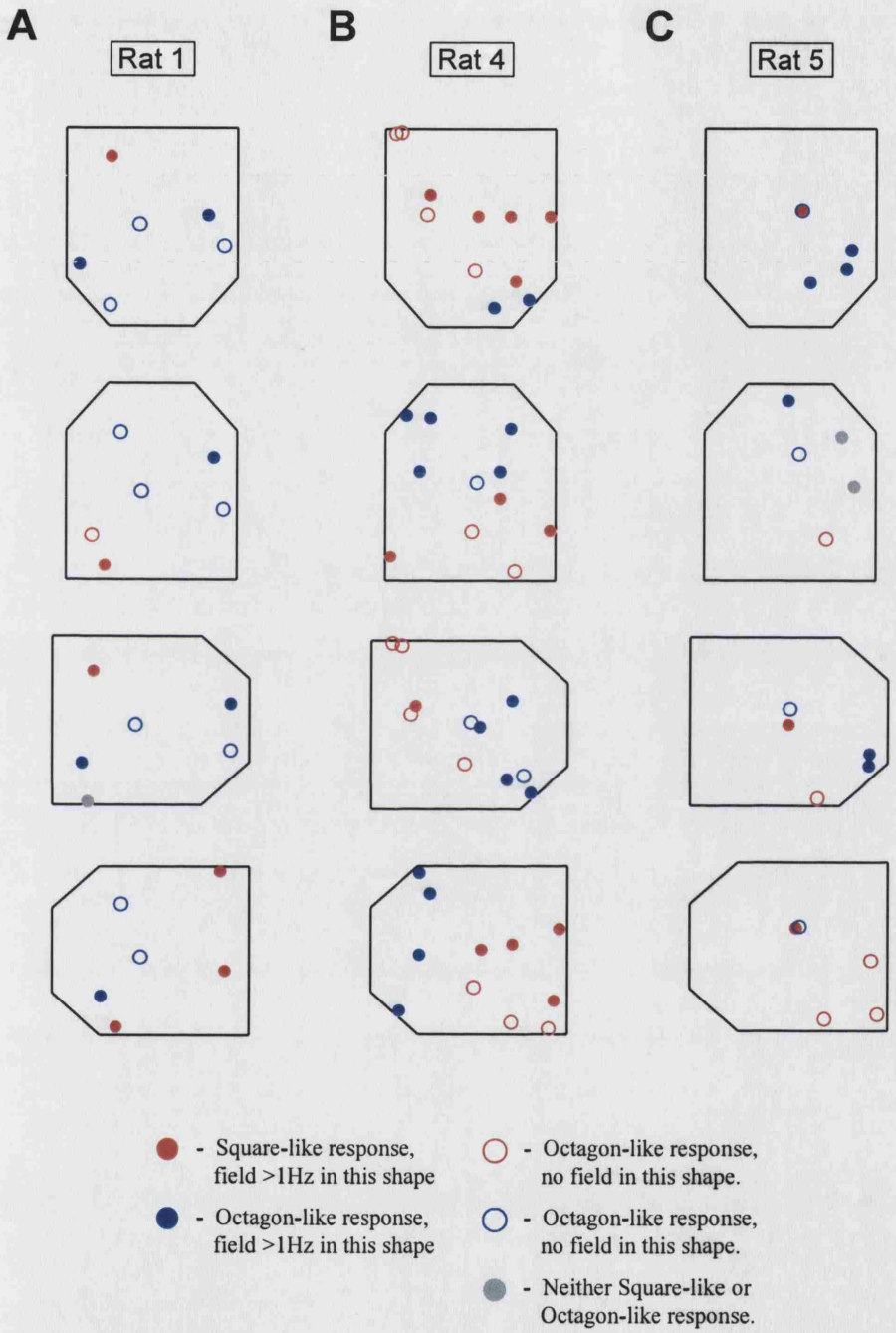

Figure 8.9. Diagrams illustrating field position and place cell response, with data for each rat shown individually. Diagrams constructed as for figure 8.7. Rat 5 chimeric shapes were transformed to match the shapes for rats 1 and 4, using standard algorithm (see Methods). Figure shows all remapped cells from; **A**) rat 1, **B**) rat 4, **C**) rat 5.

maps: there are enough remapped cells to sample responses over the whole environment, and in each trial, square-like and octagon-like areas can be clearly delineated. Interestingly, if there are two separate coherent representations, the areas of the environment over which they are active can change greatly between trials. In the north-octagon and east-octagon, the environment is split roughly in half between square-like and octagon-like areas. In the west-octagon, octagon-like responses are constrained to a smaller area, closer to the octagonal part of the chimera. In the south-octagon, the only octagon-like responses are very close to the octagonal south-west corner of the box. This variability would explain the result seen in Figure 8.8A, in which there is a graded relationship between the cell response and distance to the wall, when all cells are pooled together.

Rat 5 has few remapped cells, but the responses of two cells seem to argue against the 'map-flipping' interpretation. These cells have place fields close to each other, in the centre of the environment. In three out of four chimeric shapes, these two cells have opposite responses (see Figure 8.9C). Again, however, it is difficult to reach firm conclusions with so few cells: these place fields could be on the boundary between the two different maps.

Summary

The octagon probe experiment showed that, under certain conditions, place cells could act as a coherent representation of the environment. By contrast, in the chimeric shapes, place cells were shown not to act in a coherent manner. The chimeric shapes elicited a chimeric cell population representation, with some cells responding as if to a square, and, simultaneously, some responding as if to an octagon. However, although the place representation is chimeric at the cell population level, individual place cells display all-or-none switches between (mutually exclusive) square-like or octagon-like responses. The response of each cell is primarily influenced by the shape of the environment wall close to the place field. Overall, square-like responses occur over a larger proportion of the environment than octagon-like responses.

It could be that chimeric representations are in fact composed of two different coherent representations, between which the hippocampus switches as the rat moves around the environment. There are too few cells in each animal to test this hypothesis

properly, but data from rat 4, in which different cell responses occur in two clearly separated areas of the environment, suggests that it may be possible.

Chapter 9

Discussion

This discussion will consider the results presented in each of the preceding three chapters. It will attempt to highlight and summarise the most important results in each chapter, and place these finding in a wider context.

Remapping Training

Fast Remapping in Response to Changing Environment Shape and Colour

Rats were exposed to an alternating series of two environments that differed in the shape, colour, texture and odour of their walls. These differences induced fast remapping of CA1 place cells. By the end of day 1 (3 trials of each shape) the majority of recorded place cells were remapped in most rats (83%, 69%, 50% and 77% cells remapped in rats 1, 2, 3 and 4, respectively). Within each animal, there were a variety of cell responses, with some cells being stably remapped from the first trials, some becoming remapped during training, and some stably non-remapped throughout the day. Almost all remapping that occurred in these animals happened during day 1: the proportions of cells remapped at the beginning of day 4 were the same, or only slightly higher, than at the end of day 1 (80%, 69%, 67% and 82% cells remapped in rats 1, 2, 3 and 4, respectively).

This study shared much of its experimental protocol with that of Lever *et al* (2002), the only difference being that, in this study, recording environment walls differed in colour and material, in addition to shape. The results, however, are very different - in Lever *et al* (2002), remapping took days or weeks to occur. This suggests that the contrast of wall colour, texture and odour is crucial in bringing about fast remapping. Why does this extra change lead to fast remapping? One possibility is that wall colour alone is driving remapping. There are no directly comparable experiments which have only changed wall colour: Bostock *et al* (1991) changed only cue card colour, and saw no remapping immediately; Jeffery & Anderson (2003)

obtained complete remapping by changing wall and floor colour, but most cells were primarily responding to the colour of the floor. The best evidence for colour-based remapping is from a study by Kentros *et al* (1998), which obtained complete remapping by changing wall colour and cue card colour. Against this, the transfer experiments, of Lever *et al* (2002) and this thesis, both showed that when wall colour and wall shape are dissociated, place cells preferentially respond to wall shape. Given the finding that place cells can remap between square and circle (Muller & Kubie, 1987; Quirk *et al* 1992; Sharp, 1997; Lever *et al*, 2002), it seems most likely that all sensory contrasts together are driving the fast remapping of place cells. An interesting question is whether the multi-modal nature of the contrasts present in this study is important in producing fast remapping.

Another important issue is whether remapping involves learning or plasticity, or whether it consists of hard-wired responses to stimuli. It has been demonstrated that stabilising remapped representations requires the molecular machinery of synaptic plasticity (Kentros *et al*, 1998; Agnihotri *et al*, 2004). It is also clear that the slow remapping of Lever *et al* (2002) involves a learning process. However, whether place cells show learning in the case of 'fast' remapping has not been well studied. In this study, it is clear that, within the same animal, some cells show learning, while others show remapped responses from the first exposure to the environments. In the section below, the idea is developed that coherent place cell representations may be based on selectively strengthening connections in CA3 recurrent collaterals (see also chapter 4). The fact that place cell responses are (at least in part) learnt supports the idea that synaptic plasticity is required to form remapped representations. Furthermore, the heterogeneity of responses is interesting in itself. It is possible that some place fields are the result of hard-wired, feed-forward responses, while others are recruited to the network only after some experience.

In chapter 3, a distinction was drawn between different forms of remapping. 'Complete' remapping involves all place cells simultaneously changing their response (including turning on or off), and could correspond to an abrupt switch to a new, independent active sub-set of cells (Muller *et al*, 1987; Thompson & Best, 1989; Bostock *et al*, 1991; Kentros *et al*, 1998). By contrast, other studies have found 'partial' forms of remapping, including remapped and non-remapped responses existing simultaneously (Skaggs & McNaughton, 1998) or gradual, piecemeal changes to place cell responses (Lever *et al*, 2002). How does the remapping

described in this thesis fit into this context? It seems clear that it is close to the concept of 'complete' remapping. The proportion of place cells non-remapped is greater than that expected by chance, but is also clearly a minority (25%, on average, at the start of day 4). Furthermore, although some cells change responses during day 1, almost all remapping has occurred by the end of six trials. As was noted in chapter 3, 'complete' remapping, as seen in this study, is more compatible with the conception of place cells forming a coherent representation of space.

Remapped Representations Transfer to Shape-Only Differences

Rats were trained in alternating white circles and morph squares for 3 days. During day 4, the white circle was replaced with the morph circle. In all rats, the remapped place cell representations at least partially transferred from white circle to the morph circle, demonstrating that wall shape was capable of maintaining remapping. In two animals, transfer was complete: almost all cells transferred firing patterns from white to morph circle. In the other two animals, transfer was partial: some remapped cells converged to a non-remapped response, though overall remapping levels remained at least 50%.

In the section above, the tentative conclusion was reached that all sensory contrasts together were responsible for causing remapping. It therefore appears that shape is maintaining remapping, despite some of the sensory cues that originally caused it (colour, odour, texture) now being the same in both environments. The complete transfer seen in two animals therefore seems best explained in terms of pattern-completion, i.e. the ability of place cells to maintain their firing patterns despite the alteration or removal of some cues in the environment. Pattern completion is often postulated to depend on CA3 recurrent connections (Marr, 1971; McNaughton & Morris, 1987; Treves & Rolls, 1994), and removing NMDA receptors from CA3-CA3 synapses reduces the ability of place cells to compensate for removal of a sub-set of cues (Nakazawa *et al*, 2002). It would be interesting to investigate animals without CA3 recurrent collateral function (no CA3-CA3 synaptic plasticity, or a CA1-entorhinal only perforant pathway), and see, if they remapped at all, does white to morph transfer still occur?

For the partial transfer seen in two animals, other explanations are also possible. The fact that partial convergence of the sensory cues leads to partial convergence of remapped representations could suggest that different place cells are coding cues independently. The result bears some resemblance to the finding that the amount of CA1 remapping relates to the degree of stimuli divergence between environments (Leutgeb *et al*, 2004; Vazjardanova *et al*, 2004). In this interpretation, remapping is caused by both shape and colour, independently. Making colour similar causes those cells responding to colour to converge their responses, leaving the responses of others unaltered. However, the dynamic of place cell responses in rat 3, in which responses almost completely converged, then partially diverged, argue against this interpretation. Other factors, such as the animal's expectation of the shape, and the contrast to the shape in the last trial, seem to be required to explain the results.

Octagon Probe

Abrupt, simultaneous response switching suggests coherent representations

The octagon probe experiment was designed to test to what extent place cells constitute a coherent representation of the environment. Rats were trained until place cells were remapped between two environments, differentiated only by their shape (Square vs Circle). The animals were then exposed to a series of environments with shapes geometrically intermediate between square and circle. The rationale was that, if place cells are responding to environmental features independently, different cells should switch responses at different points in the series. Coherent representations should switch in unison.

In the main experimental group (rats 1-4), two important results were observed: first, place cells abruptly switched between responses; second, almost all cells simultaneously switched at the same point. The fact that place cells 'flip' between representations in this way suggests co-operative action between cells, based on the probability of cells independently switching at the same point. If it is assumed that cells have an equal probability of switching at any of the five transitions in the series, the probability of all cells switching responses between the same shapes would

be $0.2^{(N-1)}$, where N is the number of remapped cells. This is a very small probability, ranging from $p = 0.0016$ (for rat 3, $N = 4$) to $p < 10^{11}$ (for rat 4, $N = 17$).

The most commonly proposed model for co-operative action in the hippocampus is that CA3 pyramidal cells form an auto-associative network, based on their recurrent collateral connections (Marr, 1971; McNaughton & Morris, 1987; Treves & Rolls 1992). In a specifically spatial context, it has been proposed that place cells could represent the environment by means of connection strengths between CA3 neurones (Muller, 1996; Samsonovich & McNaughton, 1997). Remapping would then correspond to CA3 switching to a different, independent, connection matrix (Battaglia & Treves, 1998; Kali & Dayan, 2000). In the octagon probe, the switch between representations occurred in response to a very small change in sensory input. It has been proposed that, in order to reduce interference between different CA3 representations of similar environments, the dentate gyrus performs an 'orthogonalisation' function (McNaughton & Morris, 1987; Rolls 1990). The entorhinal input is projected onto large numbers of dentate granule cells, decreasing the correlation between similar representations. Such a mechanism may allow the discrimination of very similar intermediate environments. The orthogonalisation/auto-association model would, in theory, explain how the hippocampal place cell representation can 'flip' between responses when presented with the intermediate octagon series.

The model proposed above has some weaknesses. In addition to the 'tri-synaptic loop' projections described here, there are also direct projections from the entorhinal cortex to all fields of the hippocampus (see Chapter 1). In the orthogonalisation/auto-association model, the roles of these projections are not well defined. There is also little direct evidence that information processing in the hippocampus follows the orthogonalisation/auto-association principle. However, some place cell data on remapping is consistent with the model. CA3 place cells are more likely to display all-or-none remapping (Leutgeb *et al*, 2004; Vazdarjanova *et al*, 2004), and CA1 place fields are less resistant to cue removal when CA3 recurrent collateral NMDA receptors are not present. The place representation in the dentate gyrus is sparsely coded (Jung & McNaughton, 1993, Chawla *et al*, 2005) and with low overlap between remapped representations (Chawla *et al*, 2005). Despite the weaknesses of the orthogonalisation/auto-association model, therefore, it remains a useful hypothesis. The octagon probe presents a good opportunity to test the model,

by selectively removing or inactivating fields of the hippocampal formation and observing the effect on the place cell responses (for more detail, see below).

Attractor Dynamics in the Place Cell Representation

The Attractor Neural Network (ANN) is a formalism commonly used to describe the behaviour of recurrently connected networks, such as the model outlined above (Hopfield, 1982). A fixed point ANN model of the octagon probe result is illustrated in Figure 9.1. The behaviour of the network is described by a one-dimensional 'landscape' (Lyapunov function), where encoded representations (P and Q, Figure 9.1A) occupy positions in the landscape (see Amit, 1992). The dynamic properties of the network are such that it always moves 'downhill' from the starting point (input stimulus, R). In a network without attractors, the landscape is flat, and the response to intermediate octagons will be intermediate between square and circle representations (Figure 9.1B). If the square and circle representations are attractor states of the network, however, an intermediate starting point will move downhill until it reaches either one of these two states (Figure 9.1C).

If the hippocampus is acting as an ANN in the intermediate octagon experiment, it should be possible to see attractor dynamics in place cell responses: the network should take time to reach the attractor state. Furthermore, the further the stimulus is from the attractor state, the longer the network should take to reach it. This was seen in (some of) the intermediate octagons: place cell firing was ambiguous within the first few tens of seconds of a trial, and became more like the final representation within approximately two minutes. The effect was strongest in the 2:6 octagon, one of the more intermediate shapes.

There are problems with this interpretation, however. First, this effect was not seen in the 3:5 octagon, just as 'intermediate' as the 2:6. Second, the time course of the changes seen was much slower than would be predicted by ANN models. Generally, ANN models based on hippocampal anatomy require only tens of iterations before a stable attractor pattern of activity emerges. If one iteration cycle is taken to correspond to one theta cycle in the hippocampus, then a stable pattern of activity should emerge within 10 seconds. By contrast, the place cell representation in the intermediate octagons changes over the course of 100 seconds. This mismatch

Figure 9.1

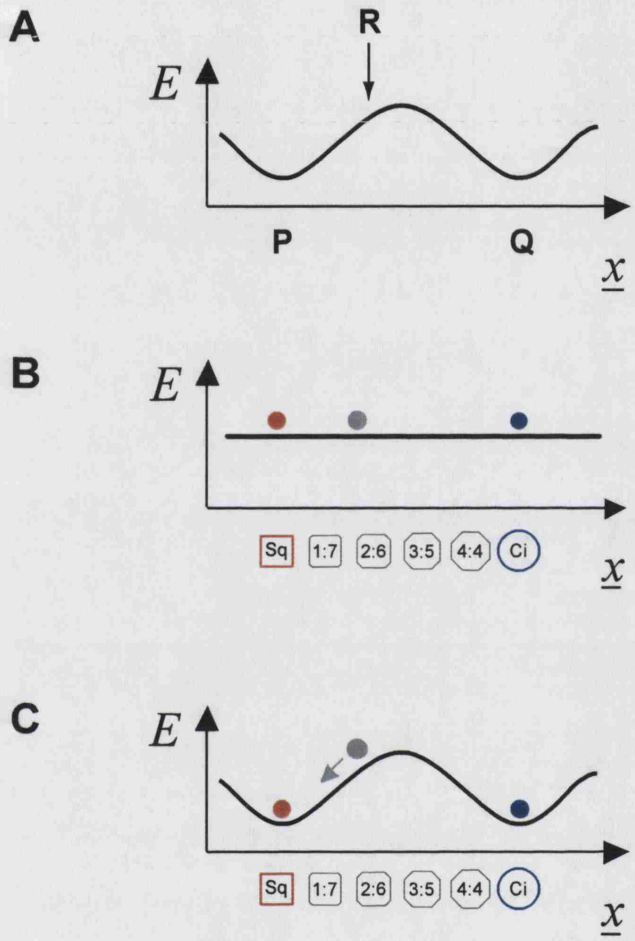

Figure 9.1. A) Dynamics of an Attractor Neural Network, illustrated by a 'landscape' function. P and Q represent attractors within the possible range of network states (x). The dynamics of the system are such that the 'energy' or Lyapunov function (*E)* of the system can only reduce. Given an input stimulus (R), the system will change state, until an attractor is reached (in this case, P). **B)** Place cell representations x (vector of activity of N place cells) in the absence of attractors. The representation of an environment of intermediate shape (grey point) is intermediate between those of the square or circular environments (red and blue points respectively) **C)** Attractor representations of square and circular environments (Sq and Ci). The place cell representation of an environment of intermediate shape (grey point) falls into the basin of attraction of the circular or square representation and converges onto that representation over time (grey arrow).

suggests that the changing state of the representation does not correspond to the classical attractor dynamics of the ANN.

The slow dynamics are also in contrast to reference frame switching in the shuttle box task (Gothard *et al*, 1996; Redish *et al*, 2000; Gothard *et al*, 2001; see below, 'Chimeric Shapes' section for a brief description). In this task, place fields switch from one position to another (from room-aligned to apparatus-aligned, or *vice versa*) over very short periods (approximately 100ms). There are, however, many contrasts between this task and the octagon probe: in the shuttle box, non-remapped place cells moved their fields along a linear track, at the start of octagon probe trials, place cells were developing either of two unrelated, remapped, responses. Expressed in terms of attractor models, the shuttle box switch corresponds to a jump in the position of a continuous attractor activity peak, whereas the changes in the octagon probe correspond to the states of a system approaching a fixed attractor. It is therefore probable that different neural mechanisms underlie these two processes.

Alternative explanations for the dynamic response include short-term plasticity, such as that seen in some cells in the Lever *et al* (2002) study. It could also be that the slow response is related to the time needed for the animal to explore the environment. If place cells are responding mainly to cues close to the animal, then the animal may need to adequately sample the environment before the hippocampal representation reaches its final state.

The interpretation described above is based on a model of global remapped representations as fixed point attractors. It should be noted, however, that this model does not account for place cell discharge in a particular location. (Unlike continuous attractor models). The model therefore describes the encoding of global representations of space in the hippocampus, but not of particular locations within that space (see Chapter 5 for further details).

Different representations elicited by the same intermediate shape

In two out of the four rats showing abrupt, simultaneous switching (rats 2 and 3), different trials in the same intermediate shape elicited different place cell representations. This result could be interpreted in different ways. It could be seen as the product of stochastic, noisy, attractor dynamics in the place cell responses. On the

other hand, it could be seen as a result of plasticity in the place cell response, induced by a single exposure to the intermediate octagons.

The smooth curve of the attractor landscape shown in figure 9.1C is an idealisation: in reality, the response of the system would also be affected by the noisy signal of biological neurones. (See, for example, Fenton & Muller (1998) for a description of how temporal variation in place cell firing is greater than can be predicted using a Poisson distribution model). The unreliability of real neurones may be an inherent weakness of a biological system, or it may be an advantageous feature of ANN systems, reducing the error from spurious attractor states (Amit, 1992). Whatever the reason for noise in the system, it could have a similar effect on the dynamics of the place cell network: if an input stimulus is on the cusp of a hill between attractors, random fluctuations in network state could cause it to fall into either one attractor or the other. In this interpretation, the 2:6 and 1:7 octagons fall on such a cusp.

Alternatively, the assumption that noise observed in cell activity carries no information may be wrong. The 'noise' may not be noise at all, but, rather, signal for which the correlate is not known. In this case, the system may chose between attractor states not on a random basis, but on the basis of subtle differences in uncontrolled variables between different trials.

A different explanation is that the changing place cell responses between the first and second series may be due to plasticity. Exposure to the first intermediate octagon series could have disrupted the place cell representation to the extent that it would respond differently to any later exposures to the same shapes. To test this hypothesis, one would need to run an extended series, of several exposures to the octagons. If responses to intermediate shapes were to be square-like or circle-like in random sequence, it would argue for the noisy attractor interpretation. If, on the other hand, place cell responses tended to change only once, then stay that way, it would argue that plasticity is responsible.

Possible Objections

The model outlined above explains abrupt, simultaneous response switching in terms of auto-associative information processing in the hippocampus. There are, however, other possible causes for the result.

One such explanation is based on the limits of rat visual perception. Vision is the most likely sensory modality for the rat to discriminate the shapes, given that odour and texture cues on wall and floor are the same in all shapes. If the rat is using vision to discriminate the shapes, the switch between representations could be due to the differentiating feature falling below a perceptual threshold in some shapes. If, for instance, the corner wall in the 1:7 and 2:6 octagons was too small to discriminate from the adjacent walls, this could lead to the animal judging these shapes to be squares. However, measurement of rat visual spatial acuity argues against this interpretation. The peak spatial sensitivity of rat vision is approximately 0.1 cycles/degree, that is, a banding pattern in which each band subtends 10° on the retina. Rat spatial acuity (the finest detail that can be discriminated) is approximately 1 cycle/degree. (Birch & Jacobs, 1979; Dean, 1981; Silveira *et al*, 1987; Keller *et al*, 2000). When viewed from the centre of the box, the angle which the 1:7 octagon corner wall subtends onto the retina is approximately 10°.

These data do not prove that the rat is able to discriminate the wall. The difference between wall appearance (due to shadows from illuminated cue card) appeared very low-contrast (though no proper reflectance measurements were taken). Furthermore, measurements of visual spatial sensitivity were performed in photopic light conditions, while experimental conditions were scotopic. However, if rats were able to discriminate walls at all, they should have been able to see even the smallest wall, the 1:7 octagon corner. It seems unlikely, therefore, that the place representation switch was due to an environmental feature crossing a visual discrimination threshold.

A further explanation is that remapping between square and circle is not purely sensory, but also based on the rat's expectation of an alternating sequence of shapes. All rats were trained with an unbroken alternating sequence, six trials per day for six days. Although remapping must be initiated by a sensory discrimination, it is possible that this is later reinforced by learning that a square always follows a circle, and visa versa. The influence of expectation on place cell firing has been seen in the

context of remapping (Skaggs & McNaughton, 1998), and in the context of directional orientation (O'Keefe & Speakman, 1987).

Learnt expectation of an alternating sequence is a valid alternative explanation for the results seen, at least on the first octagon series. The place cell representations alternate between square and circle, exactly as if they were responding to the training sequence of square/circle. However, this is not the case on the second octagon series. Trial H is a 2:6 octagon, and also directly follows a square. For place cells to display a square-like response here, therefore, would be evidence against an expectation effect. Two rats (1 and 4) do display a square-like response on trial H. Of the other two rats which do not, rat 2 displays a circle-like response on trial J, a 1:7 octagon which directly follows a circle. For 3/4 rats, therefore, an expectation effect is controlled for by the results from the second octagon series.

Interestingly, an expectation effect may be present even in rats 1 and 4. In the time series analysis for both rats (figure 7.8C, 7.9C), the strongest effect of time on place cell response was seen in trial H. The ambiguous nature of the place representation, in the early part of the trial, could have been caused by the conflict between expectation and sensory stimuli.

Comparison with Previous Studies

The broad rationale of the octagon probe experiment, investigating the nature of remapped representations using intermediate stimuli, was shared by other recent studies. Vazdarjanova *et al* (2004) and Leutgeb *et al* (2004a) both placed animals in a series of environments, dissimilar to different degrees, and then measured remapping in CA1 and CA3. Both studies claimed a similar result: that CA3 exhibited 'all-or-none' remapping, while CA1 showed partial remapping, with the amount of remapping depending on the degree of environment dissimilarity. The CA3 representation was therefore claimed to be more coherent than that of CA1 (See chapter 3 for further details). This result is appealing in the context of the functional model outlined above. Only CA3 contains the extensive recurrent network needed for auto-associative representations, whereas input into CA1 is from both CA3 and the entorhinal cortex. The entorhinal representation is assumed to be more 'sensory bound', and thus this input reduces the coherence of CA1 place cell firing.

Caveats of the above studies are discussed in chapter 3, but the most important, and a motivating factor for the intermediate octagon probe, is the need for a well controlled, systematic relationship between the environments. One study which attempted this was Leutgeb *et al* (2004b). The environments used for remapping were a square and a circle, further differentiated by a large or a small internal cue card. The intermediate environments were created using a deformable octagon. To convert a square to a circle, a corner was gradually created in the centre of the square walls, and this 'flat' side of the octagon rotated (by 45°) away from its square orientation. At the same time, cue card size was gradually increased. The results from this experiment are clear: representations change gradually and incrementally, in both CA1 and CA3. Cell-by-cell data is not presented, but exemplar firing rate maps show a mixture of different behaviours: some cells change response abruptly (but not simultaneously), some change response gradually. In one animal (out of four), an abrupt switch is claimed in CA3, but the effect is not pronounced and, furthermore, is not present when a temporal co-firing measure is used.

Why are the results of Leutgeb *et al* (2004b) in complete contrast to those of the present study? One possible reason is the nature of the intermediate shape probe. In the present study, intermediate shapes were presented in pseudo-random order, aimed at ruling out temporal hysteresis effects. By contrast, Leutgeb *et al* (2004b) presented the environments by order of shape. Starting with one baseline (for example, square), the environment in each trial became progressively more like the opposite baseline (circle). Possibly, with this design, gradual changes could have been produced by the contrast between expectation (another square) and sensory input (slightly more circular than the previous trial).

Comparison with Previous Studies: Remapping Training and the Nature of the Hippocampal Representation

Another explanation for the contrast between Leutgeb *et al* (2004b) and the present study relates to the nature of the remapping training. In this study, animals from the main group (rats 1-4) were trained with a fast remapping protocol. Almost all representation differentiation occurred on the first day of training, and many cells were remapped from the first exposure to the different environments. By contrast,

animals in the Leutgeb *et al* (2004) study remapped gradually, over 2-3 weeks of training, similar to the results seen in Lever *et al* (2002). One animal in this thesis (rat 5) was trained using the same protocol as Lever *et al* (2002), though the place cells were not recorded during the remapping training. When this animal was run on the intermediate octagon series, there was no simultaneous switch between representations. Individual cells switched abruptly, but at different points in the octagon series. The overall change in the representation, therefore, was gradual and incremental.

The similarity between the rat 5 result, and that of Leutgeb *et al* (2004), suggests the possibility that gradual remapping leads to gradual representation shifts during the octagon probe. If slow remapping involves piecemeal changes to the place representation, with different cells responding independently to environments, it is possible that the resulting remapped representations are not coherent. This would then be exposed by the intermediate octagon series, in which different cells switch responses at different points, depending on which environmental features they are tuned to.

By contrast, fast remapping might lead to coherent remapped representations. As discussed above, the remapping observed in rats 1-4 is closer to the concept of 'complete' remapping (c.f. Muller & Kubie, 1987; Bostock *et al*, 1991) than partial or piecemeal remapping (c.f. Skaggs & McNaughton, 1998; Lever *et al*, 2002), and is also more compatible with the concept of place cells as a coherent representation of the environment. Only when fast remapping is triggered, therefore, do coherent representations arise. What could determine which type of representation was formed? One possibility is that sub-cortical inputs to the hippocampus change the way in which place cells respond to novel stimuli. For example, cholinergic modulation of CA3 recurrent synapses could affect whether novel stimuli are encoded using a new, independent representation, or blended with elements of an existing one (Hasselmo *et al*, 1995; 1996).

Further Experiments

In order to test the pattern separation/completion model of coherent representations, one important experiment would be to inactivate or to modify the

dentate gyrus/CA3 input to CA1, and then test the behaviour of CA1 place cells on the octagon probe experiment. Complete inactivation of the pathway could done by lesion of CA3, or cuts of the schaffer collaterals (Brun *et al*, 2002). In this case, CA1 place cell activity would be expected to reflect activity in the entorhinal cortex. Given the differing types of spatial signal in the entorhinal cortex (Quirk *et al*, 1992; Frank *et al*, 2000; Fyhn *et al*, 2004b), it would be of interest to test whether an 'entorhinal-only' CA1 would a) remap at all, and, if so, b) display a coherent switch between representations on the octagon probe. If there was no remapping, or there was remapping, but no coherent switch, it would be good evidence that dentate-CA3 circuitry does play a part in the discrimination of representations, as commonly proposed (Marr, 1971; McNaughton & Morris, 1987; Treves & Rolls, 1994).

It would also be possible to test separately the functions of the dentate gyrus and CA3. Lesions of dentate granule cells (McNaughton *et al*, 1989) could be used to destroy selectively the dentate gyrus, but leave the perforant pathway to CA3 intact. If the dentate gyrus does play a role in decreasing the overlap of incoming sensory representations, dentate lesioned animals would be expected not to remap. (Providing remapping was not also occurring upstream in the entorhinal cortex, see above). It would also be possible to prevent selectively plasticity in CA3 recurrent synapses (Nakazawa *et al*, 2002). This should prevent auto-associative networks forming between the active cell population, which should, therefore, reduce the coherency of the switch between representations.

To test further the pattern separation/completion hypothesis, it would be useful to record simultaneously from different sub-fields of the parahippocampal region, whilst running the remapping training and octagon probe. The nature of the spatial signal in the entorhinal cortex is of particular importance. Most models of hippocampal function assume that entorhinal cells have a broadly tuned spatial signal (c.f. Quirk *et al*, 1992). If entorhinal cells can show a highly spatially specific signal, and remap in response to altered environments (Hafting *et al*, 2005; Fyhn *et al*, 2004a; Fyhn *et al*, 2004b), it reduces the need to postulate the hippocampal formation being involved in discrimination of environments. It would be important to record from spatially specific dorsolateral MEC cells during the octagon probe, to test their responses to intermediate stimuli. The categorisation of environmental stimuli, and the ability to switch abruptly between representations, may be a task for which the hippocampus is required.

Place Cell Representations and Memory

This thesis has studied the nature of place cell representations in individual animals. As place cell firing has been proposed to correspond to a cognitive representation of place (or of objects and their relations, in non-spatial models of the hippocampus), it may be asked whether remapped place cell representations constitute memories of the different environments. The definition of memory used in this thesis is that memories relate only to behavioural responses. For remapped place cell representations to be considered memory traces, therefore, it would have to be shown that cell firing correlated with behavioural responses to different environments.

Can a link be demonstrated between remapping and a behavioural discrimination of environments? Several studies have shown a relationship between the place cell representation of environment and performance on spatial behaviour tasks (for example, O'Keefe & Speakman, (1987); Markus *et al*, (1994)). The only study to address remapping directly, in this context, was Jeffery *et al* (2003), which found a dissociation between remapping and behavioural performance. However, this study only showed that performance in a spatial task (run to box corner, defined by distal cues) was preserved, despite CA1 remapping. It is easy to imagine why remapping may not have affected this task: remapping was in response to changed proximal cues (box walls), whereas the goal area was defined by distal cues.

The octagon probe experiment presents a good opportunity to test the relationship between remapped place cells and cognitive representations. Animals could be trained to discriminate behaviourally between environments (rewarded in opposite halves of the environment in square and circle, for example), then run on the octagon probe. If remapped place cells are related to cognitive discrimination of environments, behavioural responses should match the 'abrupt shift' response profile of place cells. This result would be evidence that switching between place cell representations corresponds to the animal recalling memories of the different shapes. Of particular interest would be whether, in those shapes that can elicit different place cell representations on different trials, behavioural responses match place cell responses. If they did, it would suggest that place cell responses reflect the rat's

internal opinion of which shape he is in, even when this internal opinion does not correspond one to one with the external environment.

Chimeric Shapes

Chimeric Shapes Elicit Chimeric Representations

The chimeric shapes experiment was also designed to investigate the nature of remapped hippocampal representations. In the octagon probe, environments were ambiguous and intermediate, but the degree of similarity to square or to circle was uniform throughout an environment. By contrast, the chimeric shapes experiment exposed the animal to fully square-like and fully circle-like features simultaneously, during the same trial. The experiment was designed to test whether, even under these conditions, the place cell representation is coherent. If there was no coherence, what drives the responses of individual cells?

The primary result of the chimeric shapes experiment was clear: there was no coherent representation over the whole environment. In all chimeric environments, simultaneously recorded place cells were always split between those with square-like responses, and those with circle like responses. Chimeric shapes, therefore, led to chimeric place cell representations.

Why was no coherent representation seen in this experiment, in contrast to the octagon probe? The important difference could be simultaneous exposure to strongly conflicting sensory cues, a factor absent from the octagon probe. Animals expected to see either square environment features or circle environment features, but not both during the same trial. Even if a representation is coherent under 'normal' (i.e. baseline) circumstances, it can be disrupted by sufficiently great perturbations of environmental stimuli. In this case, simultaneous exposure to two sets of environmental features, previously associated with different remapped representations, could be sufficient to 'break up' coherent representations. Similarly, studies using angular cue dissociation have shown that putting familiar cues in conflict will disrupt the CA1 place cell representation, breaking apart the topological relationship between place fields and inducing remapping in some cells (Tanila *et al*, 1997; Shapiro *et al*, 1997; Brown & Skaggs, 2002; Knierim, 2002; Lee *et al*, 2004;

see chapter 3 for further details). Interestingly, this study has clearly shown what has remained contentious in angular cue dissociation studies, i.e. split control of different CA1 place fields by the different cue sets.

The Nature of the Chimeric Representation

In order to determine what drives the response of each cell, animals were exposed to a series of chimeras, each with octagonal features at a different cardinal point of the compass. Another clear result was found: overwhelmingly, place cell response (square-like or octagon-like) depended on the shape of the environment wall close to the place field of the cell. It is also important to note that almost all cells showed either fully square-like or fully octagon-like responses. There are at least two ways in which to interpret these results. Firstly, it may be that cells are independently responding to different proximal wall features. Secondly, it is possible to see the chimeric representation as two separate coherent representations. Hippocampal activity could be flipping between these as the animal moves around the environment. Each of these interpretations raises its own set of questions.

Chimeric representations as a collection of independent responses

The chimeric nature of the place cell representation raises the possibility that, at least under these experimental circumstances, cells are responding to the environment independently. The results could be explained by place cell firing based on a local view or sensory response which was biased towards stimuli close to the animal. Alternatively, 'feature detector' responses may be more broadly tuned when the receptive field is further from the animal (as in, for example, Hartley *et al*, 2000). In this case, as octagon and square shapes are broadly similar, only feature detectors tuned to nearby features would be able to discriminate between them. This would result in place cell responses matching those wall features currently close to them. Unfortunately, too few different shapes were used to understand properly what was driving the response of each cell.

Chimeric representations as flipping between two coherent maps

In the animal with the most remapped cells (rat 4), square-like and octagon-like responses were segregated into separate spatial regions of the environment. This raises the possibility that, within each of these regions, there is a coherent map of the environment, and hippocampal activity switches between the two, as the animal moves around the environment. In this interpretation, place cell response is influenced by both the activity of other place cells (via a collateral effect) and by environment wall features (with a bias towards features close to the animals current position). The hippocampus would have a tendency to maintain the current place cell representation, unless the input mismatch from close walls was sufficient cause it to 'flip' to another. Network collateral inputs could explain why the response of some cells do not match the closest wall features: strong inputs from cells with adjacent fields could override the sensory inputs in that position.

Models of the hippocampus which include coherent maps based on CA3 recurrent collaterals (e.g. Muller, 1991; McNaughton *et al*, 1996) all propose that remapping involves switching to an independent map, based on different active cells and different connections. However, none of these models has examined how or whether switches between maps could occur repeatedly within a single exposure to an environment. One set of studies that may be relevant involve training animals to shuttle on a linear track, then moving the start box relative to the rest of the laboratory. It was found that this induced an abrupt switch between 'reference frames' (whether place fields were positioned with respect to the start box or the laboratory), as the rat ran along the track (Gothard *et al*, 1996). This result refers to switching between positions on a single coherent map, rather than switching between remapped representations. It does, however, demonstrate the principle of an abrupt change in the place cell representation, as the animal traverses the environment. Redish *et al* (2000) determined that the occurrence of the switch was best predicted by time since leaving the start box, and that the dynamics of the switch suggested an attractor-based representation. Recording dentate gyrus cells during the task, however, demonstrated that, if this effect does occur, it is upstream of the dentate, and therefore cannot be based in CA3 (Gothard *et al*, 2001).

Testing the nature of the chimeric representation

An important follow-up to the chimeric shapes experiment would be a test of the two hypotheses outlined above. The most straightforward test would be to expose animals to the chimeric shapes whilst simultaneously recording a large number of remapped cells. Only a small amount of overlap between square-like and octagon-like firing would suggest that hippocampal activity was flipping between different maps. The most simple method would be to examine spatial overlap, as was attempted in this thesis. However, the flip between maps may occur at different places at different times in a trial. It may, therefore, also be necessary to examine population vectors of temporally co-active cells within a small time window. If there are two coherent maps, the distribution of population vectors in the chimeric representation should be roughly equivalent to the square distribution plus the circle distribution. The appearance of new population vectors would indicate 'hybrid' firing, and argue against the existence of two coherent maps.

Bibliography

Agnihotri NT, Hawkins RD, Kandel ER, Kentros C (2004) The long-term stability of new hippocampal place fields requires new protein synthesis. Proc Natl Acad Sci U S A 101: 3656-3661.

Amaral DG, Dolorfo C, Alvarez-Royo P (1991) Organization of CA1 projections to the subiculum: a PHA-L analysis in the rat. Hippocampus 1: 415-435.

Amaral DG, Insausti R, Cowan WM (1984) The commissural connections of the monkey hippocampal formation. J Comp Neurol 224: 307-336.

Amaral DG, Ishizuka N, Claiborne B (1990) Neurons, numbers and the hippocampal network. Prog Brain Res 83: 1-11.

Amaral DG, Kurz J (1985) An analysis of the origins of the cholinergic and noncholinergic septal projections to the hippocampal formation of the rat. J Comp Neurol 240: 37-59.

Amaral DG, Witter MP (1995) Hippocampal Formation. In: The Rat Nervous System (Paxinos G, ed), San Diego: Academic Press.

Amit D.J. (1992) Modelling Brain Function: the World of Attractor Neural Networks. Cambridge: Cambridge University Press.

Anderson MI, Jeffery KJ (2003) Heterogeneous modulation of place cell firing by changes in context. J Neurosci 23: 8827-8835.

Barnes CA, McNaughton BL, Mizumori SJ, Leonard BW, Lin LH (1990) Comparison of spatial and temporal characteristics of neuronal activity in sequential stages of hippocampal processing. Prog Brain Res 83: 287-300.

Battaglia F.P., Treves A. (1998) Attractor neural networks storing multiple space representations: A model for hippocampal place fields. Physical Review Letters E 58: 7738-7753.

Bayer SA (1982) Changes in the total number of dentate granule cells in juvenile and adult rats: a correlated volumetric and 3H-thymidine autoradiographic study. Exp Brain Res 46: 315-323.

Bayer SA, Yackel JW, Puri PS (1982) Neurons in the rat dentate gyrus granular layer substantially increase during juvenile and adult life. Science 216: 890-892.

Birch D, Jacobs GH (1979) Spatial contrast sensitivity in albino and pigmented rats. Vision Res 19: 933-937.

Blackstad TW (1956) Commissural connections of the hippocampal region in the rat, with special reference to their mode of termination. J Comp Neurol 105: 417-537.

Bland BH, Anderson P, Ganes T (1975) Two generators of hippocampal theta activity in rabbits. Brain Res 94: 199-218.

Bland BH, Colom LV (1993) Extrinsic and intrinsic properties underlying oscillation and synchrony in limbic cortex. Prog Neurobiol 41: 157-208.

Bland BH, Colom LV, Konopacki J, Roth SH (1988) Intracellular records of carbachol-induced theta rhythm in hippocampal slices. Brain Res 447: 364-368.

Bliss TV, Collingridge GL (1993) A synaptic model of memory: long-term potentiation in the hippocampus. Nature 361: 31-39.

Bliss TV, Lomo T (1973) Long-lasting potentiation of synaptic transmission in the dentate area of the anaesthetized rabbit following stimulation of the perforant path. J Physiol 232: 331-356.

Bliss TV, Richter-Levin G (1993) Spatial learning and the saturation of long-term potentiation. Hippocampus 3: 123-125.

Bostock E, Muller RU, Kubie JL (1991) Experience-dependent modifications of hippocampal place cell firing. Hippocampus 1: 193-205.

Bragin A, Engel J, Jr., Wilson CL, Fried I, Buzsaki G (1999) High-frequency oscillations in human brain. Hippocampus 9: 137-142.

Bragin A, Jando G, Nadasdy Z, Hetke J, Wise K, Buzsaki G (1995) Gamma (40-100 Hz) oscillation in the hippocampus of the behaving rat. J Neurosci 15: 47-60.

Brankack J, Stewart M, Fox SE (1993) Current source density analysis of the hippocampal theta rhythm: associated sustained potentials and candidate synaptic generators. Brain Res 615: 310-327.

Brown JE, Skaggs WE (2002) Concordant and discordant coding of spatial location in populations of hippocampal CA1 pyramidal cells. J Neurophysiol 88: 1605-1613.

Brun VH, Otnass MK, Molden S, Steffenach HA, Witter MP, Moser MB, Moser EI (2002) Place cells and place recognition maintained by direct entorhinal-hippocampal circuitry. Science 296: 2243-2246.

Burgess N, Donnett JG, Jeffery KJ, O'Keefe J (1997) Robotic and neuronal simulation of the hippocampus and rat navigation. Philos Trans R Soc Lond B Biol Sci 352: 1535-1543.

Burgess N, Donnett JG, O'Keefe J (1998) The representation of space and the hippocampus in rats, robots and humans. Z Naturforsch [C] 53: 504-509.

Burgess N, Jackson A, Hartley T, O'Keefe J (2000) Predictions derived from modelling the hippocampal role in navigation. Biol Cybern 83: 301-312.

Burgess N, O'Keefe J (1996) Cognitive graphs, resistive grids, and the hippocampal representation of space. J Gen Physiol 107: 659-662.

Burgess N, O'Keefe J (1996) Neuronal computations underlying the firing of place cells and their role in navigation. Hippocampus 6: 749-762.

Burwell RD (2000) The parahippocampal region: corticocortical connectivity. Ann N Y Acad Sci 911: 25-42.

Burwell RD, Amaral DG (1998) Cortical afferents of the perirhinal, postrhinal, and entorhinal cortices of the rat. J Comp Neurol 398: 179-205.

Burwell RD, Amaral DG (1998) Perirhinal and postrhinal cortices of the rat: interconnectivity and connections with the entorhinal cortex. J Comp Neurol 391: 293-321.

Burwell RD, Witter MP, Amaral DG (1995) Perirhinal and postrhinal cortices of the rat: a review of the neuroanatomical literature and comparison with findings from the monkey brain. Hippocampus 5: 390-408.

Buzsaki G (1989) Two-stage model of memory trace formation: a role for "noisy" brain states. Neuroscience 31: 551-570.

Buzsaki G, Czopf J, Kondakor I, Kellenyi L (1986) Laminar distribution of hippocampal rhythmic slow activity (RSA) in the behaving rat: current-source density analysis, effects of urethane and atropine. Brain Res 365: 125-137.

Buzsaki G, Gage FH, Czopf J, Bjorklund A (1987) Restoration of rhythmic slow activity (theta) in the subcortically denervated hippocampus by fetal CNS transplants. Brain Res 400: 334-347.

Caballero-Bleda M, Witter MP (1993) Regional and laminar organization of projections from the presubiculum and parasubiculum to the entorhinal cortex: an anterograde tracing study in the rat. J Comp Neurol 328: 115-129.

Calton JL, Stackman RW, Goodridge JP, Archey WB, Dudchenko PA, Taube JS (2003) Hippocampal place cell instability after lesions of the head direction cell network. J Neurosci 23: 9719-9731.

Canteras NS, Simerly RB, Swanson LW (1992) Connections of the posterior nucleus of the amygdala. J Comp Neurol 324: 143-179.

Chawla MK, Guzowski JF, Ramirez-Amaya V, Lipa P, Hoffman KL, Marriott LK, Worley PF, McNaughton BL, Barnes CA (2005) Sparse, environmentally selective expression of Arc RNA in the upper blade of the rodent fascia dentata by brief spatial experience. Hippocampus.

Chicurel ME, Harris KM (1992) Three-dimensional analysis of the structure and composition of CA3 branched dendritic spines and their synaptic relationships with mossy fiber boutons in the rat hippocampus. J Comp Neurol 325: 169-182.

Chrobak JJ, Buzsaki G (1994) Selective activation of deep layer (V-VI) retrohippocampal cortical neurons during hippocampal sharp waves in the behaving rat. J Neurosci 14: 6160-6170.

Chrobak JJ, Buzsaki G (1996) High-frequency oscillations in the output networks of the hippocampal-entorhinal axis of the freely behaving rat. J Neurosci 16: 3056-3066.

Claiborne BJ, Amaral DG, Cowan WM (1986) A light and electron microscopic analysis of the mossy fibers of the rat dentate gyrus. J Comp Neurol 246: 435-458.

Cohen NJ, Eichenbaum H (1993) Memory, Amnesia and the Hippocampal System. Cambridge: MIT Press.

Collingridge GL, Kehl SJ, McLennan H (1983) Excitatory amino acids in synaptic transmission in the Schaffer collateral-commissural pathway of the rat hippocampus. J Physiol 334: 33-46.

Colom LV, Nassif-Caudarella S, Dickson CT, Smythe JW, Bland BH (1991) In vivo intrahippocampal microinfusion of carbachol and bicuculline induces theta-like oscillations in the septally deafferented hippocampus. Hippocampus 1: 381-390.

Conrad LC, Leonard CM, Pfaff DW (1974) Connections of the median and dorsal raphe nuclei in the rat: an autoradiographic and degeneration study. J Comp Neurol 156: 179-205.

Cressant A, Muller RU, Poucet B (1997) Failure of centrally placed objects to control the firing fields of hippocampal place cells. J Neurosci 17: 2531-2542.

Cressant A, Muller RU, Poucet B (1999) Further study of the control of place cell firing by intra-apparatus objects. Hippocampus 9: 423-431.

Csicsvari J, Hirase H, Czurko A, Mamiya A, Buzsaki G (1999) Oscillatory coupling of hippocampal pyramidal cells and interneurons in the behaving Rat. J Neurosci 19: 274-287.

Daitz HM, Powell TP (1954) Studies of the connexions of the fornix system. J Neurochem 17: 75-82.

Dean P (1981) Visual pathways and acuity hooded rats. Behav Brain Res 3: 239-271.

Dolleman-Van Der Weel MJ, Witter MP (1996) Projections from the nucleus reuniens thalami to the entorhinal cortex, hippocampal field CA1, and the subiculum in the rat arise from different populations of neurons. J Comp Neurol 364: 637-650.

Dolorfo CL, Amaral DG (1998) Entorhinal cortex of the rat: topographic organization of the cells of origin of the perforant path projection to the dentate gyrus. J Comp Neurol 398: 25-48.

Draguhn A, Traub RD, Schmitz D, Jefferys JG (1998) Electrical coupling underlies high-frequency oscillations in the hippocampus in vitro. Nature 394: 189-192.

Elgersma Y, Silva AJ (1999) Molecular mechanisms of synaptic plasticity and memory. Curr Opin Neurobiol 9: 209-213.

Fenton AA, Csizmadia G, Muller RU (2000) Conjoint control of hippocampal place cell firing by two visual stimuli. I. The effects of moving the stimuli on firing field positions. J Gen Physiol 116: 191-209.

Fenton AA, Csizmadia G, Muller RU (2000) Conjoint control of hippocampal place cell firing by two visual stimuli. Ii. A vector-field theory that predicts modifications of the representation of the environment. J Gen Physiol 116: 211-221.

Fenton AA, Muller RU (1998) Place cell discharge is extremely variable during individual passes of the rat through the firing field. Proc Natl Acad Sci U S A 95: 3182-3187.

Fox SE, Wolfson S, Ranck JB, Jr. (1986) Hippocampal theta rhythm and the firing of neurons in walking and urethane anesthetized rats. Exp Brain Res 62: 495-508.

Frank LM, Brown EN, Wilson M (2000) Trajectory encoding in the hippocampus and entorhinal cortex. Neuron 27: 169-178.

Freund TF, Antal M (1988) GABA-containing neurons in the septum control inhibitory interneurons in the hippocampus. Nature 336: 170-173.

Freund TF, Buzsaki G (1996) Interneurons of the hippocampus. Hippocampus 6: 347-470.

Frey U, Huang YY, Kandel ER (1993) Effects of cAMP simulate a late stage of LTP in hippocampal CA1 neurons. Science 260: 1661-1664.

Frotscher M, Seress L, Schwerdtfeger WK, Buhl E (1991) The mossy cells of the fascia dentata: a comparative study of their fine structure and synaptic connections in rodents and primates. J Comp Neurol 312: 145-163.

Fyhn M, Hafting T, Treves A, Moser M, Moser E.I. (2004) Pattern Separation In Hippocampus But Not Layers II And III Of Entorhinal Cortex. Soc Neurosci Abstract No 330.5.

Fyhn M, Molden S, Witter MP, Moser EI, Moser MB (2004) Spatial representation in the entorhinal cortex. Science 305: 1258-1264.

Gaykema RP, Luiten PG, Nyakas C, Traber J (1990) Cortical projection patterns of the medial septum-diagonal band complex. J Comp Neurol 293: 103-124.

Gloor P (1997) The Hippocampal System. In: The Temporal Lobe and Limbic System pp 325-589. Oxford: Oxford University Press.

Golob EJ, Taube JS (1997) Head direction cells and episodic spatial information in rats without a hippocampus. Proc Natl Acad Sci U S A 94: 7645-7650.

Golob EJ, Taube JS (1999) Head direction cells in rats with hippocampal or overlying neocortical lesions: evidence for impaired angular path integration. J Neurosci 19: 7198-7211.

Gothard KM, Hoffman KL, Battaglia FP, McNaughton BL (2001) Dentate gyrus and ca1 ensemble activity during spatial reference frame shifts in the presence and absence of visual input. J Neurosci 21: 7284-7292.

Gothard KM, Skaggs WE, McNaughton BL (1996) Dynamics of mismatch correction in the hippocampal ensemble code for space: interaction between path integration and environmental cues. J Neurosci 16: 8027-8040.

Gothard KM, Skaggs WE, Moore KM, McNaughton BL (1996) Binding of hippocampal CA1 neural activity to multiple reference frames in a landmark-based navigation task. J Neurosci 16: 823-835.

Groenewegen HJ, Vermeulen-Van der Zee E, te KA, Witter MP (1987) Organization of the projections from the subiculum to the ventral striatum in the rat. A study using anterograde transport of Phaseolus vulgaris leucoagglutinin. Neuroscience 23: 103-120.

Guzowski JF, McNaughton BL, Barnes CA, Worley PF (1999) Environment-specific expression of the immediate-early gene Arc in hippocampal neuronal ensembles. Nat Neurosci 2: 1120-1124.

Hafting T, Fyhn M, Molden S, Moser MB, Moser EI (2005) Microstructure of a spatial map in the entorhinal cortex. Nature.

Haglund L, Swanson LW, Kohler C (1984) The projection of the supramammillary nucleus to the hippocampal formation: an immunohistochemical and anterograde transport study with the lectin PHA-L in the rat. J Comp Neurol 229: 171-185.

Haring JH, Davis JN (1983) Topography of locus ceruleus neurons projecting to the area dentata. Exp Neurol 79: 785-800.

Harris EW, Cotman CW (1986) Long-term potentiation of guinea pig mossy fiber responses is not blocked by N-methyl D-aspartate antagonists. Neurosci Lett 70: 132-137.

Harris KD, Henze DA, Hirase H, Leinekugel X, Dragoi G, Czurko A, Buzsaki G (2002) Spike train dynamics predicts theta-related phase precession in hippocampal pyramidal cells. Nature 417: 738-741.

Hartley T, Burgess N, Lever C, Cacucci F, O'Keefe J (2000) Modeling place fields in terms of the cortical inputs to the hippocampus. Hippocampus 10: 369-379.

Hasselmo ME, Schnell E, Barkai E (1995) Dynamics of learning and recall at excitatory recurrent synapses and cholinergic modulation in rat hippocampal region CA3. J Neurosci 15: 5249-5262.

Hasselmo ME, Wyble BP, Wallenstein GV (1996) Encoding and retrieval of episodic memories: role of cholinergic and GABAergic modulation in the hippocampus. Hippocampus 6: 693-708.

Heale VR, Vanderwolf CH, Kavaliers M (1994) Components of weasel and fox odors elicit fast wave bursts in the dentate gyrus of rats. Behav Brain Res 63: 159-165.

Hebb D.O. (1949) The Organization of Behavior. New York: Wiley.

Hetherington PA, Shapiro ML (1997) Hippocampal place fields are altered by the removal of single visual cues in a distance-dependent manner. Behav Neurosci 111: 20-34.

Hill AJ (1978) First occurrence of hippocampal spatial firing in a new environment. Exp Neurol 62: 282-297.

Hill AJ, Best PJ (1981) Effects of deafness and blindness on the spatial correlates of hippocampal unit activity in the rat. Exp Neurol 74: 204-217.

Hopfield JJ (1982) Neural networks and physical systems with emergent collective computational abilities. Proc Natl Acad Sci U S A 79: 2554-2558.

Huxter J, Burgess N, O'Keefe J (2003) Independent rate and temporal coding in hippocampal pyramidal cells. Nature 425: 828-832.

Ishizuka N, Cowan WM, Amaral DG (1995) A quantitative analysis of the dendritic organization of pyramidal cells in the rat hippocampus. J Comp Neurol 362: 17-45.

Ishizuka N, Weber J, Amaral DG (1990) Organization of intrahippocampal projections originating from CA3 pyramidal cells in the rat. J Comp Neurol 295: 580-623.

Jeffery KJ, Anderson MI (2003) Dissociation of the geometric and contextual influences on place cells. Hippocampus 13: 868-872.

Jeffery KJ, Donnett JG, Burgess N, O'Keefe JM (1997) Directional control of hippocampal place fields. Exp Brain Res 117: 131-142.

Jeffery KJ, Gilbert A, Burton S, Strudwick A (2003) Preserved performance in a hippocampal-dependent spatial task despite complete place cell remapping. Hippocampus 13: 175-189.

Jeffery KJ, O'Keefe JM (1999) Learned interaction of visual and idiothetic cues in the control of place field orientation. Exp Brain Res 127: 151-161.

Jung MW, McNaughton BL (1993) Spatial selectivity of unit activity in the hippocampal granular layer. Hippocampus 3: 165-182.

Jung MW, Wiener SI, McNaughton BL (1994) Comparison of spatial firing characteristics of units in dorsal and ventral hippocampus of the rat. J Neurosci 14: 7347-7356.

Kahana MJ, Sekuler R, Caplan JB, Kirschen M, Madsen JR (1999) Human theta oscillations exhibit task dependence during virtual maze navigation. Nature 399: 781-784.

Kali S, Dayan P (2000) The involvement of recurrent connections in area CA3 in establishing the properties of place fields: a model. J Neurosci 20: 7463-7477.

Keller J, Strasburger H, Cerutti DT, Sabel BA (2000) Assessing spatial vision - automated measurement of the contrast-sensitivity function in the hooded rat. J Neurosci Methods 97: 103-110.

Kentros C, Hargreaves E, Hawkins RD, Kandel ER, Shapiro M, Muller RV (1998) Abolition of long-term stability of new hippocampal place cell maps by NMDA receptor blockade. Science 280: 2121-2126.

Klausberger T, Magill PJ, Marton LF, Roberts JD, Cobden PM, Buzsaki G, Somogyi P (2003) Brain-state- and cell-type-specific firing of hippocampal interneurons in vivo. Nature 421: 844-848.

Klausberger T, Marton LF, Baude A, Roberts JD, Magill PJ, Somogyi P (2004) Spike timing of dendrite-targeting bistratified cells during hippocampal network oscillations in vivo. Nat Neurosci 7: 41-47.

Knierim JJ (2002) Dynamic interactions between local surface cues, distal landmarks, and intrinsic circuitry in hippocampal place cells. J Neurosci 22.

Knierim JJ, Kudrimoti HS, McNaughton BL (1995) Place cells, head direction cells, and the learning of landmark stability. J Neurosci 15: 1648-1659.

Knierim JJ, Kudrimoti HS, McNaughton BL (1998) Interactions between idiothetic cues and external landmarks in the control of place cells and head direction cells. J Neurophysiol 80: 425-446.

Knierim JJ, McNaughton BL (2001) Hippocampal place-cell firing during movement in three-dimensional space. J Neurophysiol 85: 105-116.

Kohler C (1985) Intrinsic projections of the retrohippocampal in the rat brain. I. The subicular complex. J Comp Neurol 236: 504-522.

Kohler C, Chan-Palay V, Wu JY (1984) Septal neurons containing glutamic acid decarboxylase immunoreactivity project to the hippocampal region in the rat brain. Anat Embryol (Berl) 169: 41-44.

Kohler C, Swanson LW, Haglund L, Wu JY (1985) The cytoarchitecture, histochemistry and projections of the tuberomammillary nucleus in the rat. Neuroscience 16: 85-110.

Krettek JE, Price JL (1977) Projections from the amygdaloid complex and adjacent olfactory structures to the entorhinal cortex and to the subiculum in the rat and cat. J Comp Neurol 172: 723-752.

Kubie JL, Ranck JB (1983) Sensory-Behavioural correlates in individual hippocampus neurons in three situations: space and context. In: Neurobiology of the hippocampus. (Siefert W, ed), New York: Academic Press.

Laurberg S, Sorensen KE (1981) Associational and commissural collaterals of neurons in the hippocampal formation (hilus fasciae dentatae and subfield CA3). Brain Res 212: 287-300.

Lawson VH, Bland BH (1993) The role of the septohippocampal pathway in the regulation of hippocampal field activity and behavior: analysis by the intraseptal microinfusion of carbachol, atropine, and procaine. Exp Neurol 120: 132-144.

Lee I, Yoganarasimha D, Rao G, Knierim JJ (2004) Comparison of population coherence of place cells in hippocampal subfields CA1 and CA3. Nature 430: 456-459.

Lein ES, Callaway EM, Albright TD, Gage FH (2005) Redefining the boundaries of the hippocampal CA2 subfield in the mouse using gene expression and 3-dimensional reconstruction. J Comp Neurol 485: 1-10.

Leranth C, Ribak CE (1991) Calcium-binding proteins are concentrated in the CA2 field of the monkey hippocampus: a possible key to this region's resistance to epileptic damage. Exp Brain Res 85: 129-136.

Leutgeb JK, Leutgeb S, Treves A, Fyhn M, Meyer R, Barnes CA, McNaughton BL, Moser M, Moser EI (2004) Pattern Completion And Pattern Separation In Ca3 During Morphing Of Two Environments. Soc Neurosci Abstract No. 330.3.

Leutgeb S, Leutgeb JK, Treves A, Moser MB, Moser EI (2004) Distinct ensemble codes in hippocampal areas CA3 and CA1. Science 305: 1295-1298.

Lever C, Wills T, Cacucci F, Burgess N, O'Keefe J (2002) Long-term plasticity in hippocampal place-cell representation of environmental geometry. Nature 416: 90-94.

Lewis PR, Shute CC, Silver A (1967) Confirmation from choline acetylase analyses of a massive cholinergic innervation to the rat hippocampus. J Physiol 191: 215-224.

Li XG, Somogyi P, Ylinen A, Buzsaki G (1994) The hippocampal CA3 network: an in vivo intracellular labeling study. J Comp Neurol 339: 181-208.

Lopes da Silva FH, Witter MP, Boeijinga PH, Lohman AH (1990) Anatomic organization and physiology of the limbic cortex. Physiol Rev 70: 453-511.

Lorente de No R (1934) Studies on the structure of the cerebral cortex. II. Continuation of the study of the ammonic system. J Psychol Neurol 46: 113-177.

MacVicar BA, Tse FW (1989) Local neuronal circuitry underlying cholinergic rhythmical slow activity in CA3 area of rat hippocampal slices. J Physiol 417: 197-212.

Markus EJ, Barnes CA, McNaughton BL, Gladden VL, Skaggs WE (1994) Spatial information content and reliability of hippocampal CA1 neurons: effects of visual input. Hippocampus 4: 410-421.

Markus EJ, Qin YL, Leonard B, Skaggs WE, McNaughton BL, Barnes CA (1995) Interactions between location and task affect the spatial and directional firing of hippocampal neurons. J Neurosci 15: 7079-7094.

Marr D (1971) Simple memory: a theory for archicortex. Philos Trans R Soc Lond B Biol Sci 262.

Martin SJ, Grimwood PD, Morris RG (2000) Synaptic plasticity and memory: an evaluation of the hypothesis. Annu Rev Neurosci 23: 649-711.

McNaughton B.L., Morris R.G.M (1987) Hippocampal synaptic enhancement and information storage within a distributed memory system. Trends in Neurosciences 10: 408-415.

McNaughton BL, Barnes CA (1977) Physiological identification and analysis of dentate granule cell responses to stimulation of the medial and lateral perforant pathways in the rat. J Comp Neurol 175: 439-454.

McNaughton BL, Barnes CA, Gerrard JL, Gothard K, Jung MW, Knierim JJ, Kudrimoti H, Qin Y, Skaggs WE, Suster M, Weaver KL (1996) Deciphering the hippocampal polyglot: the hippocampus as a path integration system. J Exp Biol 199: 173-185.

McNaughton BL, Barnes CA, Meltzer J, Sutherland RJ (1989) Hippocampal granule cells are necessary for normal spatial learning but not for spatially-selective pyramidal cell discharge. Exp Brain Res 76: 485-496.

McNaughton BL, Barnes CA, O'Keefe J (1983) The contributions of position, direction, and velocity to single unit activity in the hippocampus of freely-moving rats. Exp Brain Res 52: 41-49.

Mehta MR, Lee AK, Wilson MA (2002) Role of experience and oscillations in transforming a rate code into a temporal code. Nature 417: 741-746.

Mehta MR, Quirk MC, Wilson MA (2000) Experience-dependent asymmetric shape of hippocampal receptive fields. Neuron 25: 707-715.

Mizumori SJ, Miya DY, Ward KE (1994) Reversible inactivation of the lateral dorsal thalamus disrupts hippocampal place representation and impairs spatial learning. Brain Res 644: 168-174.

Mizumori SJ, Perez GM, Alvarado MC, Barnes CA, McNaughton BL (1990) Reversible inactivation of the medial septum differentially affects two forms of learning in rats. Brain Res 528: 12-20.

Mizumori SJ, Ragozzino KE, Cooper BG, Leutgeb S (1999) Hippocampal representational organization and spatial context. Hippocampus 9: 444-451.

Mizumori SJ, Williams JD (1993) Directionally selective mnemonic properties of neurons in the lateral dorsal nucleus of the thalamus of rats. J Neurosci 13: 4015-4028.

Morris RG, Anderson E, Lynch GS, Baudry M (1986) Selective impairment of learning and blockade of long-term potentiation by an N-methyl-D-aspartate receptor antagonist, AP5. Nature 319: 774-776.

Moser EI, Krobert KA, Moser MB, Morris RG (1998) Impaired spatial learning after saturation of long-term potentiation. Science 281: 2038-2042.

Mosko S, Lynch G, Cotman CW (1973) The distribution of septal projections to the hippocampus of the rat. J Comp Neurol 152: 163-174.

Muller R (1996) A quarter of a century of place cells. Neuron 17: 813-822.

Muller RU, Bostock E, Taube JS, Kubie JL (1994) On the directional firing properties of hippocampal place cells. J Neurosci 14: 7235-7251.

Muller RU, Kubie JL (1987) The effects of changes in the environment on the spatial firing of hippocampal complex-spike cells. J Neurosci 7: 1951-1968.

Muller RU, Kubie JL, Ranck JB, Jr. (1987) Spatial firing patterns of hippocampal complex-spike cells in a fixed environment. J Neurosci 7: 1935-1950.

Muller RU, Kubie JL, Saypoff R (1991) The hippocampus as a cognitive graph (abridged version). Hippocampus 1: 243-246.

Muller RU, Stead M (1996) Hippocampal place cells connected by Hebbian synapses can solve spatial problems. Hippocampus 6: 709-719.

Muller RU, Stead M, Pach J (1996) The hippocampus as a cognitive graph. J Gen Physiol 107: 663-694.

Naber PA, Caballero-Bleda M, Jorritsma-Byham B, Witter MP (1997) Parallel input to the hippocampal memory system through peri- and postrhinal cortices. Neuroreport 8: 2617-2621.

Naber PA, Witter MP (1998) Subicular efferents are organized mostly as parallel projections: a double-labeling, retrograde-tracing study in the rat. J Comp Neurol 393: 284-297.

Naber PA, Witter MP, Lopes da Silva FH (2001) Evidence for a direct projection from the postrhinal cortex to the subiculum in the rat. Hippocampus 11: 105-117.

Nafstad PH (1967) An electron microscope study on the termination of the perforant path fibres in the hippocampus and the fascia dentata. Z Zellforsch Mikrosk Anat 76: 532-542.

Nakazawa K, Quirk MC, Chitwood RA, Watanabe M, Yeckel MF, Sun LD, Kato A, Carr CA, Johnston D, Wilson MA, Tonegawa S (2002) Requirement for hippocampal CA3 NMDA receptors in associative memory recall. Science 297: 211-218.

Nyakas C, Luiten PG, Spencer DG, Traber J (1987) Detailed projection patterns of septal and diagonal band efferents to the hippocampus in the rat with emphasis on innervation of CA1 and dentate gyrus. Brain Res Bull 18: 533-545.

O'Keefe J, Nadel L (1978) The hippocampus as a cognitive map. Oxford University Press.

O'Keefe J (1976) Place units in the hippocampus of the freely moving rat. Exp Neurol 51: 78-109.

O'Keefe J (1979) A review of the hippocampal place cells. Prog Neurobiol 13: 419-439.

O'Keefe J (1990) A computational theory of the hippocampal cognitive map. Prog Brain Res 83: 301-312.

O'Keefe J (1991) An allocentric spatial model for the hippocampal cognitive map. Hippocampus 1: 230-235.

O'Keefe J, Burgess N (1996) Geometric determinants of the place fields of hippocampal neurons. Nature 381: 425-428.

O'Keefe J, Conway DH (1978) Hippocampal place units in the freely moving rat: why they fire where they fire. Exp Brain Res 31: 573-590.

O'Keefe J, Dostrovsky J (1971) The hippocampus as a spatial map. Preliminary evidence from unit activity in the freely-moving rat. Brain Res 34: 171-175.

O'Keefe J, Recce ML (1993) Phase relationship between hippocampal place units and the EEG theta rhythm. Hippocampus 3: 317-330.

O'Keefe J, Speakman A (1987) Single unit activity in the rat hippocampus during a spatial memory task. Exp Brain Res 68: 1-27.

O'Reilly RC, McClelland JL (1994) Hippocampal conjunctive encoding, storage, and recall: avoiding a trade-off. Hippocampus 4: 661-682.

Ochiishi T, Chen L, Yukawa A, Saitoh Y, Sekino Y, Arai T, Nakata H, Miyamoto H (1999) Cellular localization of adenosine A1 receptors in rat forebrain: immunohistochemical analysis using adenosine A1 receptor-specific monoclonal antibody. J Comp Neurol 411: 301-316.

Olton DS, Branch M, Best PJ (1978) Spatial correlates of hippocampal unit activity. Exp Neurol 58: 387-409.

Pikkarainen M, Ronkko S, Savander V, Insausti R, Pitkanen A (1999) Projections from the lateral, basal, and accessory basal nuclei of the amygdala to the hippocampal formation in rat. J Comp Neurol 403: 229-260.

Poucet B, Thinus-Blanc C, Muller RU (1994) Place cells in the ventral hippocampus of rats. Neuroreport 5: 2045-2048.

Quirk GJ, Muller RU, Kubie JL, Ranck JB, Jr. (1992) The positional firing properties of medial entorhinal neurons: description and comparison with hippocampal place cells. J Neurosci 12: 1945-1963.

Ranck JB, Jr. (1973) Studies on single neurons in dorsal hippocampal formation and septum in unrestrained rats. I. Behavioral correlates and firing repertoires. Exp Neurol 41: 461-531.

Ranck JB (1984) Head-direction cells in the deep layers of dorsal presubiculum in freely moving rats. Soc Neurosci Abstract 10.

Redish AD (1999) Beyond the Cognitive Map: From Place Cells to Episodic Memory. Cambridge, Massachusetts: MIT Press.

Redish AD, Rosenzweig ES, Bohanick JD, McNaughton BL, Barnes CA (2000) Dynamics of hippocampal ensemble activity realignment: time versus space. J Neurosci 20: 9298-9309.

Redish AD, Touretzky DS (1997) Cognitive maps beyond the hippocampus. Hippocampus 7: 15-35.

Redish AD, Touretzky DS (1998) The role of the hippocampus in solving the Morris water maze. Neural Comput 10: 73-111.

Ribak CE, Seress L (1983) Five types of basket cell in the hippocampal dentate gyrus: a combined Golgi and electron microscopic study. J Neurocytol 12: 577-597.

Ribak CE, Seress L, Amaral DG (1985) The development, ultrastructure and synaptic connections of the mossy cells of the dentate gyrus. J Neurocytol 14: 835-857.

Ribak CE, Vaughn JE, Saito K (1978) Immunocytochemical localization of glutamic acid decarboxylase in neuronal somata following colchicine inhibition of axonal transport. Brain Res 140: 315-332.

Ruth RE, Collier TJ, Routtenberg A (1982) Topography between the entorhinal cortex and the dentate septotemporal axis in rats: I. Medial and intermediate entorhinal projecting cells. J Comp Neurol 209: 69-78.

Ruth RE, Collier TJ, Routtenberg A (1988) Topographical relationship between the entorhinal cortex and the septotemporal axis of the dentate gyrus in rats: II. Cells projecting from lateral entorhinal subdivisions. J Comp Neurol 270: 506-516.

Samsonovich A, McNaughton BL (1997) Path integration and cognitive mapping in a continuous attractor neural network model. J Neurosci 17: 5900-5920.

Save E, Cressant A, Thinus-Blanc C, Poucet B (1998) Spatial firing of hippocampal place cells in blind rats. J Neurosci 18: 1818-1826.

Save E, Nerad L, Poucet B (2000) Contribution of multiple sensory information to place field stability in hippocampal place cells. Hippocampus 10: 64-76.

Scharfman HE, Witter MP, Schwarcz R (2000) The parahippocampal region. Implications for neurological and psychiatric diseases. Introduction. Ann N Y Acad Sci 911: ix-xiii.

Segal M, Landis S (1974) Afferents to the hippocampus of the rat studied with the method of retrograde transport of horseradish peroxidase. Brain Res 78: 1-15.

Seress L, Ribak CE (1983) GABAergic cells in the dentate gyrus appear to be local circuit and projection neurons. Exp Brain Res 50: 173-182.

Shapiro ML, Tanila H, Eichenbaum H (1997) Cues that hippocampal place cells encode: dynamic and hierarchical representation of local and distal stimuli. Hippocampus 7: 624-642.

Sharp PE (1997) Subicular cells generate similar spatial firing patterns in two geometrically and visually distinctive environments: comparison with hippocampal place cells. Behav Brain Res 85: 71-92.

Sharp PE (1999) Subicular place cells expand or contract their spatial firing pattern to fit the size of the environment in an open field but not in the presence of barriers: comparison with hippocampal place cells. Behav Neurosci 113: 643-662.

Sharp PE, Green C (1994) Spatial correlates of firing patterns of single cells in the subiculum of the freely moving rat. J Neurosci 14: 2339-2356.

Silveira LC, Heywood CA, Cowey A (1987) Contrast sensitivity and visual acuity of the pigmented rat determined electrophysiologically. Vision Res 27: 1719-1731.

Skaggs WE, McNaughton BL (1998) Spatial firing properties of hippocampal CA1 populations in an environment containing two visually identical regions. J Neurosci 18: 8455-8466.

Skaggs WE, McNaughton BL, Gothard KM, Markus EJ (1993) An information-theoretic approach to deciphering the hippocampal code. In: Advances in neural information processing systems. (Hanson SJ, Cowan JD, Giles CL, eds), San Mateo: Morgan Kaufman.

Skaggs WE, McNaughton BL, Wilson MA, Barnes CA (1996) Theta phase precession in hippocampal neuronal populations and the compression of temporal sequences. Hippocampus 6: 149-172.

Sloviter RS, Sollas AL, Barbaro NM, Laxer KD (1991) Calcium-binding protein (calbindin-D28K) and parvalbumin immunocytochemistry in the normal and epileptic human hippocampus. J Comp Neurol 308: 381-396.

Somogyi P, Klausberger T (2005) Defined types of cortical interneurone structure space and spike timing in the hippocampus. J Physiol 562: 9-26.

Squire LR (1987) Memory and Brain. New York: Oxford University Press.

Stackman RW, Taube JS (1998) Firing properties of rat lateral mammillary single units: head direction, head pitch, and angular head velocity. J Neurosci 18: 9020-9037.

Steward O, Scoville SA (1976) Cells of origin of entorhinal cortical afferents to the hippocampus and fascia dentata of the rat. J Comp Neurol 169: 347-370.

Suzuki WA, Amaral DG (1990) Cortical inputs to the CA1 field of the monkey hippocampus originate from the perirhinal and parahippocampal cortex but not from area TE. Neurosci Lett 115: 43-48.

Swanson LW (1978) The anatomical organisation of septo-hippocampal projections. In: Functions of the septo-hippocampal system pp 25-48. Amsterdam: Elsevier.

Swanson LW (1982) The projections of the ventral tegmental area and adjacent regions: a combined fluorescent retrograde tracer and immunofluorescence study in the rat. Brain Res Bull 9: 321-353.

Swanson LW, Cowan WM (1977) An autoradiographic study of the organization of the efferent connections of the hippocampal formation in the rat. J Comp Neurol 172: 49-84.

Swanson LW, Hartman BK (1975) The central adrenergic system. An immunofluorescence study of the location of cell bodies and their efferent connections in the rat utilizing dopamine-beta-hydroxylase as a marker. J Comp Neurol 163: 467-505.

Swanson LW, Kohler C, Bjorklund A (1987) The limbic region. I. The septohippocampal system. In: Handbook of Chemical Neuroanatomy, Vol 5, Integrated Systems of the CNS, Part I. (Bjorklund A, Swanson LW, Hokfelt T, eds), pp 125-227. Amsterdam: Elsevier.

Swanson LW, Sawchenko PE, Cowan WM (1980) Evidence that the commissural, associational and septal projections of the regio inferior of the hippocampus arise from the same neurons. Brain Res 197: 207-212.

Swanson LW, Sawchenko PE, Cowan WM (1981) Evidence for collateral projections by neurons in Ammon's horn, the dentate gyrus, and the subiculum: a multiple retrograde labeling study in the rat. J Neurosci 1: 548-559.

Swanson LW, Wyss JM, Cowan WM (1978) An autoradiographic study of the organization of intrahippocampal association pathways in the rat. J Comp Neurol 181: 681-715.

Tamamaki N, Abe K, Nojyo Y (1987) Columnar organization in the subiculum formed by axon branches originating from single CA1 pyramidal neurons in the rat hippocampus. Brain Res 412: 156-160.

Tamamaki N, Abe K, Nojyo Y (1988) Three-dimensional analysis of the whole axonal arbors originating from single CA2 pyramidal neurons in the rat hippocampus with the aid of a computer graphic technique. Brain Res 452: 255-272.

Tanila H, Shapiro ML, Eichenbaum H (1997) Discordance of spatial representation in ensembles of hippocampal place cells. Hippocampus 7: 613-623.

Taube JS (1995) Head direction cells recorded in the anterior thalamic nuclei of freely moving rats. J Neurosci 15: 70-86.

Taube JS, Muller RU, Ranck JB, Jr. (1990) Head-direction cells recorded from the postsubiculum in freely moving rats. I. Description and quantitative analysis. J Neurosci 10: 420-435.

Taube JS, Muller RU, Ranck JB, Jr. (1990) Head-direction cells recorded from the postsubiculum in freely moving rats. II. Effects of environmental manipulations. J Neurosci 10: 436-447.

Tesche CD (1997) Non-invasive detection of ongoing neuronal population activity in normal human hippocampus. Brain Res 749: 53-60.

Thompson LT, Best PJ (1990) Long-term stability of the place-field activity of single units recorded from the dorsal hippocampus of freely behaving rats. Brain Res 509: 299-308.

Toth K, Freund TF (1992) Calbindin D28k-containing nonpyramidal cells in the rat hippocampus: their immunoreactivity for GABA and projection to the medial septum. Neuroscience 49: 793-805.

Touretzky DS, Redish AD (1996) Theory of rodent navigation based on interacting representations of space. Hippocampus 6: 247-270.

Touretzky DS, Weisman WE, Fuhs MC, Skaggs WE, Fenton AA, Muller RU (2004) Deforming the hippocampal map. Hippocampus.

Treves A. (1990) Graded-response neurons and information encodings in autoassociative memories. Physical Review A 42: 2418-2430.

Treves A, Rolls ET (1992) Computational constraints suggest the need for two distinct input systems to the hippocampal CA3 network. Hippocampus 2: 189-199.

Treves A, Rolls ET (1994) Computational analysis of the role of the hippocampus in memory. Hippocampus 4: 374-391.

Tucker MS, Khan I, Fuchs-Young R, Price S, Steininger TL, Greene G, Wainer BH, Rosner MR (1993) Localization of immunoreactive epidermal growth factor receptor in neonatal and adult rat hippocampus. Brain Res 631: 65-71.

van Groen T, Wyss JM (1990) Extrinsic projections from area CA1 of the rat hippocampus: olfactory, cortical, subcortical, and bilateral hippocampal formation projections. J Comp Neurol 302: 515-528.

van Groen T, Wyss JM (1990) The connections of presubiculum and parasubiculum in the rat. Brain Res 518: 227-243.

van Groen T, Wyss JM (1990) The postsubicular cortex in the rat: characterization of the fourth region of the subicular cortex and its connections. Brain Res 529: 165-177.

van Groen T, Wyss JM (1995) Projections from the anterodorsal and anteroventral nucleus of the thalamus to the limbic cortex in the rat. J Comp Neurol 358: 584-604.

Vanderwolf CH (1969) Hippocampal electrical activity and voluntary movement in the rat. Electroencephalogr Clin Neurophysiol 26: 407-418.

Vanderwolf CH (1971) Limbic-diencephalic mechanisms of voluntary movement. Psychol Rev 78: 83-113.

Vanderwolf CH (2001) The hippocampus as an olfacto-motor mechanism: were the classical anatomists right after all? Behav Brain Res 127: 25-47.

Vazdarjanova A, Guzowski JF (2004) Differences in hippocampal neuronal population responses to modifications of an environmental context: evidence for distinct, yet complementary, functions of CA3 and CA1 ensembles. J Neurosci 24: 6489-6496.

Wainer BH, Levey AI, Rye DB, Mesulam MM, Mufson EJ (1985) Cholinergic and non-cholinergic septohippocampal pathways. Neurosci Lett 54: 45-52.

Williams TE, Meshul CK, Cherry NJ, Tiffany NM, Eckenstein FP, Woodward WR (1996) Characterization and distribution of basic fibroblast growth factor-containing cells in the rat hippocampus. J Comp Neurol 370: 147-158.

Willshaw DJ, Buckingham JT (1990) An assessment of Marr's theory of the hippocampus as a temporary memory store. Philos Trans R Soc Lond B Biol Sci 329: 205-215.

Wilson MA, McNaughton BL (1993) Dynamics of the hippocampal ensemble code for space. Science 261: 1055-1058.

Witter MP (1993) Organisation of the entorhinal-hippocampal system. Hippocampus 3(suppl): 33-44.

Witter MP, Groenewegen HJ (1990) The subiculum: cytoarchitectonically a simple structure, but hodologically complex. Prog Brain Res 83: 47-58.

Witter MP, Groenewegen HJ, Lopes da Silva FH, Lohman AH (1989) Functional organization of the extrinsic and intrinsic circuitry of the parahippocampal region. Prog Neurobiol 33: 161-253.

Witter MP, Naber PA, van Haeften T, Machielsen WC, Rombouts SA, Barkhof F, Scheltens P, Lopes da Silva FH (2000) Cortico-hippocampal communication by way of parallel parahippocampal-subicular pathways. Hippocampus 10: 398-410.

Witter MP, Wouterlood FG, Naber PA, van Haeften T (2000) Anatomical organization of the parahippocampal-hippocampal network. Ann N Y Acad Sci 911: 1-24.

Wouterlood FG, Saldana E, Witter MP (1990) Projection from the nucleus reuniens thalami to the hippocampal region: light and electron microscopic tracing study in the rat with the anterograde tracer Phaseolus vulgaris-leucoagglutinin. J Comp Neurol 296: 179-203.

Wyss JM, van Groen T (1992) Connections between the retrosplenial cortex and the hippocampal formation in the rat: a review. Hippocampus 2: 1-11.

Zipp F, Nitsch R, Soriano E, Frotscher M (1989) Entorhinal fibers form synaptic contacts on parvalbumin-immunoreactive neurons in the rat fascia dentata. Brain Res 495: 161-166.

Appendix 1

List of Abbreviations

ADN.....Anterior Dorsal Nucleus of the Thalamus

ANN.....Attractor Neural Network

AP.....Anterior-Posterior

BVC.....Boundary Vector Cell

CA[1, 2, 3] .....*Cornu Ammonis* fields of the Hippocampus

CPP.....3-(2-Carboxypiperazin-4-yl)Propyl-1-Phosphonic acid

DV.....Dorso-Ventral

GABA.....Gamma-Aminobutyric Acid

HD, HD Cell.....Head Direction, Head Direction Cell

ITI.....Inter-Trial Interval

LDN.....Latero-Dorsal Nucleus of the Thalamus

LEA.....Lateral Entorhinal Area

LIA.....Large Irregular Activity (EEG state of Hippocampus)

LTP.....Long-Term Potentiation

MEA.....Lateral Entorhinal Area

MS/DBB.....Medial Septum/Diagonal Band of Broca

NMDA[-R].....N-Methyl-D-Aspartate [Receptor]

O-LM cells.....*Oriens-Lacunosum Moleculare* interneurons of the Hippocampus

REM.....Rapid Eye Movement sleep

[m]RNA.....[messenger] Ribo-Nucleic Acid

SD.....Similarity Difference score